Master's thesis

NTNU
Norwegian University of Science and Technology
Faculty of Economics and Management
Dept. of Industrial Economics and Technology Management

Nithish Kini Ullal

Zonal Level Disruption Response Considering Transmission Line Outage from Large-Scale Offshore Wind Farms

Master's thesis in Sustainable Energy Systems and Markets
Supervisor: Ruud Egging-Bratseth, Christian von Hirschhausen and Felix Jakob Fliegner
Co-supervisor: Christoph Weyhing and Jan Voet
September 2022

NTNU
Norwegian University of Science and Technology

TECHNISCHE UNIVERSITÄT BERLIN

Nithish Kini Ullal

Zonal Level Disruption Response Considering Transmission Line Outage from Large-Scale Offshore Wind Farms

Master's thesis in Sustainable Energy Systems and Markets
Supervisor: Ruud Egging-Bratseth, Christian von Hirschhausen and Felix Jakob Fliegner
Co-supervisor: Christoph Weyhing and Jan Voet
September 2022

Norwegian University of Science and Technology
Faculty of Economics and Management
Dept. of Industrial Economics and Technology Management

NTNU
Norwegian University of Science and Technology

Technical University of Berlin
Faculty VII (School of Economics and Management)
Workgroup for Infrastructure Policy

Norwegian University of Science and Technology
Department of Industrial Economics and
Technology Management

Master's Thesis

Zonal Level Disruption Response Considering Transmission Line Outage from Large-Scale Offshore Wind Farms

Author:

Nithish Kini Ullal

(458480) - ullal@campus.tu-berlin.de

(520122) - nithish.k.ullal@ntnu.no

Supervisors:

Prof. Dr. Ruud Egging-Bratseth	(NTNU)
Prof. Dr. Christian von Hirschhausen	(TU Berlin)
Jan Voet	(50hertz Transmission GmbH)
Christoph Weyhing	(TU Berlin)
Felix Jakob Fliegner	(50hertz Transmission GmbH)

Trondheim & Berlin,

Thursday 29th September, 2022

Statutory Declaration

I hereby declare that I have produced the present work independently and self-reliant, without unauthorized assistance from others, and only by using the listed sources and aids. This work solely represents my view on the matter and allows no implication on strategic or other positioning of the affiliated supervising parties and institutions. I declare no conflict of interest other than my praise for the open-source tool chain utilized in this project.

Thursday 29th September, 2022

Nithish Kini Ullal

Preface

This master thesis concludes the dual master programme *Sustainable Energy Systems and Markets (SESAM)* and *Industrial Engineering*. The dual degree programme is the result of a cooperation between Norges teknisk-naturvitenskapelige universitet (NTNU) and Technische Universität Berlin (TU Berlin). This thesis was written in cooperation with 50Hertz Transmission GmbH.

First of all, I would like to thank all my supervisors from NTNU and TU Berlin for their support throughout the thesis.

I also take this opportunity to thank Prof. Ruud Egging-Bratseth for being a constant believer in my abilities since the first semester at NTNU. I am grateful for all the valuable insights which helped me throughout the thesis.

Special thanks to Jan Voet and Felix Jakob Fliegner for providing me the opportunity to formulate my thesis at 50Hertz Transmission GmbH. I appreciate all the inputs you provided in shaping the research question and continued support throughout the period of the thesis.

Last but not the least, thanks to the NTNU Solstorm cluster, for letting me use your computational capacity. It would have been impossible to compile the results if it were not for the high-performance cluster.

Thursday 29th September, 2022

Berlin & Trondheim

Abstract

Due to its drastically reducing costs and enormous potential in Europe, energy from offshore wind will be pivotal in realizing Europe's decarbonization targets. High Voltage Direct Current (HVDC) technology and different connection topologies are proposed for the transmission of electricity from offshore wind farms to transport vast amounts of electricity to the shore. We determine that, regardless of the topology, the power required to be transmitted by individual transmission links will rapidly increase. In such a case, it is critical to understand the impact of sudden outages of offshore transmission lines, whether the onshore system can cope with them, or whether additional investments are required to address such issues. We analyze the impact of sudden disruptions of power supply from large-scale offshore wind farms located near each other where there is a possibility of interconnecting them, leading to the creation of hubs for the provision of quick balancing energy. Further, we try to answer the question, "In an electricity system with high renewable penetration and dependency on high-capacity offshore transmission lines, what are the cost-optimal investment and system operation decisions to ensure system stability in case of outages of these transmission assets? We find that no additional investments were required to the existing onshore system to handle sudden power loss greater than 3 Gigawatt (GW) caused due to the failure of power supply from large offshore wind farm clusters. Redispatch of power from gas-based power plants, lithium-ion batteries, and pumped hydro capacities was cost-optimal to deal with outage events of low probability.

Abstrakt

På grunn av de drastisk reduserende kostnadene og det enorme potensialet i Europa, vil energi fra havvind være sentralt for å realisere Europas avkarboniseringsmål. High Voltage Direct Current (HVDC)-teknologi og forskjellige tilkoblingstopologier er foreslått for overføring av elektrisitet fra havvindparker for å transportere enorme mengder elektrisitet til land. Vi fastslår at, uavhengig av topologi, vil kraften som kreves for å overføres av individuelle overføringslinker raskt øke. I et slikt tilfelle er det avgjørende å forstå virkningen av plutselige utfall av offshore overføringslinjer, om landsystemet kan takle dem, eller om det er nødvendig med ytterligere investeringer for å løse slike problemer. Vi analyserer virkningen av plutselige avbrudd i strømforsyningen fra store havvindparker som ligger i nærheten av hverandre der det er mulighet for å koble dem sammen, noe som fører til opprettelsen av knutepunkter for levering av rask balanseringsenergi. Videre prøver vi å svare på spørsmålet: "I et elektrisitetssystem med høy fornybar penetrasjon og avhengighet av høykapasitets offshore overføringslinjer, hva er de kostnadsoptimale investerings- og systemdriftsbeslutningene for å sikre systemstabilitet i tilfelle avbrudd i disse overføringene eiendeler? Vi finner at det ikke var nødvendig med ytterligere investeringer til det eksisterende landbaserte systemet for å håndtere plutselige krafttap større enn 3 Gigawatt (GW) forårsaket på grunn av svikt i strømforsyningen fra store havvindparkklynger. Videresending av kraft fra gassbaserte kraftverk, litium-ion-batterier og pumpet vannkraft var kostnadsoptimalt for å håndtere utfallshendelser med lav sannsynlighet.

Summary

To combat global warming, a sustainable reduction of Carbon Dioxide (CO_2) emissions is crucial in the fossil fuel-dependent global economic system. Increased use of renewable energy sources in the power system can help decarbonize electricity production, significantly reducing CO_2 emissions. Due to its drastically reducing costs and enormous potential in Europe, energy from offshore wind will be pivotal in realizing Europe's decarbonization targets. However, the transmission of electricity from remote offshore locations to the load centers presents one of the biggest challenges to realizing the vast potential. HVDC technology and different connection topologies are proposed to transmit electricity from offshore wind farms to transport vast amounts of electricity to the shore. We determine that, regardless of the topology, the power required to be transmitted by individual transmission links will rapidly increase. In such a case, it is critical to understand the impact of sudden outages of offshore transmission lines, whether the onshore system can cope with them, or whether additional investments are required to address such issues.

Power transmission through sea-based HVDC interconnectors is similar to power transmission from large offshore wind farms as both are in the sea environment. Hence, investigating the causes and likelihood of failures related to sea-based HVDC interconnectors gives us an idea about offshore power transmission's reliability. We identify that the faults arising in the converters and physical disruptions of the offshore transmission line can cause sudden loss of power transmission capacity. However, a sudden loss of capacity up to 3 GW can be handled by the European Frequency Containment Reserve (FCR). Hence, in this thesis, we analyze disruptions in offshore transmission causing a power loss greater than 3 GW. The setting is in 2030, when there is a likelihood of such significant outages in transmission lines of offshore wind farms because of the increase in power capacity of the offshore wind farms. Further, we identify the following options that can potentially help the system during such power losses.

- Battery storage systems.
- Increased interconnection between market zones.
- Vehicle to Grid (V2G) services from battery electric vehicles.
- Installation of additional natural gas based balancing power plants.
- Installation of parallel transmission lines from offshore wind farms.

We develop a three-stage stochastic model which aims to assess optimal investments in generation, transmission, and storage systems to counter high-capacity transmission disruptions. The model consists of one investment period, followed by the Day Ahead (DA) market opti-

mization for different seasons or time periods, and finally, the redispatch in the Intraday (ID) markets. By using temporal aggregation we consider representative hours for different seasons along with two additional extreme load (peak) seasons in a year instead of all 8760 hours. Using open-source offshore wind farms data, we identify offshore wind farms which will be commissioned by the year 2030 and manually cluster them into hubs. Initially, we run the model in a deterministic setting without introducing any outages of transmission lines in the system at different gas and CO_2 prices. We do so to obtain the following information about the system:

- Identify how the selected wind farm hubs interconnect *at lowest cost*.
- Determine the connection capacities of the offshore transmission lines from the hubs to the shore.
- To find the hours when offshore transmission lines carry maximum power.

Using this information from the deterministic analysis, we perform a stochastic analysis in which we introduce outages in specific transmission lines for specific hours of operation. We examine the stochastic results to determine if the system can manage transmission outages well, or if further investments are needed. Further, we identify a base case and conduct a sensitivity analysis, in which we vary the fixed investment costs for the parallel transmission link, followed by a sensitivity analysis on the probability of outages. In each sensitivity analysis, we compare the investments and disruption responses with identified base case and look for a potential investment in a parallel line.

Based on our analysis, we find that CO_2 and gas prices are negatively correlated to the curtailment of offshore wind in a system with high offshore wind penetration. Increasing CO_2 price pushed CO_2 intensive plants out of the merit order and increased production from gas-based power plants instead. Increasing gas prices caused a slight decrease in export from market zones, causing the installation of gas power plants in import-dependent market zones. No additional investments were required to the existing onshore system to handle sudden power loss greater than 3 GW caused due to the failure of power supply from large offshore wind farm clusters. Redispatch of power from gas-based power plants, lithium-ion batteries, and pumped hydro capacities was cost-optimal to deal with outage events of low probability. Increased interconnection between market zones provides sufficient flexibility in the system by allowing access to system-wide redispatch options. Increasing the outage probability and decreasing the fixed investment cost to construct a parallel line connecting the offshore wind farm to the shore caused the model to invest in a parallel line.

Sammendrag

For å bekjempe global oppvarming er en bærekraftig reduksjon av karbondioksid (CO2)-utslipp avgjørende i det fossile brenselavhengige globale økonomiske systemet. Økt bruk av fornybare energikilder i kraftsystemet kan bidra til å dekarbonisere elektrisitetsproduksjonen, og redusere CO_2-utslippene betydelig. På grunn av de drastisk reduserende kostnadene og det enorme potensialet i Europa, vil energi fra havvind være sentralt for å realisere Europas avkarboniseringsmål. Imidlertid utgjør overføring av elektrisitet fra avsidesliggende offshore-lokasjoner til lastesentrene en av de største utfordringene for å realisere det enorme potensialet. HVDC-teknologi og forskjellige tilkoblingstopologier er foreslått for å overføre elektrisitet fra havvindparker for å transportere enorme mengder elektrisitet til land. Vi fastslår at, uavhengig av topologi, vil kraften som kreves for å overføres av individuelle overføringslinker raskt øke. I et slikt tilfelle er det avgjørende å forstå virkningen av plutselige utfall av offshore overføringslinjer, om landsystemet kan takle dem, eller om det er nødvendig med ytterligere investeringer for å løse slike problemer.

Kraftoverføring gjennom sjøbaserte HVDC-forbindelser ligner på kraftoverføring fra store havvindparker ettersom begge er i havmiljøet. Å undersøke årsakene til og sannsynligheten for feil relatert til sjøbaserte HVDC-forbindelser gir oss derfor en idé om offshore kraftoverførings pålitelighet. Vi identifiserer at feil som oppstår i omformere og fysiske forstyrrelser i offshore overføringslinjen kan forårsake plutselig tap av kraftoverføringskapasitet. Imidlertid kan et plutselig tap av kapasitet opp til 3 GW håndteres av European Frequency Containment Reserve (FCR). Derfor analyserer vi i denne oppgaven forstyrrelser i offshore overføring som forårsaker et effekttap større enn 3 GW. Innstillingen er i 2030, da det er sannsynlighet for slike betydelige utfall i overføringslinjene til havvindparker på grunn av økningen i kraftkapasiteten til havvindparkene. Videre identifiserer vi følgende alternativer som potensielt kan hjelpe systemet under slike strømtap.

- Batterilagringssystemer.
- Økt sammenkobling mellom markedssoner.
- V2G tjenester fra batteridrevne elektriske kjøretøy.
- Installasjon av ytterligere naturgassbaserte balansekraftverk.
- Installasjon av parallelle overføringslinjer fra havvindparker.

Vi utvikler en tre-trinns stokastisk modell som tar sikte på å vurdere optimale investeringer i generasjons-, overførings- og lagringssystemer for å motvirke overføringsforstyrrelser med høy kapasitet. Modellen består av én investeringsperiode, etterfulgt av DA markedsoptimaliser-

ing for ulike sesonger eller tidsperioder, og til slutt redispatsjen i ID-markedene. Ved å bruke tidsmessig aggregering vurderer vi representative timer for forskjellige årstider sammen med to ekstra ekstrembelastnings- (høytids) sesonger i løpet av et år i stedet for alle 8760 timer. Ved å bruke åpen kildekode offshore vindparkdata identifiserer vi havvindparker som skal settes i drift innen år 2030, og grupperer dem manuelt i knutepunkter. I første omgang kjører vi modellen i en deterministisk setting uten å introdusere utfall av overføringslinjer i systemet til forskjellige gass- og CO_2-priser. Vi gjør det for å få følgende informasjon om systemet:

- Identifiser hvordan de valgte vindparkknutepunktene kobler sammen *til lavest kostnad*.
- Bestem tilkoblingskapasiteten til offshore overføringslinjene fra navene til land.
- For å finne timene når offshore overføringslinjer har maksimal effekt.

Ved å bruke denne informasjonen fra den deterministiske analysen utfører vi en stokastisk analyse der vi introduserer strømbrudd i spesifikke overføringslinjer for spesifikke driftstimer. Vi undersøker de stokastiske resultatene for å finne ut om systemet kan håndtere overføringsavbrudd godt, eller om det er behov for ytterligere investeringer. Videre identifiserer vi et basistilfelle og gjennomfører en sensitivitetsanalyse, der vi varierer de faste investeringskostnadene for den parallelle overføringsforbindelsen, etterfulgt av en sensitivitetsanalyse på sannsynligheten for utfall. I hver sensitivitetsanalyse, vi sammenligner investeringene og avbruddsreaksjonene med identifiserte base case og ser etter en potensiell investering i en parallell linje.

Basert på vår analyse finner vi at CO_2- og gasspriser er negativt korrelert til innskrenkning av havvind i et system med høy havvindpenetrasjon. Økende CO_2-pris presset CO_2-intensive anlegg ut av merittordren og økte produksjonen fra gassbaserte kraftverk i stedet. Økende gasspriser førte til en liten nedgang i eksporten fra markedssoner, noe som førte til installasjon av gasskraftverk i importavhengige markedssoner. Det var ikke nødvendig med ytterligere investeringer til det eksisterende landbaserte systemet for å håndtere plutselige strømtap større enn 3 GW forårsaket av svikt i strømforsyningen fra store havvindparkklynger. Videresending av kraft fra gassbaserte kraftverk, litium-ion-batterier og pumpet vannkraft var kostnadsoptimalt for å håndtere utfallshendelser med lav sannsynlighet. Økt sammenkobling mellom markedssoner gir tilstrekkelig fleksibilitet i systemet ved å gi tilgang til systemomfattende videresendingsalternativer. Økning av utfallssannsynligheten og reduksjon av den faste investeringskostnaden for å bygge en parallell linje som forbinder havvindparken til land førte til at modellen investerte i en parallell linje.

Contents

List of Figures

List of Tables

Acronyms

AC	Alternating Current
BEV	Battery Electric Vehicle
CAPEX	Capital Expenditure
CCGT	Closed Cycle Gas Turbine
CGS	Combined Grid Solution
CO_2	Carbon Dioxide
COP	Conference of Parties
DA	Day Ahead
DC	Direct Current
DE	Distributed Energy
EEZ	Exclusive Economic Zone
EMPIRE	European Model for Power System Investment with (high shares of) Renewable Energy
ENTSO-E	European Network of Transmission System Operators for Electricity
EU	European Union
FCR	Frequency Containment Reserve
FRR	Frequency Restoration Reserve
GB	Great Britain
GHG	Greenhouse Gas
GIS	Geographic Information System
Gt	Gigatonnes
GW	Gigawatt
H_2	Hydrogen
HFGT	Hydrogen Fired Gas Turbine
HVAC	High Voltage Alternating Current
HVDC	High Voltage Direct Current
IC	Interconnector
ID	Intraday
IEA	International Energy Agency
kV	Kilovolts

LCOE	Levelized Cost of Energy Generation
MW	Megawatt
nmi	Nautical Miles
NSEC	North Sea Energy Cooperation
NTC	Net Transfer Capacity
OWF	Offshore Wind Farm
PH	Pumped Hydro
PtX	Power to X
PV	Photovoltaic
RES	Renewable Energy Sources
SoC	State of Charge
TSO	Transmission System Operator
TWh	Terawatt hours
UK	United Kingdom
V2G	Vehicle to Grid
VoLL	Value of Lost Load
VRE	Variable Renewable Energy

1 Introduction

CO_2 emissions from various human activities such as burning fossil fuels cause an increase in the concentration of CO_2 in the atmosphere. The accumulated CO_2 traps infrared radiation through the greenhouse effect, responsible for increasing the average global temperature, commonly referred to as global warming. Adverse effects of global warming include droughts, severe weather patterns, glacier ice melting, and wildfires, all of which impact global ecosystems (Anderson et al., 2016). As a recent example, widespread wildfires ravaged parts of California and the Mediterranean region in the summer of 2021, damaging wildlife, vegetation, and residential properties. That same summer, unexpectedly heavy rainfall in Germany and Belgium led to floods claiming the lives of many residents in the low-lying areas. Even though these specific events cannot be proven to be caused by global warming alone, they illustrate the type of consequences global warming can have and raise a topic for debate and further research. Since global warming will have far-reaching consequences in the years to come, action against it is imperative today.

In order to combat global warming, a sustainable reduction of CO_2 emissions is crucial in the fossil fuel-dependent global economic system. This process is referred to as decarbonization. It is one of the imminent challenges the world will face in the years to come. On a global level, various efforts toward reducing global warming are currently underway. The Paris Climate Agreement at the Conference of Parties (COP) 21 outlines a commitment by 196 countries worldwide to limit global warming to well below 2 °C and preferably to 1.5 °C in comparison with levels in 1990 (IPCC, 2022). Through its *Green Deal*, the European Union (EU) aims to be climate neutral by 2050. Further, the EU introduced its *Fit for 55 package* to reduce CO_2 emissions by 55% compared to 1990 levels by 2030 (IEA, 2021c). Internationally coordinated efforts such as those mentioned and individual efforts from countries globally are essential to tackle the challenge of rapid decarbonization.

The first step toward reducing CO_2 emissions is identifying the anthropogenic activities contributing to it. When examining the sources, the usage of fossil fuels to generate electricity, transportation, and industry stand out as the primary causes (Amaral et al., 2019). According IEA (2021a), global CO_2 emissions from fossil fuel combustion and industrial processes stood at 36.3 Gigatonnes (Gt) in 2021, which is approximately 89% of the total anthropogenic Greenhouse Gas (GHG) emissions (40.9 Gt CO_2 equivalent). Major industrial processes such as the manufacturing of fertilizer, cement, and steel are highly energy- and carbon-intensive as they depend on the heat produced from combusting CO_2-intensive coal. Currently, emissions related to coal usage account for 42% of the energy-related CO_2 emissions, with oil (30%) and

natural gas (20%) usage being other significant sources (IEA, 2021a).

To limit global warming below 1.5℃, in 2018 Hausfather (2018) has estimated a remaining global anthropogenic carbon budget of around 416 Gt CO_2. This budget was projected to be used by the end of the current decade based on CO_2 emission rates in 2018. With the current rate of CO_2 emissions and the expected rise in energy consumption, the global temperature rise would surpass the 1.5℃ mark even sooner (EIA, 2021). According to UNEP (2011), decoupling resource use from economic growth is essential to realizing the goal of decarbonization. One of the most fundamental resources of the modern economy, energy is a resource common to most carbon-intensive sectors thanks to its utility and versatility. Hence, it is evident that decarbonizing the energy sector will significantly limit global temperature rise.

1.1 Decarbonization through Electricity from Renewable Energy Sources

The choice of energy carrier plays an essential role in decarbonizing the energy system (Elia Group, 2021). Electricity is an energy carrier of high quality due to its ease of conversion to other forms of energy with high efficiencies. Hence, electricity is a suitable energy carrier to satisfy direct and indirect energy demands. Globally, from 2010 to 2020, the electricity demand rose by 25%. In order to reach the net-zero emissions target of 2050, electricity demand must rise by more than 30% of what it is today by 2030 (IEA, 2021c). Elia Group (2021) suggests that a direct electrification approach will lead to a 75% increase in the European total electricity demand by 2050 (5600 Terawatt hours (TWh)) compared to 2018 (3200 TWh). This increased future demand for electricity will require higher electricity production from clean energy sources to avoid further CO_2 emissions. In sectors where electricity cannot contribute directly, producing alternate energy carriers like hydrogen, e-gas, and e-fuels by utilizing the ease of conversion of electricity may play a crucial role in decarbonization.

Focusing on electricity generation sources, currently, renewables produce less than 30% of the world's electricity, a low figure compared to the requirement that renewable sources generate 88% of power to achieve net-zero emissions by 2050 (IEA, 2021c). The International Energy Agency (IEA) stresses the need to rapidly incorporate renewable energy technologies such as wind and solar Photovoltaic (PV) in the national energy mix, which are expected to produce the lion's share (68%) of renewable electricity globally. The current rate of renewable expansion in Europe has been deemed insufficient, and it will require a tripling of the current rate to meet the objectives of the Green Deal (Elia Group, 2021). In addition to incorporating renewables in the energy system, continued efforts from nations to decommission existing fossil-based power generators are required. Several European countries have instituted phase-out plans for coal-based power plants. Austria, Belgium, Portugal, and Sweden have decommissioned all

domestic coal-based power plants (Europe Beyond Coal, 2021a; Europe Beyond Coal, 2020; Europe Beyond Coal, 2021b)). In 2020, Germany passed legislation mandating all coal-based power plants to be decommissioned by 2038 (Brauers et al., 2020). With the reduction in generation capacity due to decommissioning existing fossil-based capacity and the need to satisfy greater electricity demand, the onus is now on solar PV and wind to deliver more energy.

1.1.1 Offshore Wind Energy

Energy production from offshore wind turbines is steadily gaining importance globally. Compared to the global operational capacity in 2010, the current operational capacity has grown thirteen-fold (IEA, 2021b). At the end of 2021, the global offshore wind capacity stood at 57.2 GW, with over 36% (21.1 GW) of this capacity was connected to the shore in 2021 (GWEC, 2022). One of the primary reasons for its adoption worldwide is its decreasing Levelized Cost of Energy Generation (LCOE). According to Fraunhofer ISE (2021), the LCOE of offshore wind currently varies between 7.2-12.1 €¢/kWh and is expected to fall to 5.4-7.9 €¢/kWh by 2040. Despite its slightly higher costs compared to utility-scale solar PV (4.0-5.0 €¢/kWh) and onshore wind (4.0-8.3 €¢/kWh), offshore wind has advantages that may make it a viable option from a societal and energy system perspective. These advantages include higher wind speeds, more full load hours, greater availability of project area, and increased distance from human settlements that might be affected by visual and noise-based externalities (Bilgili et al., 2011). Owing to these advantages, the IEA (2021b) expects offshore wind to play a massive role in decarbonizing the energy system, requiring nearly $1 trillion investment over the next two decades.

With the advantages mentioned above in mind, the EU aims to increase its offshore wind capacity in the range of 240-450 GW (an eight-to-fifteen-fold increase compared to the 2020 level of 30 GW) (European Union, 2020). Wind Europe (2019) presents a possible allocation of 450 GW offshore-wind capacity in four different offshore locations: around 212 GW in the North Sea (consists of the area between the west coast of Norway and the east coast of Britain), 85 GW in the European Atlantic (consists of Celtic Seas, Bay of Biscay and Iberian Coast), 83 GW in the Baltic Sea (including The Gulf of Bothnia), and 70 GW in the southern European waters (consists of the eastern and the western Mediterranean Sea). As a large chunk of the offshore wind potential in Europe is in deeper sea waters, advancement in floating offshore wind technology will be pivotal in realizing the potential identified by Wind Europe in the European waters. Many floating offshore wind demonstration projects are being carried out in Europe, signaling a positive technological development.

1.1.2 Challenges in Deploying Offshore Wind

Over the next three decades, deploying up to 450 GW offshore wind in Europe will be challenging. The crucial challenges that must be overcome are listed below (Wind Europe, 2019):

Intermittency and Spatial disparity

Like all weather-dependent renewable energy sources, wind generation is intermittent. Another general challenge of offshore wind is its spatial disparity with existing load centers.

Connections to shore

The locations of some offshore wind farms being explored extend further from the coast in deeper waters. As the distance from the shore and water depth increases, the cost and technical complexity of installing cables and converter stations also increase.

Strengthening the onshore grid

Onshore grid upgrades are required to use the electricity generated from offshore wind farms. Additional transmission lines and transformers to withstand the increased influx of electricity, especially where the offshore HVDC lines have their landfall, will be essential to maintain the stability of the electrical system.

Attracting investments in offshore wind

Offshore wind farms are Capital Expenditure (CAPEX) intensive. Large-scale investments are crucial to developing the targeted capacities. It is expected that offshore wind farms will see a threefold increase in their CAPEX by 2025. Attracting developers to invest in offshore wind farms through government policies is one of the essential steps to achieving offshore wind targets.

Developing supply chains

Supply chains play a vital role in the large-scale deployment of any technology. Considering high volumes of offshore wind capacity deployment in the future, every constituent of the offshore supply chain, from the production of the turbines to the carrier vessels required to install the wind turbines offshore, needs significant ramp-up.

Marine spatial planning to allow multiple uses of maritime space

The marine space is rich with natural resources, attracting interest from several stakeholders. Activities such as energy production, industrial fishing, and maritime transport require the use of marine space. Intricate planning to allow the coexistence of these activities is essential; in other words, marine spatial planning is vital to allow multiple uses of maritime space.

Reducing impacts on the marine environment

Installing giant wind turbines in the sea may impact the local marine environment. Careful pre-evaluation of the risks of offshore wind development strategies is necessary to take precautionary measures to reduce potential environmental impacts.

Developing storage and Power to X solutions

Developing storage and energy conversion technologies is essential to avoid the curtailment of energy produced from offshore wind farms. Due to operational limitations, surplus energy generated from offshore wind farms that cannot be used offshore or transported onshore can be stored as Hydrogen (H_2) using Power to X (PtX). These molecules can be used as raw materials for specific industrial processes or converted into electricity if needed.

One of the primary challenges presented here is connecting offshore wind farms to the shore while ensuring system stability onshore is the main topic of the thesis. In this setting, relevant technical challenges include the choice of connection topology and technology, protection, operation, and maintenance of the connections, and reducing the environmental impact of marine space usage (Perveen et al., 2014).

1.2 Connection Topologies for Offshore Wind Projects

A country's Exclusive Economic Zone (EEZ) extends from the shore up to 200 Nautical Miles (nmi). Within this zone, the country owns the seafloor and is permitted to access the natural resources in the area. The EEZs of different European countries possessing a coastline are shown in Figure 1.

The EU mandates each member state to develop a marine spatial plan that includes identifying offshore wind development regions within their EEZ. The member states identify suitable locations for the deployment of offshore wind and create designated wind energy zones. These zones are then leased to developers to build offshore wind farms through appropriate auction mechanisms. This allocation may result in multiple offshore wind farms planned in the vicinity of each other. In addition to the planned offshore wind zones, several sea-based HVDC Interconnector (IC) exists between the countries that transport electricity. The presence of multiple offshore wind regions in different EEZs and ICs gives rise to multiple possibilities of offshore wind connection topologies (c.f., Figure 2 (Gephart et al., 2020; Hannah et al., 2020).)

1.2.1 Radial Connection

Radial connections are the simplest among the topologies of offshore wind connections. Offshore wind farms in an EEZ can be connected directly to the shore by employing appropriate transmission technology. Depending on the agreement between countries, it is possible to

connect offshore wind farms located in one country's EEZ with the shorelines of another.

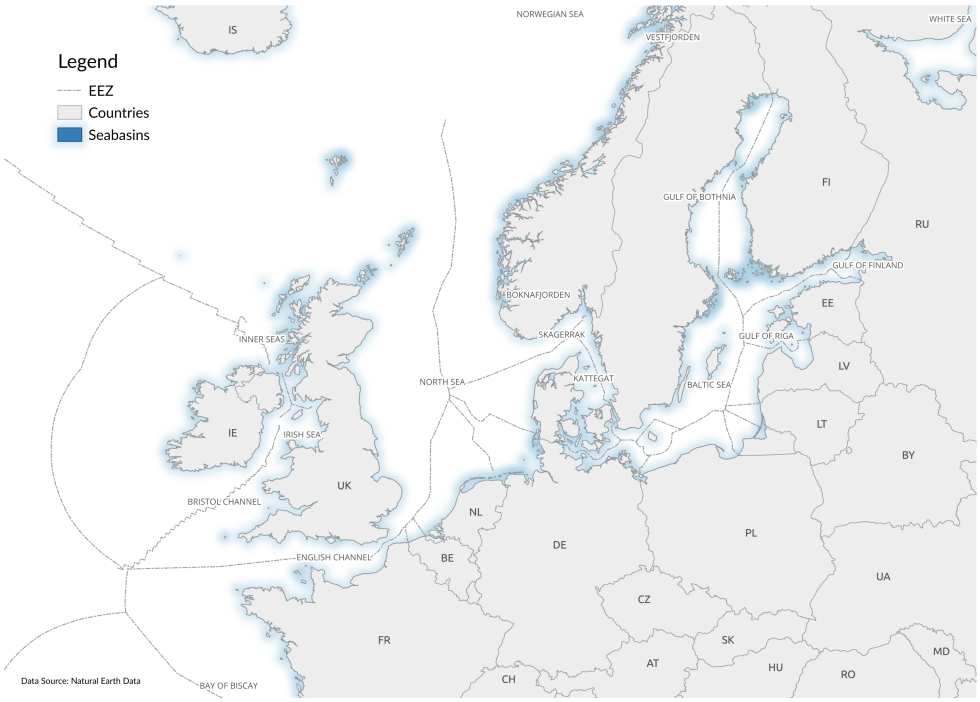

Figure 1: European Exclusive Economic Zones, Source: Own illustration based on the data from Natural Earth Dataset

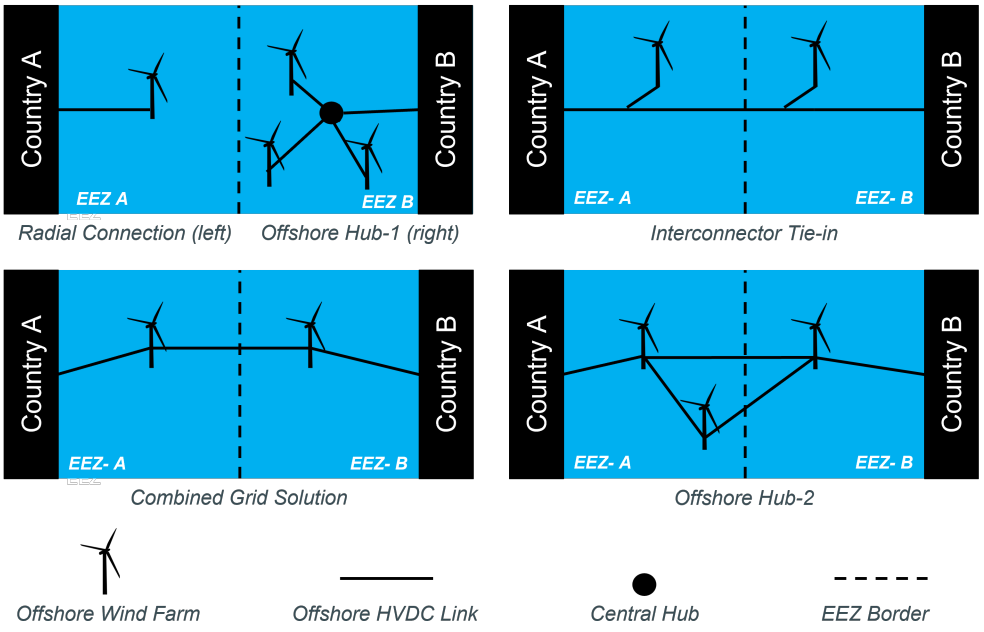

Figure 2: Offshore wind farms connection topologies, Own illustration based on Gephart et al. (2020) and Hannah et al. (2020)

1.2.2 Interconnector Tie-in

Owing to the unequal potential of renewable resources all over Europe, optimal electricity use is possible by developing interconnections between countries. ICs are transmission links that connect the electricity system of two countries and are either land-based or sea-based. ICs

allow the trading of surplus electricity from one country to another resulting in increased social welfare. Subsequently, interconnections increase the reliability of the electricity system. The Elia Group (2021) study stresses the need for increased interconnection among European countries to cope with the increased electricity demand and shield against the location-based intermittency of renewable sources.

Sea-based HVDC ICs between countries are the preferred solutions in multiple European projects. Projects such as NorNed connecting Norway and Netherland, BritNed connecting the United Kingdom (UK) to the Netherland, and the North Sea Link connecting Norway to the UK are prominent examples. The concept of IC tie-in for offshore wind farms is connecting the wind farms to the sea-based ICs instead of connecting them separately to the shore. This arrangement provides the double benefit of transfer of electricity from offshore wind farms and the opportunity to trade surplus electricity between the countries.

1.2.3 Combined Grid Solution

Two radially connected offshore wind farms in different EEZs are mutually connected through the Combined Grid Solution (CGS) solution, creating a link between both countries. This solution also enables the radial links to serve as ICs between the countries. In 2020, the German transmission system operator 50Hertz and their Danish counterparts from Energinet developed the world's first CGS solution in the Baltic Sea. The Kriegers Flak CGS solution connects the German Baltic-1 & Baltic-2 wind farms to the Danish Kriegers Flak wind farm through two cables with a transmission capacity of 400MW (50Hertz Transmission GmbH, 2020).

1.2.4 Offshore Hub

Offshore hubs are relatively more complex compared to the other topologies. Multiple offshore wind farms in the vicinity of each other are interconnected, allowing the power to be pooled and transmitted to the shore rather than directly connecting each offshore wind farm to the shore. Two possible ways of realizing a hub setup include: one where a central hub collects power from multiple offshore wind farms and transmits the power to the shore (see Figure 2, Offshore Hub-1), and the other way is to interconnect offshore wind farms with each other forming a ring-like structure and then building connections to the shore as required (see Figure 2, Offshore Hub-2). The former arrangement is an example of an energy island setup, whereas the latter is used where creating a central hub is difficult due to greater water depths in far offshore regions. Globally, offshore hub projects are yet to be realized and face significant challenges. Additionally, the development of numerous hubs all over European marine space will provide an opportunity to interconnect several hubs leading to the development of a meshed offshore grid interconnecting several European countries by 2050 (Hannah et al., 2020).

1.3 Transmission Technology

Transmission of offshore wind energy to load centers will be crucial based on the above explanation. Irrespective of the connection topology, the technology that facilitates bulk electricity transmission over long distances is fundamental. High Voltage Alternating Current (HVAC) has been the dominant technology for land-based transmission from an early period, but its shortcomings in transmitting electricity over long distances make it inefficient for sub-sea power transmission. HVDC technology has witnessed tremendous development and continuous adoption in several projects globally. Some of the advantages of HVDC compared to HVAC are (Ryndzionek and Sienkiewicz, 2020):

- Reduced transmission losses.
- Absence of the skin effect.
- Increased active power control.
- Cheaper cables due to less complex manufacturing methods.

Considering these benefits, multiple offshore wind farms have used HVDC technology to connect radially to the shore. BorWin-1 (400 Megawatt (MW)) was the first offshore wind farm to use the HVDC technology as early as 2009, and since then, multiple projects, including SylWin-1 (864MW), Nordsee Ost (422MW), and BorWin-2 & 3 (800MW, 690MW) have been realized (TenneT Holding B.V., 2020). Even though the highest capacity of current HVDC projects is around the 2 GW mark, it is apparent that this will rise with the foreseen higher penetration of offshore wind in the energy mix and the increasing size of individual wind farms.

1.3.1 HVDC Transmission Value Chain

An overview of the process and steps involved in the transmission of power from an offshore wind farm using HVDC transmission technology is provided in Figure 3. Multiple transmission

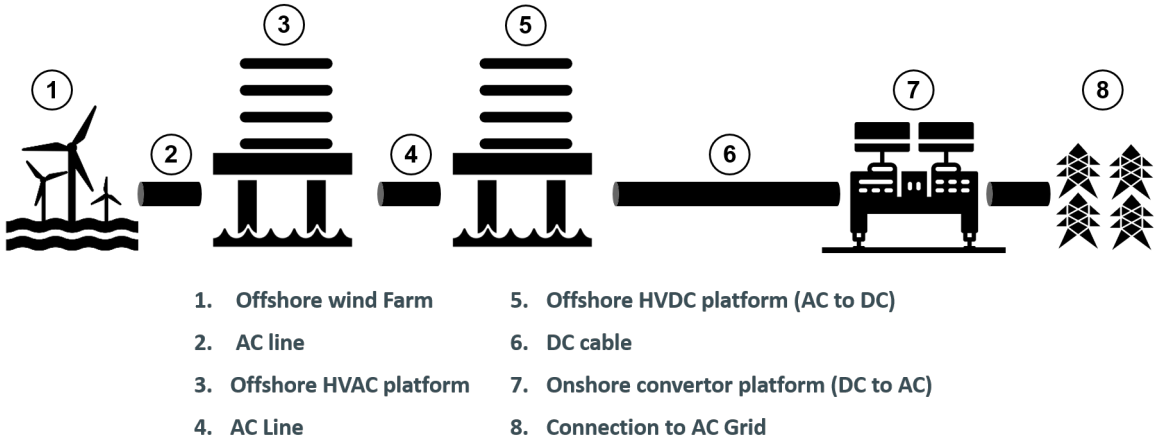

Figure 3: HVDC Transmission Technology, Own illustration

arrangements are possible based on operational needs, connection topology, and distance from the shore, but the fundamental operation is explained based on the setting shown above. Electric power from individual wind turbines is transported to an HVDC offshore platform equipped with transformers through Alternating Current (AC) cables. The platform collects the electric power from all connected wind turbines and steps up the voltage from 33/66 Kilovolts (kV) AC to 150-320kV AC (Ryndzionek and Sienkiewicz, 2020). HVAC lines further transmit the power to an HVDC offshore platform where HVAC power is converted to HVDC through converters. Different variety of converters are in use depending on the application. However, the primary function is the conversion of AC source voltage to Direct Current (DC). The DC cables enable the transmission of the converted HVDC power over long distances. On the other end of the cable, onshore converter platforms capable of converting HVDC to AC voltage are present. This step is essential to feed the power to the onshore AC grid.

1.4 Ancillary Services

Balancing demand and supply during real-time operation is critical to ensuring consistent power supply throughout the energy system; otherwise, variations in operating frequency, voltage, and current occur, harming the electricity grid. Because the Transmission System Operator (TSO) is responsible for the safe and secure operation of the electric grid, they use ancillary services to prevent any harm to the grid. Figure 4 gives an overview of the classification of ancillary services.

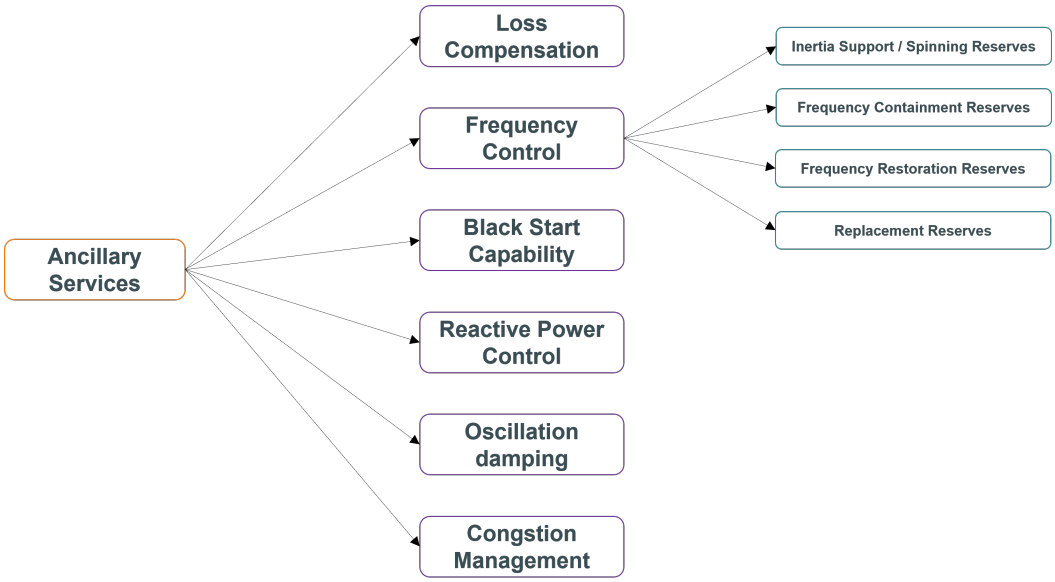

Figure 4: Classification of ancillary services, Source: Own illustration

We see that frequency variations occur due to unforeseen events such as power plant outages, transmission capacity loss, or sudden electric demand increases. In such cases, spinning

reserves act first to control the frequency variation. However, providing quick balancing energy is of utmost importance if the imbalance is significant and the spinning reserves are insufficient. The provision of balancing energy necessitates activation of balancing services which the TSO has to procure in the balancing markets.

1.5 Connecting the Dots

Based on the explanations provided, it is conclusive that the integration of large offshore wind capacities will contribute immensely toward realizing Europe's climate goals. The choice of connection topology and technology will significantly impact the realization of 450 GW offshore wind capacity in Europe. The realization of such high capacities may increase reliance on offshore wind farms to satisfy a more significant proportion of electricity demand in the future. Sudden disruptions of the transmission link that transports large quantities of power from offshore wind farms to the shore will disrupt the system if such events are not analyzed prior. In this context, this thesis analyses the impact of sudden disruptions of power supply from large-scale offshore wind farms located near each other where there is a possibility of interconnecting them, leading to the creation of hubs for the provision of quick balancing energy. The next chapter will provide further insight into the operation of balancing markets, followed by the findings on outages and limitations of HVDC transmission, which is the preferred transmission technology for future offshore wind farms.

2 Literature Review

The chapter reviews some of the essential topics in energy system planning in the academic literature. The insights from these topics highlight the necessity to address the sudden failure of the future high-capacity HVDC transmission system. To this end, we review past and recent publications that assess transmission system failures, potential solutions, and the modeling approach to address the problem. At the end of this chapter, Table 1 and Table 2 provide an overview of literature reviewed and main findings relevant for this thesis.

2.1 Electricity Markets

Electricity market operation is broadly classified into three distinct constituents based on the operation timeline: forward markets, spot markets, and balancing markets. Figure 5 shows a timeline of operation of these markets. The forward and the spot markets are financial markets with financial obligations, whereas the balancing market involves a physical balance of demand and supply in the transmission grid. The spot market is further classified into DA markets and ID markets.

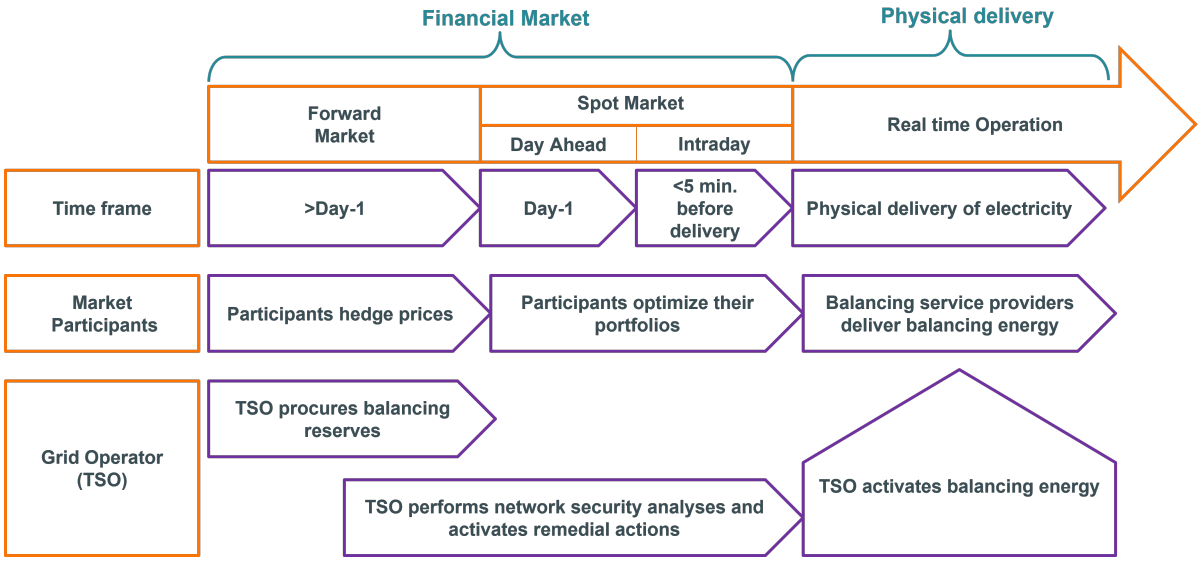

Figure 5: Overview of electricity markets, Source: Own illustration based on TenneT Holding B.V. (2021)

2.1.1 Forward Markets

By participating in the forward market, large industrial power consumers and generators, suppliers, or traders often need to balance their portfolios before the actual power delivery. A forward market consists of direct bilateral contracts, also known as Over-The-Counter trading (Zweifel et al., 2017). In forward markets, the participants can sign contracts three to four years before the actual delivery. However, in cross-border trade, the participants can do so only up to a year before the actual delivery. Additionally, it would require explicitly acquiring cross-zonal

transmission rights to facilitate this cross-border trade. The forward markets generally hedge future prices in the electricity market against volatility.

2.1.2 Day Ahead Markets

As the name suggests, DA auction takes place one day before the scheduled delivery. Market participants submit their bids and offer before midday to the exchange. The market operator (like EPEX and NORDPOOL) generates a merit order of all the bids and offers collected. Wholesale prices are determined by the merit order and fluctuate every hour based on the demand-supply balance. Along with the DA prices, the DA market provides a cost-optimal economic dispatch. If a market participant has to deviate from the decided DA dispatch, they may do so by participating in the ID market.

2.1.3 Intraday Market

Buying and selling electricity in the DA market involves decisions made by many market participants who look to maximize their profits. However, as the name suggests, the DA economic dispatch is ex-ante, making the system vulnerable to uncertain future events. To manage the deviations from the DA dispatch, electricity markets such as the ID and the balancing energy markets came into existence. The ID market opens after the DA market is cleared. The ID market allows market participants to correct their positions closer to real-time dispatch of electricity which minimizes their exposure to a penalty for deviating from the DA schedule. Currently, the ID market uses a pay-as-bid pricing model. The gate closure (commencement of physical delivery) time differs in different market areas and if the trade is cross-border. Ocker and Jaenisch (2020) present a comprehensive overview of ID gate closure time across different European markets, which typically vary between 15-60 minutes for cross-border trade and approximately 5 minutes for trade within the market zone.

2.1.4 Balancing Markets and Services

After the closure of the ID markets, the real-time delivery of power commences. During this phase of real-time operation, unplanned changes in demand, the output from Variable Renewable Energy (VRE) sources, or supply disruptions from large power plants can offset the system frequency, which is a crucial indicator that helps the TSO ensure the electric system's safe operation. A sudden increase or decrease of load or supply affects the system frequency, which must be maintained between preset limits (positive or negative deviation of max. 0.2 Hertz from 50 Hertz in the EU) and is the responsibility of the TSO. The TSO makes use of the balancing markets to deal with real-time deviations post-closure of the ID market. The TSO contracts balancing capacity ex-ante (up to one year ahead), and the procured balancing energy is accessed through different balancing services as and when needed. Balancing markets ensure

that the TSO has access to adequate energy to achieve a real-time balance of electricity supply and demand at the lowest cost possible to consumers (van der Veen and Hakvoort, 2016). In addition to being an efficient and transparent tool, balancing markets will play a crucial role in achieving one of the goals of the EU energy policy, of increasing energy security (European Commission, 2019). Additionally, as it is expensive to store large quantities of electricity in grid-scale batteries, balance management becomes crucial for ensuring the real-time balancing of electricity (van der Veen and Hakvoort, 2016). The TSOs are the sole buyers in the balancing markets, whereas other market participants offer various essential balancing services. The European Network of Transmission System Operators for Electricity (ENTSO-E) has developed a common framework to categorize the frequency control services based on their usage and activation time. Figure 6 provides an overview of the different frequency control services.

Within the synchronous area, during the initial fifteen minutes of the occurrence of an incident causing a frequency deviation, the TSOs jointly act to arrest the deviation by activating the European FCR (Poplavskaya et al., 2021). FCR arrests upward or downward frequency deviations and prevents any sudden harm to the system within a synchronous area. In the next fifteen minutes, each TSO has to act upon the area control error in their load frequency control area to restore normalcy in operating frequency. The imbalance netting method calculates the net required power by considering positive and negative imbalances within the control area. The Frequency Restoration Reserve (FRR) reserves will then be activated. For the Continental Europe synchronous area, a total capacity of 3 GW (upwards and downward) is available for activation at any time. If a control area loses 3 GW of generation or demand at any instance of time, the FCR capacity must be able to support the system for 15 minutes, maintaining system stability (ENTSO-e, 2018b). This 3 GW capacity is known as the power deviation of the reference incident, and the TSOs within the synchronous area are obligated to procure this capacity in the balancing market cumulatively. Based on the guidelines provided by the ENTSO-E, each TSO calculates their share of the FCR capacity every year. The calculation is based on the formula developed by all TSOs of Continental Europe synchronous area (ENTSO-e, 2018a).

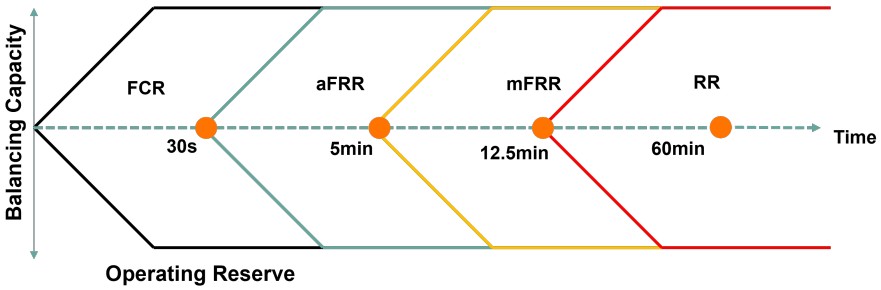

Figure 6: Overview of the timeline of Balancing Services, Source: Own illustration

2.2 HVDC Interconnectors

In addition to being used in the transmission of power from offshore wind farms, as highlighted in Chapter 1, HVDC technology is also widely used as a means of transferring power between market zones through ICs. Increased interconnection between different market zones is essential for efficient electricity use from renewable sources, as it allows for balancing intermittent supply over a larger area. This necessity has prompted the construction of several HVDC interconnections. In Europe, the UK and Sweden are the countries with the highest number of offshore-based HVDC interconnections with other market regions (ENTSO-e, 2021). Moreover, sea-based HVDC ICs through the North, and the Baltic Sea have reached transmission capacities up to 2 GW. The North Sea region alone has twelve transnational HVDC ICs, with sixteen more planned before 2030 (Benjamin et al., 2020). Compared to HVDC lines used for transmitting power from offshore wind farms, IC lines currently have a higher transmission capacity. However, with the expected growth of offshore wind generation capacity, HVDC lines from offshore wind farms will require greater transport capacity. Failure of such large-capacity lines may cause a significant imbalance in the power system. Modifications to the existing European FCR level or adopting alternate solutions to support FCRs are needed to manage such disruptions, and currently, it is unclear how to do this in a cost-optimal manner. Analyzing the causes and likelihood of failures related to HVDC ICs would be beneficial since similar failures can occur during transmission from large offshore wind farms.

2.2.1 HVDC Interconnector Disruptions

The ENTSO-E provides information regarding the failure of ICs in Europe through its transparency platform. The data includes the duration of failure, the loss of NTC between the connected regions, and (often very brief) comments indicating the causes of failure. In addition, ENTSO-E publishes an annual report on the utilization and unavailability statistics of the HVDC ICs in the Nordic and Baltic regions. (ENTSO-e, 2021)

We summarize critical insights about the sea-based HVDC ICs from the report and the data. According to the *HVDC Utilisation and Unavailability Statistics 2020* by ENTSO-e (2021), the combined HVDC interconnection capacity in the Nordic and Baltic regions is approximately 11 GW, which facilitated about 95TWh of electricity transmission in 2020. The amount of transmitted electricity has constantly risen since 2015 (69TWh), which signifies the increasing importance of interconnection between geographical regions. Additionally, based on a review of the outage statistics provided in the report, we note the following insights about sea-based HVDC ICs in the Baltic and the Nordic region:

- Due to the vicinity of HVDC submarine cables to the shipping routes, there is a rela-

tively high chance of cable severance. The anchors from the ships and fishing boats can disrupt transmission, leading to long stretches of IC unavailability. In 2020, the HVDC links between Norway and Denmark Skagerrak-1 and Skagerrak-2 experienced cable faults lasting up to 88 and 123 days, respectively, caused by ship anchors. Similarly, the Netherlands-Denmark COBRA IC was also affected by a cable fault that lasted four months. Cable outages rarely occur, but they have a high impact when they do occur.

- The probability of outage is higher as the length of the transmission line increases, in the case of subsea transmission.
- One of the most common causes of HVDC outages is failures in control, protection, and communication systems at the converter stations. These causes have a lower impact when compared to cable outages, as total transmission capacity may not be lost.
- On average, over the year, around 10% of the maximum energy that could be transmitted, has been unavailable due to planned maintenance and sudden outages causing total or partial transmission unavailability.
- Often, the IC capacity is not fully utilized, either due to onshore grid requirements or not requiring more transmission capacity.
- The utilization of the ICs is highly dependent on the electricity market.
- Performing planned maintenance to ensure the system's safety is standard practice. However, their planned nature does not cause a shock effect on the system's functioning.

The ICs in the North Sea region towards France, Belgium, and the UK are also subjected to similar outages causing a loss of available transmission capacity. However, the newly built NEMO Link IC between Belgium and the UK has performed better than its older counterparts since its commissioning in 2019.

According to the review by Zhou et al. (2022), faults in the onshore AC system can cause a common failure called commutation failure in the HVDC transmission system. Commutation failure causes a sudden increase in DC current and a steep fall in the DC voltage, which leads to a power shortage at the receiving end of a line. The authors also point out that between 2010 and 2019, these events occurred approximately nine times per HVDC system per year in China, posing a significant threat to the power system's safety. Zhu et al. (2019) also gives an in-depth analysis of the severity of the problem and possible methods to limit such failures.

2.3 Potential solutions to deal with high-capacity HVDC disruptions

We are hypothesizing that disruptions similar to those witnessed for HVDC ICs are likely to occur on transmission lines from offshore wind farms, too; we have also identified four potential

options to deal with such high-capacity disruptions.

2.3.1 Battery Storage Systems

Storage systems can play an essential role in bridging supply and demand in an electrical system with a high share of renewables. According to Østergaard (2012), in a 100% renewable energy system, electricity-based storages enable better integration of wind power compared to other heat and biogas-based storage. Properties of batteries, such as swift ramp-up times, easily controllable output, and high efficiency, make them a perfect contender to participate in providing various balancing services. In Germany, for example, amid the ongoing decommissioning of fossil and nuclear-based generation capacities, batteries have stepped up and are now providing primary balancing services (Olk et al., 2019). Further, with a combination of batteries and power plants, batteries have the potential to also participate in the secondary balancing market by adopting a co-optimized bidding strategy (Olk et al., 2019). Cole and Frazier (2021) project a decline in costs of utility-scale batteries, providing a further boost for considering batteries as a solution to sudden transmission losses.

2.3.2 Increased Interconnection between Market zones

Becker et al. (2014) point out that increasing interconnection between countries leads to a significant reduction in the requirement of backup capacity to accommodate higher penetration of VRE sources. Ramezanzadeh et al. (2021) have conducted a reliability assessment of different subsea HVDC transmission arrangements by developing a reliability model that calculates the probability and frequency of failures. Their analyses show a low overall probability of failure for transmission configurations without redundancy. However, the expected energy not-served, and the expected load curtailment of such configurations are higher than those with redundancy, indicating that redundancy in the transmission is beneficial. With the help of robust optimization considering uncertain N-k contingency failure rates, Yuan et al. (2022) account for outages of transmission lines in the ENTSO-E transmission expansion plan and conclude that transmission expansion planning results are less conservative when considering uncertain component failure rates. To conclude, increased interconnection, consideration of transmission component failures in system modeling, and accommodating redundancy can help tackle unforeseen high-capacity transmission disruptions.

2.3.3 V2G services from Battery Electric Vehicles

With the share of BEV users in Europe surpassing 4% in 2019,BEVs are meeting an increasing proportion of transportation demand (Kucukvar et al., 2022). Further, with increased BEV adoption planned in many European countries, TSOs can take advantage of BEVs' fast response time and low energy consumption for grid balancing services. The Belgian TSO Elia

successfully tested a pilot project to assess the suitability of BEV to provide FCR for the Belgian market. The study revealed that BEVs complied with all necessary technical pre-qualification requirements specified in Article 154 of the Commission Regulation (EU) 2017/1485 to provide power in the balancing market (European Commission, 2017). However, financial and regulatory barriers exist to a mass rollout (Vral, 2018). To address the financial barriers, Bañol Arias et al. (2020) argue that BEV owners can earn additional income between 100€-1100€per year by participating in balancing markets. Techno-economic analysis conducted by Gough et al. (2017) shows that providing energy to the wholesale electricity market and participating in the capacity market is the most effective method for BEV owners to increase their return on investment. Further, Elliott et al. (2020) also discuss the possibility of using the batteries from BEVs after they have outlived their usable lifespan providing transportation services. Their paper claims that BEV batteries can be used for frequency regulation for as long as eight years during their second life and that frequency regulation causes less battery degradation when compared to peak shaving, energy arbitrage, or time-shifting. We conclude that BEVs can provide immediate balancing power to the grid when needed, and participating in balancing power provision can provide direct monetary benefits to their users.

2.3.4 Balancing Power Plants

Traditionally, large power producers and industries with significant ramping capabilities dominated the balancing market. However, with the greater incorporation of renewables in recent years, the ability to swiftly respond to changing market conditions has become the most sought-after property for balancing power plants. New market players such as aggregators with flexible generation capabilities are making inroads into the balancing market, forcing conventional power plants to undertake technical changes in how they operate (Hu et al., 2019). Glensk and Madlener (2019) suggest that among the conventional power plants, Closed Cycle Gas Turbine (CCGT) technology is the most suited to provide balancing power owing to their high efficiency and flexibility compared to other thermal power plants. According to Vorushylo et al. (2016) energy storage solutions coupled with CCGT plants is an emerging technology to operate in the DA and balancing markets, but the solution needs governmental support to be sufficiently attractive to potential investors.

Natural gas has traditionally been used to power gas turbines, a fuel heavily reliant on imports. Despite its low CO_2 intensity in comparison to other fossil fuels, natural gas is fossil-based and must be strategically displaced by cleaner energy sources, as described in Chapter 1 of this thesis. It opens up the possibility of exploring other, low-carbon fuels for CCGT, such as H_2. Öberg et al. (2022) analyze the possibility of fueling gas turbines in Europe using H_2. They conclude that H_2-fueled gas turbines can be competitive if CO_2 emissions are strictly capped, and

VRE penetration is high. Their model sees significant investments in H_2 gas turbines powered by 30 vol.-% H_2 and 70 vol.-% biogas. An analysis of the cost of replacing the energy produced by natural gas-fired gas turbines in California with either Hydrogen Fired Gas Turbine (HFGT) or Lithium-ion batteries fueled by curtailed power was carried out by Hernandez and Gençer (2021) assuming that HFGTs could counter seasonal variations from VRE sources. They concluded that HFGT might be a viable investment opportunity in the future due to rising power prices and a higher share of VRE sources. The EU project GRid ASSisting Modular HydrOgen Pem PowER Plant (GRASSHOPPER) aims to develop a new generation of MW-sized H_2 fuel cell power plants that are more efficient and flexible in terms of output. Fast response characteristics of fuel cell-based systems could let them contribute to grid balancing services. Overall, dispatchable power plants fuelled with natural gas in the short term and non-CO_2 emitting fuels in the long term are viable options to provide quick balancing services.

2.4 Stochastic Optimization

Changes in the DA operating schedule can occur due to several reasons, such as changes in weather, electricity demand, power plant failure, and transmission loss. Due to the uncertain nature of these events, balancing demand and supply in real-time would require changes to decisions made ex-ante (DA operational decisions). Stochastic optimization is a preferred method to solve problems involving uncertainty (Fodstad et al., 2022). Splitting power system operations into multiple stages makes it possible to take corrective action in each stage after (partial) realization of uncertainty and assuming a certain probability distribution for possible future outcomes. For example, when a stochastic model has two stages, the first stage entails a here-and-now decision under uncertainty, and the second involves taking corrective action once the uncertain event occurs. A review of modeling approaches in energy planning that account for uncertainty was provided by Bakirtzis et al. (2012).

Multi-stage stochastic optimization is a popular technique for power system modeling that, when combined with a multi-horizon scenario tree approach, reduces the computational burden (Fodstad et al., 2022). Li and Huang (2012) formulated a multi-stage stochastic model with integer decisions to manage GHG emissions and plan future electric-power systems under uncertainty. Thangavelu et al. (2015) propose a stochastic model for long-term energy planning of regions with a diverse energy mix to address future uncertainties. Krukanont and Tezuka (2007) investigate various conversion technologies' role in capacity expansion under uncertainty with a two-stage stochastic linear model. The European Model for Power System Investment with (high shares of) Renewable Energy (EMPIRE), developed by Skar et al. (2014) to assess ways to develop the European electricity system under different policy scenarios, involves two stages of stochastic optimization. Well-known energy modeling frameworks such as MARKAL, MES-

SAGE, and TIMES have been extended with stochastic programming methods, strengthening the need to address uncertainty in energy modeling (Fodstad et al., 2022).

2.5 Research Gaps and Contribution

In conclusion, HVDC transmission is essential to connecting renewable capacities in remote areas to load centers. An event of a sudden failure in transmission causing a significant loss of transmission capacity can adversely affect the electricity system's stability. An increase in capacity of transmission links beyond 3 GW, combined with increased penetration of renewables, may imply that the current levels of FCR are insufficient for maintaining system stability. To the best of our knowledge, thus far, no one has considered the need for balancing services in the case of sudden, larger than 3 GW, transmission line disruptions. We aim to contribute cost-optimal solutions via several deterministic and stochastic analyses considering ex-post system resilience of given topologies and balancing options, as well as an attempt to cost-optimally provide such services while considering an investment in balancing options as well as transmission lines. By considering the possible outages of high-capacity offshore transmission lines stochastically in an energy system model, we can gain insights into potential solutions to counteract these sudden failures. From the literature review, we find that battery storage system, redundancy in transmission lines, and the utilization of BEVs can provide balancing services.

Table 1: Overview of literature review, Source: Own Illustration

Reference	Focus	Findings
Østergaard (2012)	Battery storage systems for FCR	• Electricity-based storages enable better integration of wind power compared to other storage types.
Olk et al. (2019)	Battery storage systems for secondary balancing market	• Increased provision of balancing services provided by batteries in Germany • Co-optimization of battery and power plants by asset owners will enable penetration of batteries into the secondary balancing market.
Cole and Frazier (2021)	Cost of utility-scale battery storage systems	• The costs of utility-scale battery storage is projected to decline, increasing their usage in power system.
ENTSO-e (2018b)	Balancing Service, FCR	• Power deviation of the reference incident set at 3000 MW for Continental Europe • The system can withstand a sudden disruption of up to 3000MW for 15 minutes.
van der Veen and Hakvoort (2016)	Need for balancing services	• Highlight the need to focus on balancing markets due to the increasing penetration of VRE sources.
Poplavskaya et al. (2021)	Operation of ancillary services	• TSOs maintain the system balance during disruptions step-by-step by activating different balancing services on offer.
Zhou et al. (2022)	HVDC interconnection failures	• Commutation failures are common in HVDC systems as transmission capacity increases.
Zhu et al. (2019)	HVDC interconnection failures	• Commutation failures can cause cascading effects leading to power system failure.

Table 2: Overview of literature review contd., Source: Own Illustration

Reference	Focus	Findings
ENTSO-e (2021)	HVDC interconnection failures	• Outages in HVDC transmission can mainly occur due to cable disruptions or faults at the converter level. • Sudden disruptions limit the maximized usage of transmission lines and can cause a shock effect on the system.
Bakirtzis et al. (2012)	Modeling Uncertainty	• Overview of power system modeling approaches with uncertainty
Li and Huang (2012)	Multi-stage stochastic modeling	• Uncertainty can be modelled by splitting decisions into multiple stages.
Thangavelu et al. (2015)	Stochastic modeling	• Stochastic optimization is a viable option for Long-term energy planning with increased Renewable Energy Sources (RES) penetration.
Krukanont and Tezuka (2007)	Two-stage stochastic modeling	• Stochastic optimization is a viable option in capacity expansion planning where uncertainty exists in various cost parameters.
Skar et al. (2014)	Two-stage stochastic modeling	• Stochastic programming can be beneficial for investment planning required to achieve a predefined low-carbon power generation mix.
Bañol Arias et al. (2020)	Utilization of BEVs in balancing markets	• BEVs can provide FCR-N services which can generate additional income for BEV owners.
Gough et al. (2017)	Utilization of BEVs in balancing markets	• By participating in balancing markets, BEV owners increase their return on investment.
Elliott et al. (2020)	Second life of BEV batteries	• BEV batteries can be used for FCR services up to eight years post their usage in transportation. • Co-optimization of battery and power plants by asset owners will enable penetration of batteries into the secondary balancing market
Glensk and Madlener (2019)	Suitable technology for balancing power plants	• CCGT technology is the best suited technology for operating conventional power plants in future balancing markets.
Vorushylo et al. (2016)	Co-using batteries and balancing plants	• A generation portfolio of CCGT along with batteries can provide required flexibility in balancing markets of the future.
Bañol Arias et al. (2020)	Utilization of BEVs in balancing markets	• BEVs can provide FCR-N services which can generate additional income for BEV owners.
Öberg et al. (2022)	H_2 fueled gas turbines	• H_2-fueled gas turbines can be competitive if CO_2 emissions are strictly capped, and VRE penetration is high.
Öberg et al. (2022)	H_2 fueled gas turbines	• H_2-fueled gas turbines can be competitive if CO_2 emissions are strictly capped, and VRE penetration is high.
Hernandez and Gençer (2021)	H_2 fueled gas turbines	• HFGT might be a viable investment opportunity in the future due to rising power prices and a higher share of VRE sources
Ramezanzadeh et al. (2021)	Reliability of HVDC interconnections	• Adopting redundancy in transmission configurations reduces expected energy not served and the expected load curtailment
Yuan et al. (2022)	Transmission expansion planning	• Accounting for component failure rates in transmission expansion planning produces less conservative results.

3 Problem Description

This chapter describes the problem we analyze in this thesis, its main characteristics, the necessary information for mathematically modeling the problem, and the assumptions needed to simplify the problem at hand. The thesis aims to assess the effect of loss of transmission capacity in high-capacity HVDC links and identify potential investment and operational decisions that could achieve reliable operation of the electricity system.

3.1 Problem Definition

Increased incorporation of electricity from offshore wind and interconnection requirements between countries will likely push the capacities of the HVDC links beyond the 3 GW mark. The current level of European FCR is at 3 GW for 15 minutes, which means that a sudden loss of capacity in the network, up to 3 GW, should be manageable for the system at all times ensuring secure operation. The system, however, may not be capable of handling a transmission capacity loss larger than 3 GW due to the disruption of these high-capacity links, whose occurrence is uncertain.

There is a high share of fossil-fuel-based capacity in the current FCR fleet, along with hydroelectric plants wherever they are available and batteries. With the growing capacity of renewables and implementation of climate policies, CO_2 intensive power plants will no longer be able to provide the spinning reserve as they will move out of the dispatch decided by the merit order. As a result, quick dispatchable plants are not scheduled in the DA market making them unable to provide spinning reserve capacity. As more such dispatchable plants move out of the DA dispatch, the spinning reserve capacity decreases, requiring a need for plausible solutions to the problem. Additionally, due to the inherent variable characteristic of renewables, adequate backing by investments in robust offshore transmission and storage-based solutions becomes of paramount importance. Hence, the thesis aims to identify the optimal investments in transmission and backup capacity in the present, keeping in mind future operational scenarios.

Figures 7 and 8 display a stylized instance of the identified problem that may occur in the future. Figure 7, shows the operation of a two-node (M_A & M_B) system interconnected with a capacity of 3 GW with node M_A connected to an offshore wind farm of 5 GW capacity. The total FCR capacity of the system is assumed to be 3 GW (1 GW at node M_B & 2 GW at node M_B) which is ready to provide capacity in times of a sudden outage. Figure 8 exhibits an outage scenario of the offshore wind farm line causing the activation of balancing plants. The figure highlights a potential high capacity disruption incident where the existing FCR capacity would not be enough to compensate for the power lost due to the disruption.

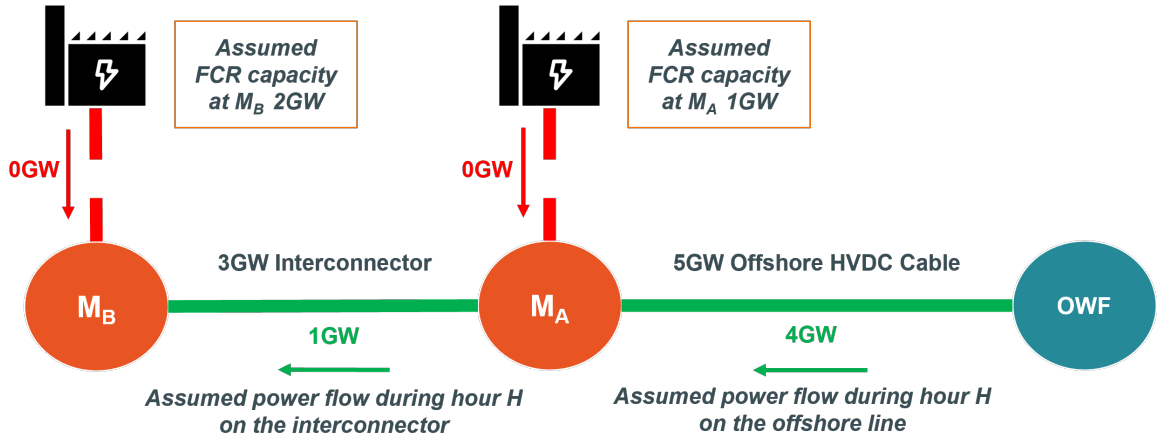

Figure 7: A partial two node (M_A) network wherein a high-capacity offshore link is connecting a OWF cluster (Source: Own illustration)

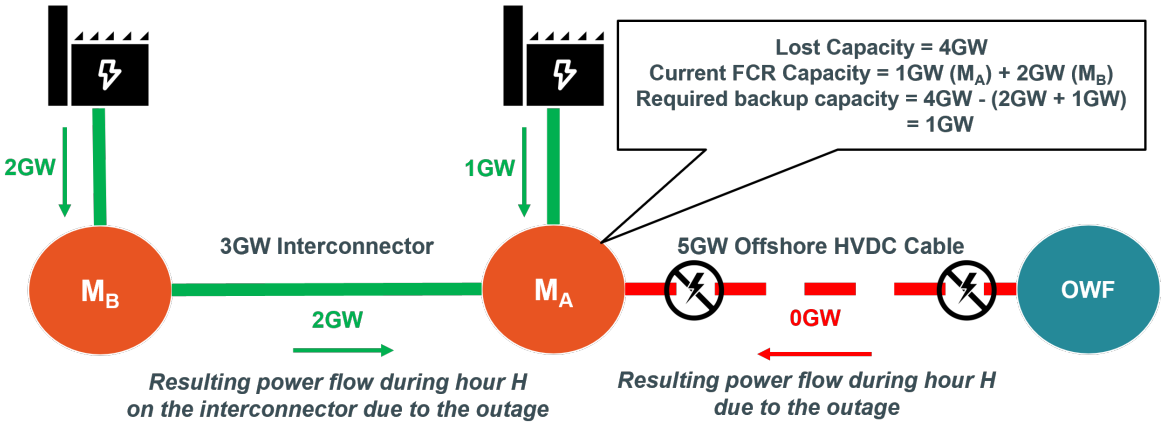

Figure 8: Disruption of the Offshore link of 5 GW creating a need for additional backup capacity (1 GW) in excess to the current FCR levels (3 GW), Own illustration

3.2 Objective

The main objective of the problem is to ensure the reliable operation of the electricity system while minimizing expected system costs. The expected system costs combine long-term investment costs and short-term operational costs. The investment costs are related to expanding the HVDC transmission system (between countries and offshore wind energy incorporation) and investing in backup capacities to ensure system stability. Backup capacities include storage and generation capacity for providing balancing power. The operational costs are the costs of energy dispatch to satisfy hourly energy demand and can vary by operational scenario.

3.3 Decisions

We propose a stochastic model with three decision-making stages. The first decision is about system investment, followed by operational decisions about day-ahead electricity dispatch for different representative cases of demand and renewable availability in the second stage. Both stages involve here-and-now decisions made under uncertainty. In the third stage, several operational scenarios are considered, including one with the realization of the DA scheduling

without transmission disruptions and others in which they occur. Additionally, for the scenarios with transmission disruptions, the third stage includes the generation and network redispatch decisions to address imbalances caused by the random failures of high-capacity transmission. Any imbalances up to 3 GW will activate the FCR, which is a no-cost decision according to the model. The model must decide upon the optimal investment from a set of investment choices. The investment choices include:

- Investing in parallel links to transmit the power to the shore which splits the transmission capacity instead of depending on a single link to transmit power to the shore.
- Investment in Li-Ion batteries.
- Expanding capacity of balancing power plants that can provide quick backup capacity.

The operational decisions include:

- In the second stage, the day-ahead dispatch based for several representative days.
- In the third stage, when a link disruption may or may not have occurred, balancing plant activation and optimal re-dispatch of storage and generation plants.

3.4 Assumptions

In order to balance technical accuracy, computational complexity, and result quality, the following assumptions are established:

- The initial transmission network between the nodes is given.
- We pool transmission capacity between market zones.
- There are only two transmission options to interconnect two nodes or a node and an offshore wind farm, i.e., by a single or two parallel transmission links.
- The length of the transmission links is chosen as the shortest distance to the shore for offshore wind farm links, and for the interconnectors, it is the straight line distance between the two market nodes, but this may not be practical in all cases due to physical and network constraints onshore.
- The DA dispatch is obtained assuming conditions of perfect competition existing in the electricity market.
- The DA market allows the curtailment of power from renewable energy sources, however the power that has been curtailed is still available during the balancing stage and is compensated with the variable cost of production.
- All plants can provide power during outages based on their activity in the DA market.
- For a generation asset to provide backup capacity during an outage, it must be scheduled

to produce in the DA market.

- The cost of balancing energy for any generator is equal to its variable cost of production.
- Storages and other flexibility providers can operate in the day-ahead market and be relied upon to provide instant backup in the events of need.
- All capacities and costs of generators, renewables, and interconnection are known with certainty.
- As total operational costs are calculated for one year, they are made comparable to investment costs by annualizing investment costs over the asset's lifetime.
- The only uncertainty considered is for the disruption of HVDC links in the system.
- In each disruption scenario, not more than one HVDC link shall experience an outage.
- In the event of a disruption in the parallel lines setup, only one line will be affected.
- The model is based on the assumption that FCR backup is applicable for an hour even though it only offers coverage for the first fifteen minutes of an outage event.
- Peak seasons of demand occur simultaneously at all market zones.
- The only generation assets the model can invest in are gas-based power plants.

3.5 Restrictions

The model takes into consideration the following set of constraints:

- The nodal electricity balance must be maintained at all times in every node.
- Charging and discharging of storage technologies involves losses.
- The initial and final energy levels of storage devices must be the same.
- The amount of balancing power that the power plants can provide is restricted by the level of its operation in the DA market.
- Ramping of dispatchable generators is limited to their respective ramping capabilities (% of their maximum operational capacity)
- The seasonal capacity of the reservoirs restricts the generation from hydropower plants both in the DA and ID market.

3.6 Wrapping Up

Based on the information provided the model attempts to answer the question "In an electricity system with high renewable penetration and dependency on high-capacity HVDC links, what are the cost-optimal investment and system operation decisions to ensure system stability in case of outages of these HVDC transmission assets?".

4 Model Framework

4.1 Modelling Approach

The model aims to assess optimal investments in generation, transmission, and storage systems to counter high-capacity HVDC transmission disruptions that may arise. These disruptions are uncertain, favoring a stochastic programming approach to tackle the problem. Stochastic programming can capture the effects of short-term uncertainty about the operating condition of a system on investment decisions (Birge and Louveaux, 2011). The approach facilitates viewing the problem from two perspectives: long-term investment decisions that must be made in the present and future operational decisions that may have to deal with transmission capacity loss. The methodology used is based on EMPIRE by Skar et al. (2014). EMPIRE is a country-level capacity expansion model for Europe that assesses optimal investments and system operation over medium to long-term planning horizons. It involves multiple investment periods, each considering of set of stochastic scenarios with uncertain demand fluctuations and the availability of renewables. Based on the approach from the EMPIRE model, we implement a three-stage stochastic model consisting of one investment period, followed by the DA market optimization for different seasons or time periods, and finally, the redispatch in the intraday markets. Several scenarios of HVDC transmission failures are considered, each of which includes the failure of one HVDC link in the system. In doing so, the aim is to optimize investments considering several possible future disruptions. Figure 9 gives an overview of the model stages.

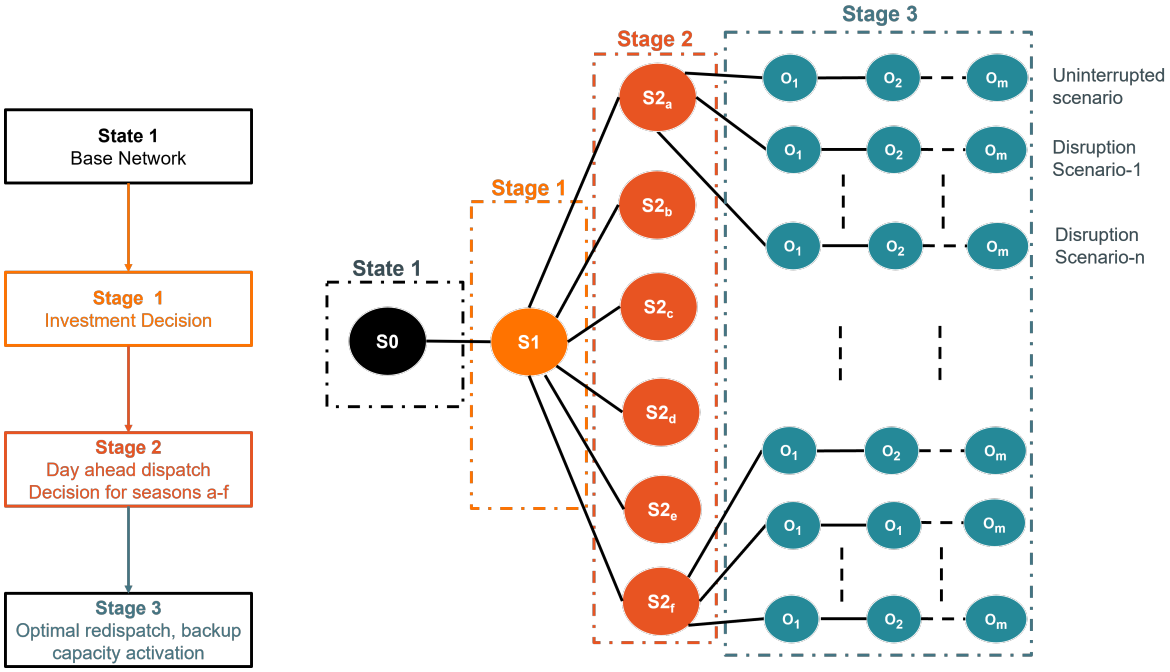

Figure 9: Schematic overview of model setup, Own illustration

4.2 Mathematical Formulation

With the general structure of the model explained, this section focuses on mathematically formulating the model. The model objective function and technical constraints are formulated using the principles of mixed integer linear programming. To explain the objective function and constraints, a list of model terminology, including sets, variables, and parameters, is included.

4.2.1 Model Terminology

Sets

Sets are denoted by scripted, uppercase letters and contain a finite number of indices used in the mathematical model.

$\mathcal{B}$	Set of storages: b
$\mathcal{H}$	Set of time-periods : h
$\mathcal{L}$	Set of transmission configurations : l
$\mathcal{N}$	Set of nodes: n,m
$\mathcal{P}$	Set of generators: p
$\mathcal{P}^{\mathcal{NR}}$	Non-Renewable generator units: nr
$\mathcal{P}^{\mathcal{RE}}$	Renewable generators units: re
$\mathcal{P}^{\mathcal{U}}$	Balancing generator units: u
$\mathcal{P}^{\mathcal{V}}$	Regulated hydro generator units: u
$\mathcal{S}$	Set of seasons represented by a typical day s
Ω	Set of scenarios: ω

Variables

Variables are represented by uppercase letters and are endogenously optimised by the model. They can span over multiple sets.

$CU_{n,p,h}$	Curtailment at node
$D^{LL}_{n,h,\omega}$	Lost load at node
$F_{(n,m),l,s,h}$	Flow from node n to node m on transmission type l
$G_{n,p,s,h}$	Production of each generator
$I_{n,b,s,h}$	Power Injection to storage
$J^{T}_{(n,m),l}$	Binary variable for investment options of transmission line between nodes n&m
$K^{E}_{n,b}$	Installed storage energy capacity after investment (MWh)
$K^{P}_{n,b}$	Installed storage power capacity after investment (MW)
$W_{n,b,s,h}$	DA Storage level (MWh)
$W_{n,b,s,h,\omega}$	ID Storage level (MWh)
$X_{n,b,s,h}$	Power Extraction from storage (MW)
$\Delta I^{+}_{n,b,s,h,\omega}$	Upward adjustment of power injected from storage

$\Delta F^{-}_{(n,m),l,s,h,\omega}$	Downward adjustment of exported power
$\Delta F^{+}_{(n,m),l,s,h,\omega}$	Upward adjustment of exported power
$\Delta I^{-}_{n,b,s,h,\omega}$	Downward adjustment of power injected from storage
$\Delta X^{+}_{n,b,s,h,\omega}$	Upward adjustment of power extracted from storage
$\Delta X^{-}_{n,b,s,h,\omega}$	Downward adjustment of power extracted from storage

Parameters

Parameters are denoted by lowercase letters and are exogenously determined by input data. Their dimension can span over multiple sets.

af	Annuity Factor
$\mathrm{av}_{p,s,h}$	Availability of generator
$\mathrm{av}^{\mathrm{L}}_{(n,m),s,h,\omega}$	Availability of link (n,m)
$\mathrm{c}^{\mathrm{G}}_{v}$	Investment cost of balancing power providing generator (€/MW)
$\mathrm{c}^{\mathrm{E}}_{b}$	Investment cost of storage energy (€/MWh)
$\mathrm{c}^{\mathrm{P}}_{b}$	Investment cost of storage power (€/MW)
$\mathrm{c}^{\mathrm{T}}_{(n,m),l}$	Investment cost of link between nodes n and m of transmission type l
$\mathrm{c}^{\mathrm{CO_2}}_{n,p}$	CO_2 Price (€/MtCO_2)
$\mathrm{c}^{\mathrm{LL}}_{n}$	Value of Lost Load (€/MWh)
dsf_{s}	Dispatch scale factor
$\mathrm{d}_{n,s,h}$	Electrical demand at node (MW_{el})
$\overline{\mathrm{g}}_{p,n}$	Maximum generator capacity in (MW)
$\overline{\mathrm{k}}^{\mathrm{E}}_{b,n}$	Maximum storage energy capacity of storage that can be built (MWh)
$\overline{\mathrm{k}}^{\mathrm{P}}_{b,n}$	Maximum storage power capacity of storage that can be built (MW)
$\overline{\mathrm{k}}^{\mathrm{T}}_{(n,m),l}$	Maximum transmission capacity between n&m of transmission type l (MW)
$\overline{\mathrm{k}}^{\mathrm{G}}_{n,v}$	Maximum capacity of balancing generator that can be installed (MW)
$\mathrm{mc}_{n,p}$	Marginal cost of generator (€/ MWh)
r_{p}	Ramping rate of generator (%)
$\mathrm{w}^{\mathrm{end}}_{b}$	Final storage level of storage (%)
$\mathrm{w}^{\mathrm{start}}_{b}$	Initial storage level of storage (%)
η^{C}_{b}	Charging efficiency of storage (%)
η^{D}_{b}	Discharging efficiency of storage (%)
$\eta^{\mathrm{T}}_{(n,m)}$	Line Efficiency (%)
λ_{b}	Energy retention efficiency (%)
$\xi_{n,p,s}$	Net seasonal hydro generation capacity at each node (MWh)
$\xi_{n,\omega}$	Net annual hydro generation capacity at each node (MWh)
ρ_{b}	Storage Discharge to Charge power ratio
π_{ω}	Probability of occurrence of each scenario ω
τ	Minimum capacity the plant must be operating to provide balancing power (%)

4.2.2 Model Objective

The objective function (Eq. 4.1) minimizes the total expected cost, the sum of investment and operational cost. The operational cost (Eq. 4.2) is summed up over all scenarios and hours in seasons, including the cost of redispatch, carbon price, and a penalty cost for lost load. The investment cost (Eq. 4.3) is divided into three main components: generation investment cost (i.e., investment in additional gas power plant capacity), storage investment cost, and transmission investment cost (investment in single or double HVDC transmission lines). Investment cost is divided into equal installments over the lifetime of the asset by multiplying the investment cost of each investment option with the annuity factor.

$$\textit{Minimize}\ \mathrm{Cost} = \mathrm{COST}^{\mathrm{OPER}} + \mathrm{COST}^{\mathrm{INV}} \cdot \mathrm{af} \tag{4.1}$$

$$\begin{aligned}\mathrm{COST}^{\mathrm{OPER}} = \Bigg[\sum_{\omega \in \Omega} \pi_{\omega} \cdot \sum_{s \in S} \mathrm{dsf_s} \cdot \Bigg\{ \sum_{h \in H} \sum_{n \in N} \sum_{p \in P} \Big[(G_{p,n,h,\omega} + \Delta G^{+}_{n,p,s,h} - \Delta G^{-}_{n,p,s,h,\omega}) \\ \cdot \left(\mathrm{mc_{n,p}} + \mathrm{c}^{\mathrm{CO_2}}_{\mathrm{n,p}}\right) + d^{LL}_{n,s,h,\omega} \cdot \mathrm{c^{LL}_n} \Big] \Bigg\} \Bigg]\end{aligned} \tag{4.2}$$

$$\begin{aligned}\mathrm{COST}^{\mathrm{INV}} = \Bigg[\sum_{l \in L} \sum_{n,m \in N, m \neq n} \mathrm{c^T_{(n,m),l}} \cdot K^{\mathrm{T}}_{(n,m),l} \cdot \mathrm{J^T_{(n,m),l}} + \sum_{n \in N} \sum_{b \in B} \left(\mathrm{c^P_b} \cdot K^{P}_{n,b} + \mathrm{c^E_b} \cdot K^{E}_{n,b}\right) \\ + \sum_{n \in N} \sum_{v \in P^V} \mathrm{c^G_v} \cdot K^{G}_{n,v} \Bigg]\end{aligned} \tag{4.3}$$

$$\mathrm{mc_{n,p}} = \text{Variable Maintenance Costs} + \frac{3.6 \cdot \text{Fuel Costs}}{\text{Generator Efficiency}} \tag{4.4}$$

$$\mathrm{af} = \frac{\text{Discount Rate}}{1 - \frac{1}{(1 + (\text{Discount Rate})^{\text{Years}})}} \tag{4.5}$$

4.2.3 Model Constraints

DA Energy Balance

The DA energy balance (4.6) ensures that in the day-ahead schedule demand is satisfied at each node during all operational hours in all seasons. We do not allow lost load in the day-ahead dispatch.

$$\begin{aligned}\sum_{p \in P} G_{n,p,s,h} + \sum_{b \in B} \left(\eta^{\mathrm{D}}_{\mathrm{b}} \cdot X_{n,b,s,h} - I_{n,b,s,h}\right) + \sum_{l \in L} \sum_{m \neq n} \left(\eta^{\mathrm{T}}_{\mathrm{(m,n)}} \cdot F_{(m,n),l,s,h} - F_{(n,m),l,s,h}\right) \\ = d_{n,s,h} \quad , n \in \mathcal{N}, s \in \mathcal{S}, h \in \mathcal{H}\end{aligned} \tag{4.6}$$

ID Energy Balance

After the DA market closes, the ID energy balance (4.7) allows power plants to correct their dispatch. These corrections may be required to redispatch power in the event of a sudden

transmission capacity loss. Such a loss would distort the DA energy balance by forcing the flow downward (c.f. Eq.(4.33) in Subsection Flow on Transmission Lines). The redispatch can change upward and downward the amounts of power generated, imported, exported, and flowing into or out of the energy storage assets. Hence, superscripts' +' and '-' are used to indicate the direction of change for the variables. If necessary, load can be shed. The sum of all the changes relative to the day-ahead balance must add up to zero.

$$\begin{aligned}
&\sum_{p\varepsilon P}\left[\Delta G^{+}_{n,p,s,h,\omega}-\Delta G^{-}_{n,p,s,h,\omega}\right]\\
&+\sum_{b\in B}\left[\eta^{\mathrm{D}}_{\mathrm{b}}\cdot\left(\Delta X^{+}_{n,b,s,h,\omega}-\frac{\Delta X^{-}_{n,b,s,h,\omega}}{\eta^{\mathrm{D}}_{\mathrm{b}}}\right)-\left(\Delta \mathrm{I}^{+}_{n,b,s,h,\omega}-\Delta \mathrm{I}^{-}_{n,b,s,h,\omega}\right)\right]\\
+\sum_{l\in L}\sum_{m\neq n}&\left[\eta^{\mathrm{T}}_{(\mathrm{m,n})}\cdot\left(\Delta F^{+}_{(m,n),l,s,h,\omega}-\frac{\Delta F^{-}_{(m,n),l,s,h,\omega}}{\eta^{\mathrm{T}}_{(\mathrm{m,n})}}\right)-\left(\Delta F^{+}_{(n,m),l,s,h,\omega}-\Delta F^{-}_{(n,m),l,s,h,\omega}\right)\right]\\
&+D^{LL}_{n,h,\omega}=0\quad ,n\in\mathcal{N},s\in\mathcal{S},h\in\mathcal{H},\omega\in\Omega
\end{aligned}\tag{4.7}$$

DA Storage Balance

The storage balance (Eq. 4.9) governs a battery's storage level at the end of each hour in the DA market. According to the equation, the current hour's storage level equals the previous hour's storage level minus the loss-corrected power withdrawn (discharged) in the current hour plus the loss-corrected power injected (charged) into the battery during the current hour. λ_b denotes the storage energy retention efficiency, which is the amount of energy retained by the battery after each operational hour. Because the model considers pooled nationwide BEV V2G capacities, we can assume that the number of BEVs connected to the grid will change over time. Using the Energy retention efficiency parameter, we assume that 10% of the energy stored is lost during each time period as the BEVs disconnect from the grid and use the energy stored for personal transportation. The efficiency parameter η^{C}_{b} represents efficiency losses during power injection . Eq. 4.8 does not allow the model to have access to any free energy in the system through the storage assets by forcing the model maintain the same energy level at the first and the last hour of the each season.

$$W_{b,n,s,h_{start}}=W_{n,b,s,h_{end}}\quad ,b\in\mathcal{B},n\in\mathcal{N},s\in\mathcal{S} \tag{4.8}$$

$$W_{n,b,s,h}=\lambda_{\mathrm{b}}\cdot W_{n,b,s,(h-1)}-X_{n,b,s,h}+I_{n,b,s,h}\cdot\eta^{\mathrm{C}}_{\mathrm{b}}\quad ,n\in\mathcal{N},b\in\mathcal{B},s\in\mathcal{S},h\in\mathcal{H} \tag{4.9}$$

ID Storage Balance

The ID storage balance incorporates an additional index for each operational scenario compared to the DA storage balance equations. While the DA storage variables remain fixed over all scenarios, the ID storage variables can vary in each operational scenario as required. Eq. 4.10, Eq. 4.11, and EQ. 4.12, govern this deviation of the ID storage variables in the ID market.

$$W_{b,n,s,h_{start},\omega} = \mathrm{w}_{\mathrm{n,b}}^{\mathrm{start}} \quad , b \in \mathcal{B}, s \in \mathcal{S}, n \in \mathcal{N}, \omega \in \Omega \tag{4.10}$$

$$W_{n,b,s,h_{end},\omega} = \mathrm{w}_{\mathrm{n,b}}^{\mathrm{end}} \quad , n \in \mathcal{N}, b \in \mathcal{B}, s \in \mathcal{S}, \omega \in \Omega \tag{4.11}$$

$$\begin{aligned} W_{n,b,s,h,\omega} = W_{n,b,,s,(h-1),\omega} - \Big(X_{n,b,s,h} + \Delta X^{+}_{n,b,s,h,\omega} - \Delta X^{-}_{n,b,s,h,\omega}\Big) \\ + \Big(I_{n,b,s,h} + \Delta I^{+}_{n,b,s,h,\omega} - \Delta \mathrm{I}^{-}_{n,b,s,h,\omega}\Big) \cdot \eta^{\mathrm{c}}_{\mathrm{b}} \quad , n \in \mathcal{N}, b \in \mathcal{B}, s \in \mathcal{S}, h \in \mathcal{H}, \omega \in \Omega \end{aligned} \tag{4.12}$$

Power Generation

The constraints related to power generation govern the functioning of the generation assets. Eq. 4.13 and Eq. 4.14 defines an upper limit to the power generated from non-renewable generators and renewable generators respectively during every hour of the season in the DA market. Both generators' maximum power production capacity depends upon the installed capacity and availability factor. For non-renewable generators, the availability factor is a fixed value for all operational hours, whereas it varies depending on the resource (wind and sun) availability profile for renewable generators. Additionally, for renewable generators, there is a possibility to curtail their output during a period of oversupply. Eq. 4.15 and Eq. 4.16 generation capability during redispatch. All generators eligible for quick balancing power can do so, provided their increased power production stays within the maximum generation capacity during that hour. The generators can also decrease their power output during operational hours if required.

$$G_{n,p,s,h} \leq \mathrm{av}_{\mathrm{n,p,s,h}} \cdot \bar{\mathrm{g}}_{\mathrm{n,p}} \quad , n \in \mathcal{N}, p \in \mathcal{P}^{\mathcal{NR}}, s \in \mathcal{S}, h \in \mathcal{H} \tag{4.13}$$

$$G_{n,p,s,h} + CU_{n,p,s,h} = \mathrm{av}_{\mathrm{n,p,s,h}} \cdot \bar{\mathrm{g}}_{\mathrm{n,p,s,h}} \quad , n \in \mathcal{N}, p \in \mathcal{P}^{\mathcal{RE}}, s \in \mathcal{S}, h \in \mathcal{H} \tag{4.14}$$

$$G_{n,p,s,h} + \Delta G^{+}_{n,p,s,h,\omega} \leq \mathrm{av}_{\mathrm{n,p,s,h}} \cdot \bar{\mathrm{g}}_{\mathrm{n,p}} \quad , n \in \mathcal{N}, p \in \mathcal{P}, s \in \mathcal{S}, h \in \mathcal{H}, \omega \in \Omega \tag{4.15}$$

$$\Delta G^{-}_{n,p,s,h,\omega} \leq G_{n,p,s,h} - \mathrm{av}_{\mathrm{n,p,s,h}} \cdot \quad , n \in \mathcal{N}, p \in \mathcal{P}, s \in \mathcal{S}, h \in \mathcal{H}, \omega \in \Omega \tag{4.16}$$

Generator Ramping

Ramping is the ability of a generator to increase or decrease its output at any point in time. For non-renewable generators, ramping depends on the availability of fuel and the technology of production, whereas renewables depend on the availability of natural resources. The ramping parameter $\mathrm{r_p}$ constrains the increase of power production to simulate the actual ramping capabilities of the generator. Another factor that affects the ramping capability during an operational

hour is the level of operation during the previous hour. Eq. 4.17 regulates the ramping of generators in the DA market whereas the Eq. 4.18 during redispatch. Redispatch needs are limited by the ability of the generator to ramp up or down from the DA dispatch level. Eq. 4.19 controls the amount of power a plant can provide during the redispatch based upon its scheduled power capacity in the DA market. The power plant must operate at a specific minimum capacity in the DA to ramp up and provide quick power. The upper limit is set based on the parameter τ.

$$G_{n,p,h} - G_{n,p,(h-1)} \leq \mathrm{r_p} \cdot \bar{\mathrm{g}}_{\mathrm{n,p}} \quad , n \in \mathcal{N}, p \in \mathcal{P}^{\mathcal{V}}, s \in \mathcal{S}, h \in \mathcal{H} : h \neq h_{start} \tag{4.17}$$

$$\begin{aligned} G_{n,p,s,h} + \Delta G^{+}_{n,p,s,h,\omega} - G_{n,p,(h-1)} \leq \mathrm{r_p} \cdot \bar{\mathrm{g}}_{\mathrm{n,p}} \quad , n \in \mathcal{N}, p \in \mathcal{P}^{\mathcal{V}}, s \in \mathcal{S}, \\ h \in \mathcal{H} : h \neq h_{start}, \omega \in \Omega \end{aligned} \tag{4.18}$$

$$\Delta G^{+}_{n,p,s,h,\omega} \leq \frac{1}{\tau} \cdot G_{n,p,s,h} \tag{4.19}$$

Storage Power Charging and Discharging

The installed storage power capacity limits the rate at which storage assets can charge or discharge during the DA market(c.f. Eq. 4.20 and 4.21). During redispatch Eq. 4.22 and Eq. 4.23 ensure that the additional power injection or extraction from the storage assets do not violate the power capacity limits. Similarly, Eq. 4.24 and Eq. 4.25 ensure that reduction in power extraction or injection during redispatch does not exceed the power scheduled in the DA market.

$$I_{n,b,s,h} \leq K^{P}_{b,n} \quad , n \in \mathcal{N}, b \in \mathcal{B}, s \in \mathcal{S}, h \in \mathcal{H} \tag{4.20}$$

$$X_{n,b,s,h} \leq \rho_{\mathrm{b}} \cdot K^{P}_{n,b} \quad , n \in \mathcal{N}, b \in \mathcal{B}, s \in \mathcal{S}, h \in \mathcal{H} \tag{4.21}$$

$$I_{n,b,s,h} + \Delta I^{+}_{n,b,s,h,\omega} \leq K^{P}_{n,b} \quad , n \in \mathcal{N}, b \in \mathcal{B}, s \in \mathcal{S}, h \in \mathcal{H}, \omega \in \Omega \tag{4.22}$$

$$X_{n,b,s,h} + \Delta X^{+}_{n,b,s,h,\omega} \leq \rho_{\mathrm{b}} \cdot K^{P}_{n,b} \quad , n \in \mathcal{N}, b \in \mathcal{B}, s \in \mathcal{S}, h \in \mathcal{H}, \omega \in \Omega \tag{4.23}$$

$$\Delta I^{-}_{n,b,s,h,\omega} \leq I_{n,b,s,h} \quad , n \in \mathcal{N}, b \in \mathcal{B}, s \in \mathcal{S}, h \in \mathcal{H}, \omega \in \Omega \tag{4.24}$$

$$\Delta X^{-}_{n,b,s,h,\omega} \leq X_{n,b,s,h} \quad , n \in \mathcal{N}, b \in \mathcal{B}, s \in \mathcal{S}, h \in \mathcal{H}, \omega \in \Omega \tag{4.25}$$

Storage Operational Capacity Level

Eq. 4.26 sets the upper limit of storage level in the DA ahead market, i.e., the amount of charge the storage system can hold at any time is lesser than the installed energy capacity. However, this storage level may vary due to redispatch decisions in different operational scenarios. Eq. 4.27 limits the storage energy capacity in the ID market.

$$W_{n,b,s,h} \leq K^{E}_{n,b} \quad , n \in \mathcal{N}, b \in \mathcal{B}, s \in \mathcal{S}, h \in \mathcal{H} \tag{4.26}$$

$$W_{n,b,s,h,\omega} \leq K^{E}_{n,b} \quad , n \in \mathcal{N}, b \in \mathcal{B}, s \in \mathcal{S}, h \in \mathcal{H}, \omega \in \Omega \tag{4.27}$$

Flow on transmission lines

The maximum power flow on any transmission line is restricted by its installed capacity (c.f. Eq. 4.28). Eqns.(4.31)-(4.30) implement the operational disruptions. Additionally, a parameter ($\mathrm{av}^{\mathrm{L}}_{(\mathrm{n,m}),\mathrm{s,h},\omega)}$) is introduced that addresses the availability of the transmission links. Eq 4.30 ensures that for any value of the transmission availability parameter of a transmission line other than unity, a corresponding decrease in the power flow on that line occurs, simulating an outage. The ID flow term in the equation signifies the reduction in power flow occurring due to the simulated outage. Eq. 4.31 imposes that an increase of power flow on any transmission line during the ID operation does not exceed the maximum transmission capacity, which also depends on the transmission availability factor during all periods. At the same time, Eq. 4.32 ensures that the sum of the scheduled power flow during the DA market and the increase of power flow during the ID operation is bound by an upper limit which is the maximum transmission capacity of the transmission line. Moreover, Eq. 4.33 enforces the restriction that the reduction in transmission flow during redispatch does not exceed the scheduled flow in the DA market.

$$F_{(n,m),l,s,h} \leq K^{T}_{(n,m),l} \quad , n,m \in \mathcal{N} : n \neq m, s \in \mathcal{S}, h \in \mathcal{H}, l \in \mathcal{L} \tag{4.28}$$

$$F_{(n,m),l,s,h} - \Delta F^{-}_{(n,m),l,s,h,\omega} \leq K^{T}_{(n,m),l} \cdot av_{(n,m),l,s,h,\omega} \tag{4.29}$$

$$, n,m \in \mathcal{N} : n \neq m, s \in \mathcal{S}, h \in \mathcal{H}, l \in \mathcal{L}, \omega \in \Omega \tag{4.30}$$

$$\Delta F^{+}_{(n,m),l,s,h} \leq K^{T}_{(n,m),l} \cdot av_{(n,m),s,h,\omega} \quad , n,m \in \mathcal{N} : n \neq m, s \in \mathcal{S}, , h \in \mathcal{H}, l \in \mathcal{L}, \omega \in \Omega \tag{4.31}$$

$$\Delta F^{+}_{(n,m),l,s,h,\omega} + F_{(n,m),l,s,h} \leq K^{T}_{(n,m),l} \quad , n,m \in \mathcal{N} : n \neq m, s \in \mathcal{S}, h \in \mathcal{H}, l \in \mathcal{L}, \omega \in \Omega \tag{4.32}$$

$$\Delta F^{-}_{(n,m),l,s,h,\omega} \leq F_{(n,m),l,s,h} \quad , n,m \in \mathcal{N} : n \neq m, s \in \mathcal{S}, h \in \mathcal{H}, l \in \mathcal{L}, \omega \in \Omega \tag{4.33}$$

Binary Transmission Investment Decision

A binary variable ($J^{T}_{(n,m),l}$) assures that the model can either invest in a single transmission line or a double transmission line and not in both. In the case of the double transmission line, the total required capacity will be split equally between the two lines. The constraint facilitates this by restricting the sum of all possible binary investment decision variables to equal one.

$$\sum_{l \in L} J^{T}_{(n,m),l} = 1 \quad , n,m \in \mathcal{N} : n \neq m \tag{4.34}$$

$$J^{T}_{(n,m),l} = \{0,1\} \tag{4.35}$$

Capacity Investment: Generation, Storage and Transmission

The model also limits the allowed capacity investments in generation (Eq. 4.36) , storage (Eq. 4.37 and Eq. 4.38), and transmission (Eq. 4.39) at all nodes by introducing an upper limit

denoted by parameters with an $\overline{overline}$. As the installation of transmission links involves a choice between a single and a double line setup, the binary variable $(J^T_{(n,m),l})$ in Eq. 4.39, ensures that the model considers the upper bound of the transmission capacity based on the installed line setup.

$$K^G_{n,v} \leq \bar{\mathrm{k}}^{\mathrm{G}}_{\mathrm{n,v}} \quad , n \in \mathcal{N}, v \in \mathcal{P}^{\mathcal{V}} \tag{4.36}$$

$$K^P_{n,b} \leq \bar{\mathrm{k}}^{\mathrm{P}}_{\mathrm{n,b}} \quad , n \in \mathcal{N}, b \in \mathcal{B} \tag{4.37}$$

$$K^E_{n,b} \leq \bar{\mathrm{k}}^{\mathrm{E}}_{\mathrm{n,b}} \quad , n \in \mathcal{N}, b \in \mathcal{B} \tag{4.38}$$

$$K^T_{(n,m),l} \leq \bar{\mathrm{k}}^{\mathrm{T}}_{\mathrm{(n,m),l}} \cdot J^T_{(n,m),l} \quad , n, m \in N : n \neq m, l \in L \tag{4.39}$$

Hydro Generation Seasonal Capacity

The water availability in the reservoirs defines the potential of the hydropower plants to generate power. The amount of water flowing into the reservoirs is limited every season throughout the year; hence, the sum of hourly output in a season cannot be greater than the net seasonal production capacity.

$$\sum_{p \in P} G_{n,p,s,h} \leq \xi_{n,p,s} \quad , n \in \mathcal{N}, p \in \mathcal{P}^{\mathcal{U}}, s \in \mathcal{S} \tag{4.40}$$

Hydro Generation Annual Capacity

The annual hydroelectric generation at each node is limited based on the net water level during the year. Eq. 4.41 enforces this in the DA market whereas Eq. 4.42 for the redispatch.

$$\sum_{s \in S} \alpha_s \cdot \sum_{h \in H} \sum_{p \in P^U} G_{n,p,s,h} \leq \xi_{n,p,s} \quad , n \in \mathcal{N} \tag{4.41}$$

$$\sum_{s \in S} \alpha_s \cdot \sum_{h \in H} \sum_{p \in P^U} G_{n,p,s,h} + \Delta G^+_{n,p,s,h,\omega} \leq \xi_{n,p,s} \quad , n \in \mathcal{N}, \omega \in \Omega \tag{4.42}$$

Non negativity constraints

All variables considered in the model are non-negative.

$$\begin{gathered} d^{LL}_{n,s,h}, F_{(n,m),l,s,h}, G_{n,p,s,h}, I_{n,b,s,h}, W_{n,b,s,h}, X_{n,b,s,h}, CU_{n,p,s,h} \geq 0 \\ \Delta F^+_{(n,m),l,s,h,\omega}, \Delta F^-_{(n,m),l,s,h,\omega}, \Delta G^+_{n,p,s,h,\omega}, \Delta G^-_{n,p,s,h,\omega}, W_{n,b,s,h,\omega}, \Delta I^+_{n,b,s,h,\omega}, \Delta I^-_{n,b,s,h,\omega}, \\ \Delta X^+_{n,b,s,h,\omega}, \Delta X^-_{n,b,s,h,\omega} \geq 0 \\ K^E_{n,b}, K^P_{n,b}, K^T_{(n,m),l} \geq 0 \\ J^T_{(n,m),l} = \{0,1\} \\ \delta_{n,p,s,h} = \{0,1\} \end{gathered} \tag{4.43}$$

The above formulation constitutes a three-stage model with an investment stage, a DA scheduling stage, and an ID operational for redispatch decisions. Uncertain disruptions in the opera-

tional stage can be anticipated by earlier stages, potentially triggering capacity investment into a more robust system and DA scheduling choices that are more flexible against disruptions. ID corrective measures can be taken. A main part of this work are all the equations needed to appropriately govern the ID corrective measures.

4.3 Implementation and Software Toolbox

The described model is implemented using the open-source language Python and the Pyomo framework for optimization models.

5 Data Processing and Data

The model developed in Chapter 4 assesses the optimal responses to disruptions of high-capacity HVDC lines from clustered offshore wind farms. The analysis done in this research includes member states of the NSEC, the Great Britain (GB), and Poland. We introduce the collected data and underlying assumptions and data processing necessary to answer the research question, followed by a broader explanation of the case setup.

5.1 Data Processing

This section explains different data processing techniques applied to compile the data sets used in this thesis, such as the temporal aggregation, stochastic scenario generation routine, and the procedure followed to cluster identified offshore wind farms.

5.1.1 Temporal Aggregation

A full-blown representation of a power network with an hourly resolution for an entire year leads to large data instances that, depending on the representation detail of other aspects, may or may not be tractable even when just considering a deterministic setting. When considering uncertainty in large-scale models, numerical tractability often becomes an issue. Skar et al. (2014) propose two temporal aggregation methods to reduce the problem's computational complexity. The two methods include aggregating investment periods into five-year blocks instead of annual blocks, and the other is to consider representative hours in a year instead of all 8760 hours. However, in our model, we limit ourselves to only one investment period; hence, we focus on building a representative set of operational scenarios. A year can be considered to consist of two season categories, namely peak and regular seasons. The set of regular seasons in the model includes winter, spring, summer, and fall, while the peak seasons include two extreme load seasons. Despite comprising just a small fraction of the year, extreme load seasons can provide helpful insight into the need for backup capacity. In a system increasingly reliant on renewable energy, a period of low production from renewable generators when demand is high is particularly stressful. Since there is a shortage of available power in the system during such peak periods, disruptions will test the system's ability to cope with an outage of high-capacity HVDC links. Figure 10 depicts an overview of a year from the model's point of view. After some testing for solution times, we have decided to reduce each regular season to 48 hours, along with two peak seasons of 24 hours, results in the total number of hours considered in the year to be 240. We implement this simplification because the computing power is inadequate to increase the number of hours modeled and to obtain results within reasonable timeframes. In the model objective, the number of hours in each regular season is multiplied by a seasonal scaling factor (45.38), whereas the hours in the peak seasons are assumed to occur only for

48 hours in an entire year and have a scaling factor equal to unity. As a result, using temporal aggregation, the entire year is simulated with less computational effort, probably at the expense of a potential loss of quality. According to Göke and Kendziorski (2022), one of the methods to reduce the loss of the quality of results due to time series reduction is by incorporating extreme situations threatening system adequacy, which we implement by adding 48 hours of peak demand in our model.

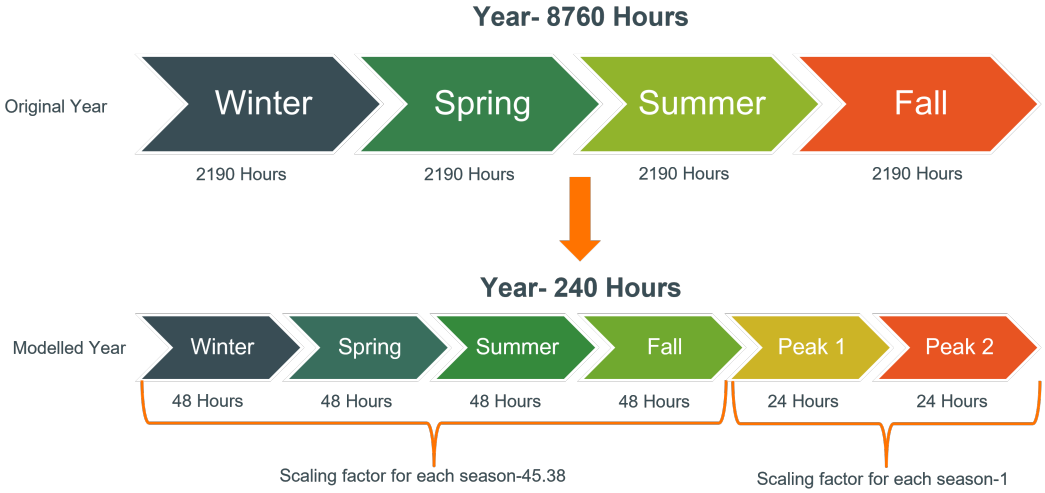

Figure 10: Annual operational hours, Own illustration

5.1.2 Stochastic Scenario Generation

We modify the scenario generation routine developed by Skar et al. (2014) to generate transmission disruption scenarios in our model. Hourly profiles for the availability of different renewable generators were collected across multiple years. Additionally, a stylized availability time series for transmission assets was developed to simulate the disruption of HVDC links. Based on the low disruption probabilities found in ENTSO-e (2021), we assume that, at most, one disruption happens simultaneously. In the event of a disruption, the transmission link's availability during that hour is reduced to zero or half, depending on the type of transmission link (single or double line). As shown in Figure 9, stochastic disruption scenarios are part of Stage 3. For every season, there is one operational scenario without disruptions, other scenarios consider one disruption only (we ignore situations with two disruptions simultaneously, somewhat comparable to $(N-1)$-security). The number of disruption scenarios depends on the number of transmission links in the system. The specific link disruptions are repeated in the operational scenarios for each of the six seasons. The data for generation assets and the load remains consistent across all scenarios in the same season, whereas transmission availability varies by operational scenario. Therefore, in each disruption scenario, an outage occurs on exactly one of the transmission links. The six seasons considered in the model are designed as six separate blocks, which causes the storage cycle to reset at the end of each season.

5.1.3 Offshore Wind Farm Clustering

As described in Chapter 1, the North and Baltic Sea regions will see the construction of several offshore wind farms within the next decade. The increased number of offshore wind farms in both seas makes it possible to cluster them, reducing the number of transmission lines required to connect them to the shore. Using open-source offshore wind farms data from 4C Offshore (2021) and the open-source wind database The Wind Power (2021), we formulated a procedure for manually clustering these upcoming offshore wind farms. The overarching, intuitive guiding principles that we have applied in this clustering are the following:

- Identification of offshore wind farms commissioned by 2030.
- Categorisation of identified offshore wind farms.
- Manual clustering based on distance.

Identification and Categorization Procedure

This section explains the how we identify and categorize offshore wind farms.

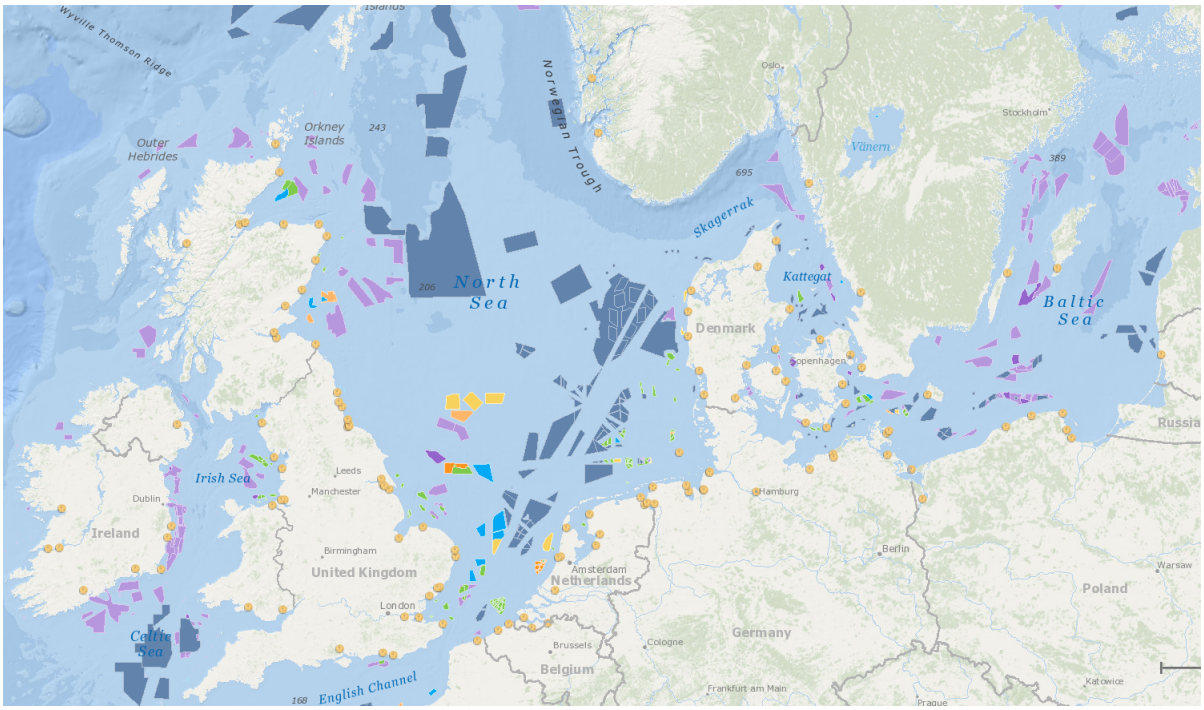

Figure 11: An overview of marine space used for offshore wind energy generation in the North and Baltic Seas (The different coloured patches represent different offshore wind farm project categories), Source: 4C Offshore (2021)

- Initially, by using the offshore interactive map provided by 4C Offshore (2021), an overview of the marine space with different categories of offshore wind farm projects for each country is obtained (Figure 11). Table 3 shows seven different types of offshore wind farm projects.

- The next step is to identify the offshore wind farm capacity that a country aims for within a fixed timeline, for example, 2030.
- Upon identification of the target, the difference between a country's targeted capacity and the existing offshore wind farm capacity provides an estimate of the upcoming offshore wind farm capacity. (For example, if a country is targeting 10 GW of offshore wind farm capacity by 2030 and has an operational offshore wind farm capacity of 2 GW, then the planned capacity to be made operational by 2030 is 8 GW).
- All offshore wind farm projects in a country are collected and categorized into the categories mentioned above using the 4C map.
- The grouped projects are picked to achieve the targeted capacity of the country. The projects are first chosen from the under-construction category, followed by the category order listed in Table 3. (Continuing from the earlier example, if 2 GW worth of project capacity is under construction, then 2 GW worth of capacity from the planned 8 GW capacity is picked from this category which leaves a possibility to further select 6 GW worth of projects from the following categories).
- Following the planned offshore wind capacity mapping to individual offshore wind farms, data such as their approximate point location (latitude and longitude) and distance to shore is collected from The Wind Power (2021).
- Further, the distance between nearby offshore wind farms is calculated using their approximate location.

Figure 12 provides an overview of all the identified offshore wind farms belonging to the NSEC countries, the GB and Poland, that are expected to be functional by 2030.

Table 3: Categorisation of offshore wind farm projects, Source: 4C Offshore (2021)

Category	**Description**
Fully Commissioned	These are existing offshore wind farms that are fully operational.
Under Construction	Offshore wind farm projects undergoing construction and projected to be operational within the chosen timeline, for example, 2030.
Pre-Construction	Currently approved offshore wind farm projects, with construction scheduled to begin.
Consent Authorized	Offshore wind farms approved but not ready to begin construction.
Consent Application Submitted	Evaluation phase of the proposed offshore wind farm project.
Concept/Early Planning	Projects that are in the initial phase of the proposal.
Development Zone	Large marine regions identified with high potential for offshore wind development with no concrete projects planned.

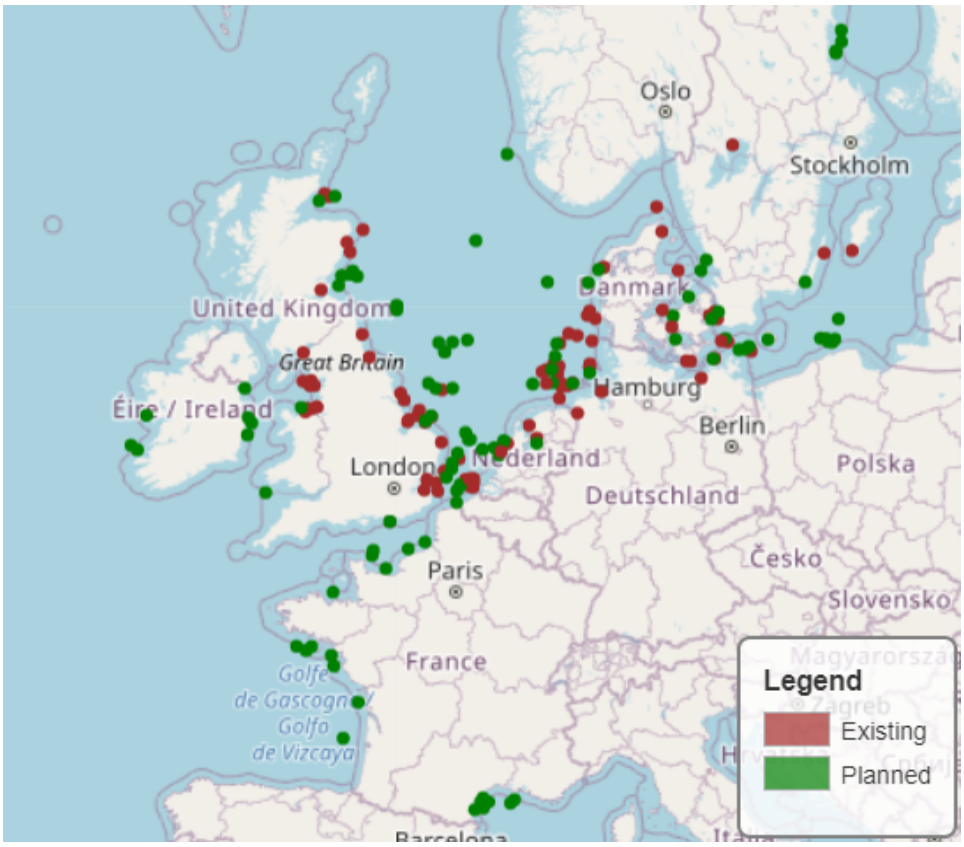

Figure 12: Approximate locations of existing and planned offshore wind farms for the NSEC countries, the GB and Poland until 2030, Source: Own creation based on the data from 4C Offshore (2021) and The Wind Power (2021)

Clustering Procedure

- After identifying the offshore wind farms that each country intends to build and gathering the necessary data, the offshore wind farms of each country are clustered based on the distance between them.
- Offshore wind farms are plotted using geodata, and those within a 50km radius and with a combined capacity greater than 3 GW are manually grouped as hubs (c.f. Figure 2 in Chapter 1).
- Offshore wind farms that cannot be clustered as hubs because they are not in the vicinity of other offshore wind farms or their cumulative capacity is less than 3 GW are grouped as a single node and are excluded from transmission outage scenarios.
- If the combined capacity of non-hub offshore wind farms exceeds 4 GW, the offshore wind farms are divided into multiple nodes, each with a capacity less than 4 GW, and each with a different wind availability series.
- The same procedure is repeated for existing offshore wind farms as they are not considered for transmission outage scenarios.

By being grouped as hubs, the model can decide whether to interconnect these offshore wind farms and then have a single transmission corridor to the shore or radially connect each offshore wind farm to the shore without any connection between them. For simplicity, among the clustered offshore wind farms, the farthest among them to the shore has no option to connect radially to the shore, forcing it to connect to at least one other offshore wind farm to transmit the power generated onshore. A hub can have more than one offshore wind farm connecting the hub to the shore, a decision the model has to make. Because the model represents each offshore wind farm as a node, each offshore wind farm has its own wind availability time series based on its location. Figure 13 displays offshore wind farms that are clustered together based on the method explained.

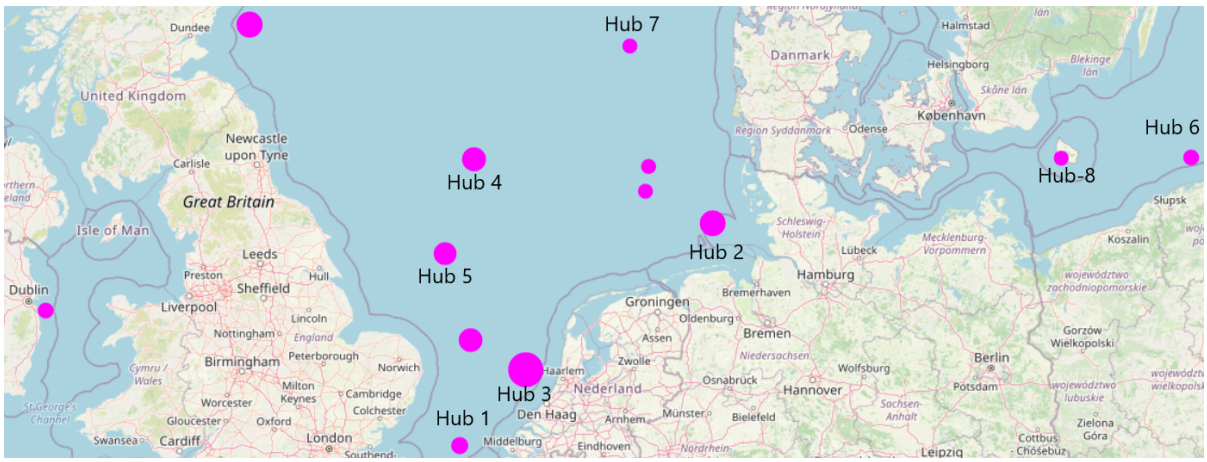

Figure 13: Approximate locations of hubs identified by the clustering of planned offshore wind farms, Source: Own creation based on the data from 4C Offshore (2021) and The Wind Power (2021)

From the identified offshore wind farms that are eligible to be clustered as a hub, we choose to analyze eight hubs in this thesis. These selected hubs are numbered in Figure 13. The capacities of the individual wind farms that constitute the hub along with the distance between them and their distances to the shore are as shown in the Figures 14, 15, & 16.

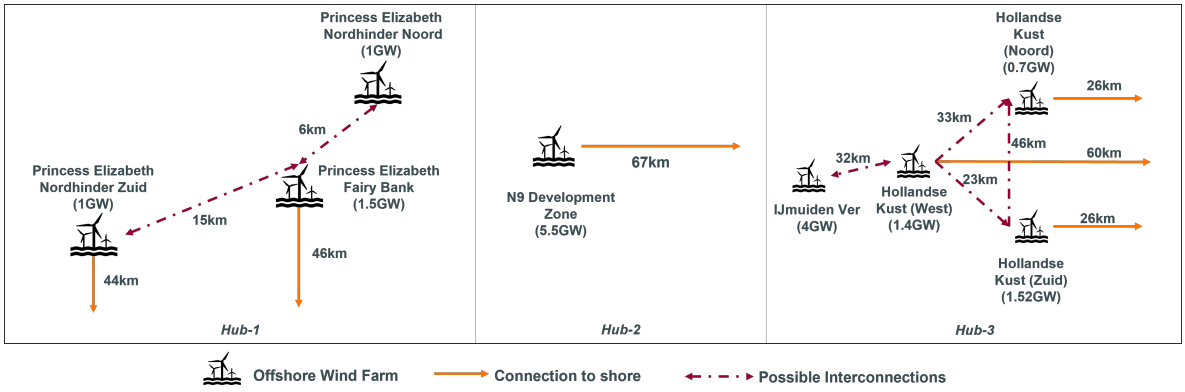

Figure 14: Wind farm clusters with capacity greater than 3 GW (BE,DE and NL)

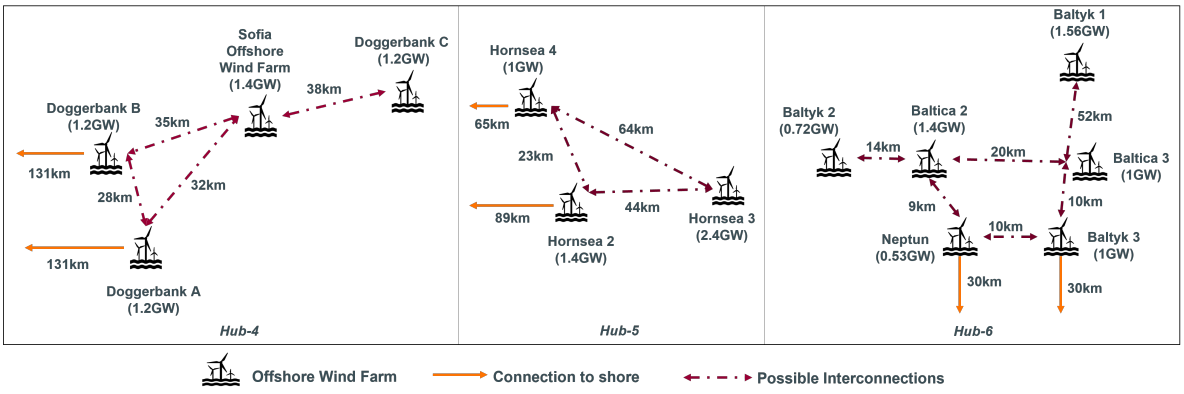

Figure 15: Wind farm clusters with capacity greater than 3 GW (GB and PL)

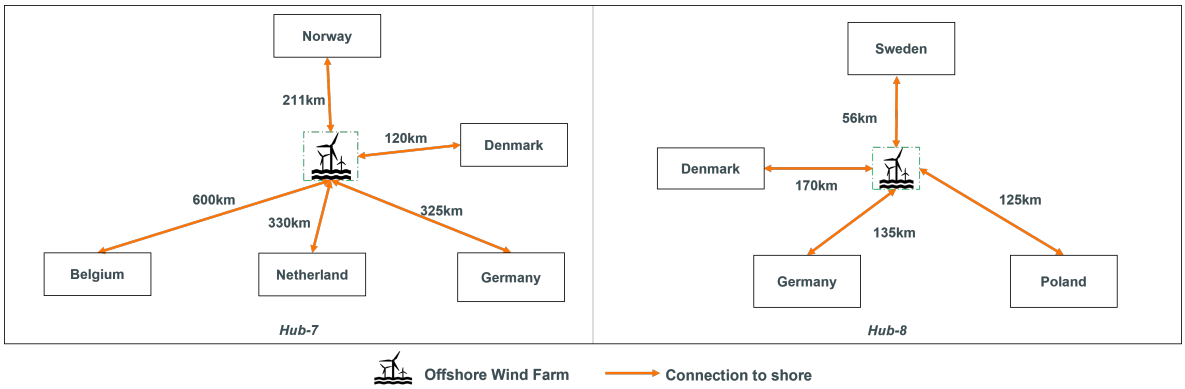

Figure 16: Wind farm clusters with capacity greater than 3 GW (DK-1 and DK-2)

5.2 Load, Generation, Network and Storage Data

We utilize the data from the Distributed Energy (DE) scenario from the *Ten-Year Network Development Plan (TYNDP) 2022* and OpenEMPIRE model data compiled by Backe et al. (2022). From the TYNDP data, we take future installed capacities for the year 2030, annual system load, and interconnection capacities between market zones [1]. From the OpenEMPIRE dataset, we use investment cost values for gas-fired power plants and Lithium-Ion batteries. Vrana and Härtel (2018) provide detailed investment cost values for developing an HVDC transmission system for offshore generation and interconnectors. The nodes, in our case, are set up according to the market zones and do not always reflect the territorial borders of the member states. The following paragraphs further explain the input data used in the thesis.

Generation

The data set contains generation technologies such as renewable, fossil-fueled, and reservoir-based hydropower plants with the capacities of the power plants in each market zone corresponding to the expected aggregate capacities in the year 2030, as per the DE scenario in

[1] In the model, there is a 1-1 relation between market zones and nodes.

ENTSO-e (2022) (c.f. Table 6 in Appendix 1 for generation capacity of each market zone). Table 5 shows the average availability, operating efficiencies, ramp rates, and carbon content per unit generation for dispatchable power plants. We collect weather data at an hourly resolution for all nodes that determine the availability of renewable power plants and their hourly generation capability, using the Renewables Ninja platform based on the work by Pfenninger et al. (2014). The model uses the data in Backe et al. (2022) to estimate the hydro reservoir level for each season with the help of the database comprising weather and reservoir data from 2015 to 2019. This sets a limit on the total hydropower capacity that is available during a season. Additionally, an annual generation limit at each market zone constrains the total hydro generation capability (c.f. equations 4.40, 4.41, 4.42).

Storage

Three storage-based technologies are considered in this study: Lithium-ion batteries, Pumped Hydro (PH), and BEV to provide flexibility to the system. Each of the storage technologies is subject to charging and discharging efficiencies. BEVs are modeled using an energy retention efficiency parameter, which roughly simulates the energy used by driving a BEV during each time period. The parameter causes the BEV to lose 10% of the stored energy every hour if unused. In the model we pool capacities of BEV in the entire market zone. Additionally, we find that majority of the BEVs are driven for less than two hours a day utilizing low amounts of stored energy Liu et al., 2015. For the remaining twenty two hours, the BEVs are idle and connected to the charging station either at home or at work. In case the user decides to disconnect the car from the charger, we lose the energy capacity of the BEV available to provide grid services. We assume that not more than 10% of the users on average per hour will disconnect the car at the same time and hence the 10% loss in energy capacity every hour. Additionally, this parameter assumption does not affect the result because of the pooling of BEV capacities. All storage technologies' initial and final State of Charge (SoC) has to be the same. We assume that the PH and BEV capacities exist already and are available, whereas to make lithium-ion battery capacity available, it must be invested in. Table 7 in Appendix 1 provides an overview of the parameter values related to storage technologies. ENTSO-e (2022) also provides projections of V2G enabled BEV capacity in each market zone for the year 2030 (c.f. Table 10).

Transmission

Transmission exchanges between market zones are restricted by the NTC, which are based on ENTSO-e (2021) data. The NTCs are assumed to be equal in both directions, and transmission efficiency of 98% is assumed for all transmission links considered in the system (Ludin et al.,

2022). The NTCs between different market zones are shown in Table 8. Investment in new transmission capacity is possible on a set of defined links. We consider several investible link types: connecting offshore wind farms with each other, connecting offshore wind clusters with multiple market zones, or connecting offshore wind clusters to a single market zone based on their location. Connecting offshore wind farm clusters to multiple market zones can also serve power flows between market zones. For each link, the model can invest in either a high-capacity single line or parallel, double lines[2]. A single transmission link interconnects clustered offshore wind farms. The model decides the capacity of all investible transmission links. Like the hourly availability of renewable power plants, the transmission lines have an availability parameter for each operational hour. For a single line, the value can either be one or zero, with one denoting the availability of the total transmission capacity, whereas zero refers to an outage of the line during a particular hour of operation. For a double line, a value of half is considered instead of zero, which signifies that only one of the lines is experiencing an outage, reducing the total transmission capacity to half the transfer capacity (c.f. Transmission Flow constraint).

Electricity Demand

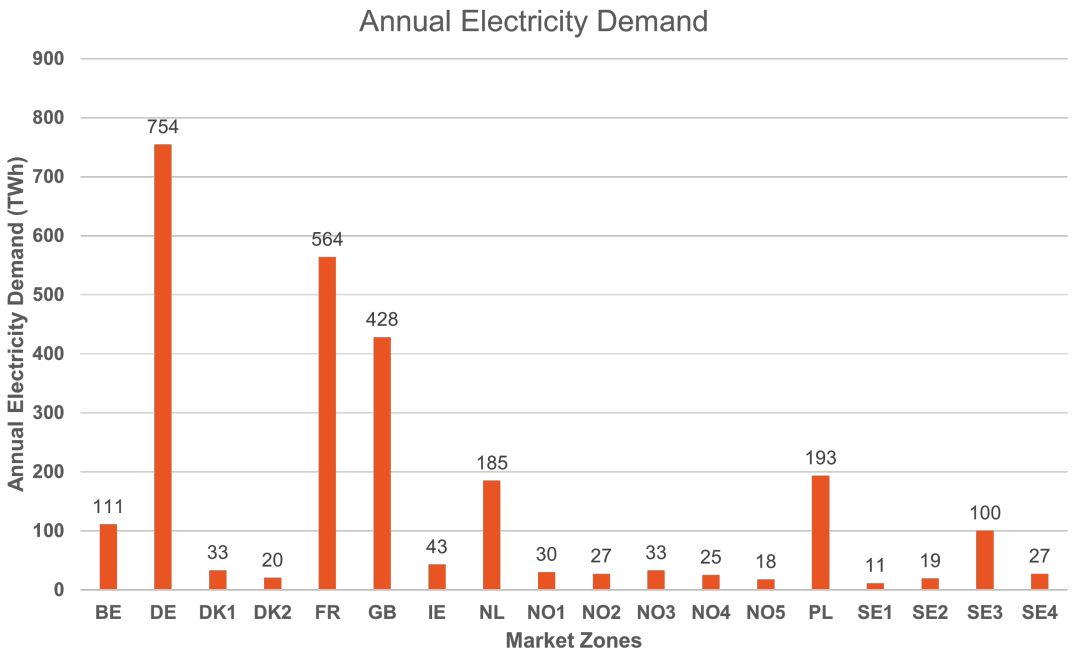

Figure 17: Annual electric demand in different market zones, (ENTSO-e, 2022)

The annual demand at each node is as per the Distributed Energy scenario of the ENTSO-e (2022) data. Figure 17 displays the net annual electricity demand for all market zones con-

[2] The double lines are enforced to both have the same capacity, but not necessarily the same aggregate capacity as the single line would have had.

sidered in the study. The historic hourly demand data from Backe et al. (2022) is scaled so that the sum of all the hourly demand considered in the operational scenario equals the net annual electric demand in each market node. The scaling retains the typical characteristics of the demand curve and adjusts it to match the projected annual electric demand in the year 2030.The demand varies in the four regular seasons and the two peak demand seasons. One peak season considers the highest combined load of all the market zone during a chosen year, and the other is based on the highest load of a single node during the same year.

Costs

Costs are categorized into fixed investment and operational. The investment costs are further divided based on the type of investment, namely gas-based balancing power plants, offshore transmission links, and lithium-ion batteries. Investment costs relating to energy storage systems include capital costs for energy storage capacity, while those relating to transmission systems include fixed costs, power costs, cable length costs, and combined length and power costs (Vrana and Härtel, 2018). Investment costs for gas-based balancing power plants include capital costs and fixed operation and maintenance costs. Table 13 , Table 12, Table 11, and Table 9 provide an overview of the costs considered.

Data

As the Value of Lost Load (VoLL) we take 3000 €/MWh, which is the EPEX spot market price cap. For the sensitivity analysis we consider low and high carbon price of 33 €/tCO_2 (approximately the average price across years 2019, 2020 and 2021) and 300 €/tCO_2 (Rodrigues et al., 2022) respectively. For the gas price sensitivity, we consider low and high gas prices from the EU Dutch TTF market, which is 31 €/MWh (half of the average gas price in Europe in 2021) and 227 €/MWh (highest recorded gas price till the end of July 2022) respectively.

6 Results and Discussion

In this chapter, we apply the model formulated in Chapter 4 to assess the possible solutions to the research question based on the following methodology. We divide the analysis into two parts. The first part consists of a deterministic analysis that does not consider outages on offshore transmission lines. We do so to obtain the following information about the system:

- Identify how the selected wind farm hubs interconnect *at lowest cost*.
- Determine the connection capacities of the offshore transmission lines from the hubs to the shore.
- To find the hours when offshore transmission lines carry maximum power.

The model is run in a deterministic setting without disruptions for three[3] cases: high and low CO_2 and high and low gas prices to identify a base system and benchmark for the stochastic analysis . Using this information from the deterministic analysis, we perform a stochastic analysis in which we introduce outages in specific transmission lines for specific hours of operation. We examine the stochastic results to determine if the system can manage transmission outages well, or if further investments are needed. After identifying a base case, we then conduct a sensitivity analysis, in which we vary the fixed investment costs for the parallel transmission link, followed by a sensitivity analysis on the probability of outages. In each sensitivity analysis, we compare the investments and disruption responses with identified base case and look for a potential investment in a parallel line. Figure 18 provides an overview of the structure followed for the overall analysis.

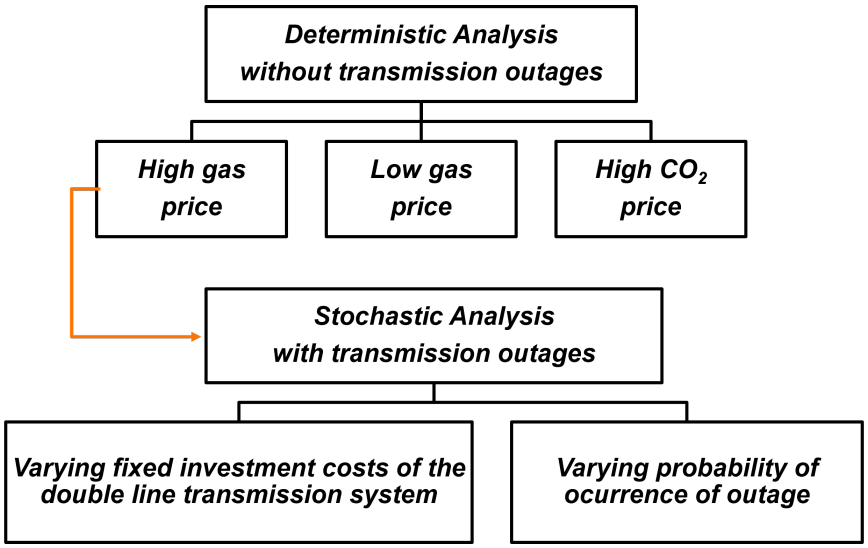

Figure 18: Methodology of the analysis - starting from the top

In the following paragraphs, we highlight our findings and interpret the deterministic results.

[3] The low gas price and the low CO_2 price case are the same as both prices are set to low for the first run.

6.1 Deterministic Analysis

For the deterministic analysis, the model is first run using low natural gas (31 €/MWh) and CO_2 (33 €/tCO_2) prices. At these prices, Figure 19, Figure 20 and Figure 21 shows the transmission capacities of the offshore wind farm hubs. All the connections and capacities are decided by the model.

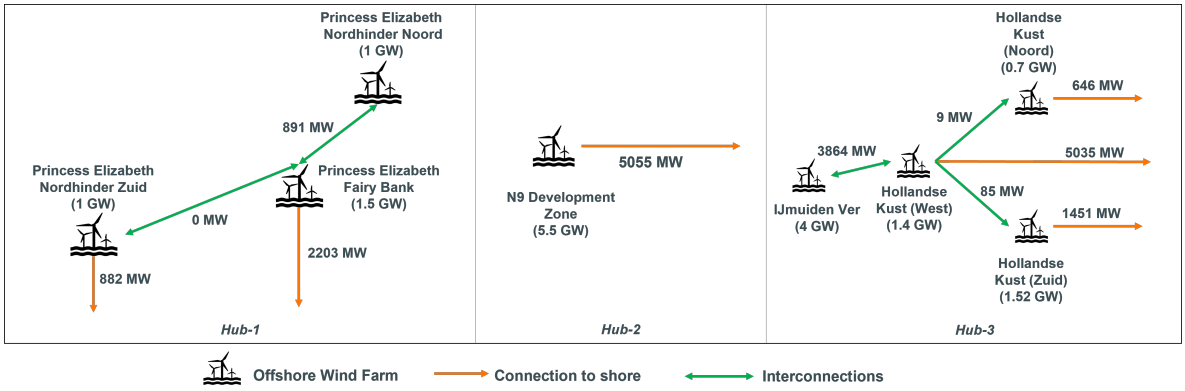

Figure 19: Wind farm Hubs 1-3 with transmission capacities at low gas and low CO_2 price

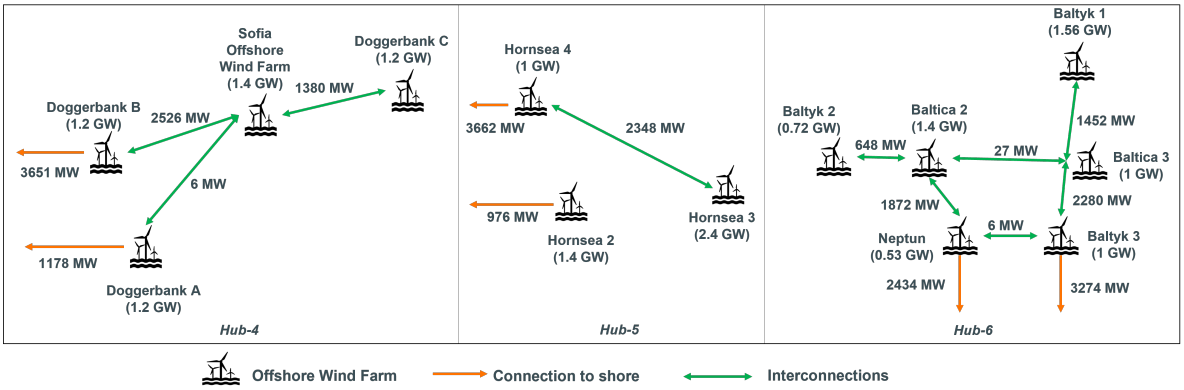

Figure 20: Wind farm Hubs 4-6 with transmission capacities at low gas and low CO_2 price

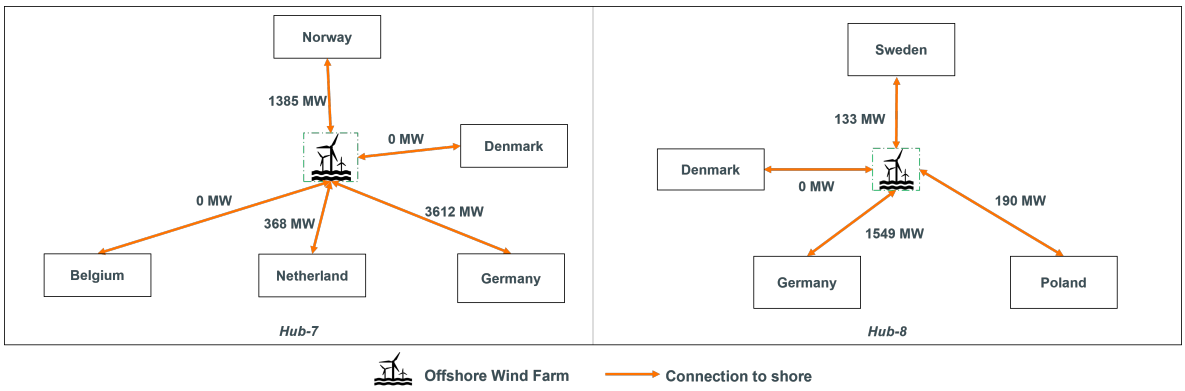

Figure 21: Wind farm Hubs 7 & 8 with transmission capacities at low gas and low CO_2 price

Some of the other major observations include:

- The annual operation cost of the system amounts to €66.5 Billion.
- The annual investment costs equal €7.5 Billion, which includes investment in additional gas-based generation capacity and transmission lines connecting offshore wind farms to the shore.
- The investment costs are lower than operational costs because in the model we start with a base system and allow only investments in storage, gas plants and transmission to connect future offshore wind farms.
- There is no investment in Li-Ion batteries at low gas and CO_2 prices in any market zone.
- Countries such as Germany (30 GW) , France (34 GW), and Great Britain (16 GW) invest significantly in additional gas-based power plant capacity.
- Not all the offshore wind farms which are grouped as a wind farm hub connect with each other. In some of the cases such as Hub 1 (Figure 19 and Hub 5 (Figure 20 nearby offshore wind farms choose not to connect with each other and instead radially connect to the shore.
- The total curtailment of energy from offshore wind farms is around 3.3 TWh which is less than 0.1% of the annual electric demand of all nodes, and about 0.5% of total offshore wind generation.
- In Hub 7, we observe an investment in high capacity (3.7 GW) of the hybrid interconnector from Germany to the Danish offshore wind farm. Even though the offshore wind farm belongs to Denmark, the model chooses not to connect the wind farm to the DK1 market zone because Denmark has sufficient capacity to match its system load during most of the year. We see the same effect in Hub 8, where the Danish offshore wind farm connects to Germany, Poland (PL), and Sweden instead of the Denmark (DK2) market zone.
- Furthermore, in Hub 7, the model does not connect the offshore wind farm to the Belgian (BE) market zone and connects to the Dutch market zone with a modest capacity due to the significant distance between the wind farm and these market zones.

We run the model two more times. First, by increasing the gas price to 227 €/MWh while the CO_2 price remains low. Next, we increase the CO_2 price to 300 €/tCO_2 while maintaining a low gas price. We observe the following effects when the prices are varied.

6.1.1 Effect of increase in natural gas and CO_2 price on transmission capacity from offshore wind farms

Generally, we observe from all the hubs that the power capacity of offshore transmission lines correlates positively with natural gas and CO_2 prices. However, as Figure 22 shows, the values of the capacity changes are rather modest. When increasing natural gas or CO_2 prices, we find that the investment in net landing capacity of the offshore transmission lines from the hubs is larger, although not by a large amount. Higher CO_2 and natural gas prices imply that, producing energy from gas and other fossil fuel-based power plants becomes more expensive. Therefore, renewable energy from offshore wind farms, which would be curtailed when natural gas and CO_2 prices are low, becomes more valuable.

On the other hand, to utilize this curtailed offshore wind energy, the model must invest in additional transmission capacity hence, causing the increase in capacity. In Figure 22 on the left, we see the optimal investments when the gas and CO_2 prices are low, whereas in the middle and on the right, we see the transmission capacity of the hub with increased gas and CO_2 prices respectively. The numbers in green and red below the lines show the change in transmission capacity of lines after increasing the gas and CO_2 prices. Figure 23 compares the curtailment of annual curtailed offshore wind energy at high and low CO_2 and natural gas prices and helps to infer that the curtailment of energy from offshore wind farms negatively correlates to the prices of natural gas and CO_2. We observe an 80% decrease in offshore wind curtailment when the natural gas prices increased and 65% decrease when CO_2 price is increased compared to the low price case.

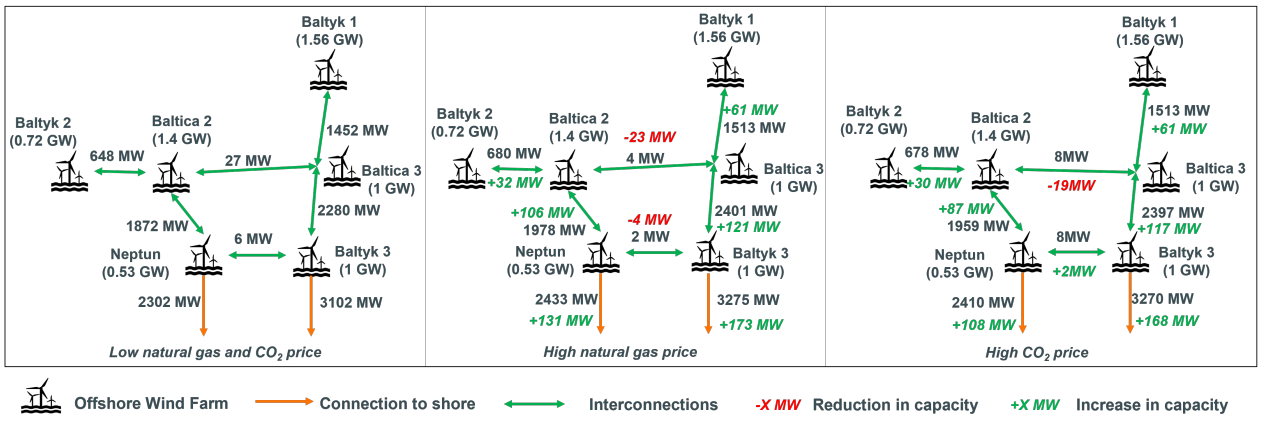

Figure 22: Transmission capacities for Hub 6 for three deterministic cases

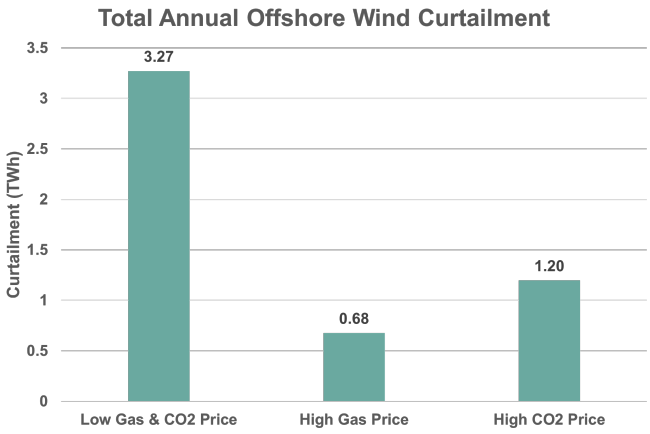

Figure 23: Overall change in annual curtailment from offshore wind farms

6.1.2 Effect of natural gas and CO_2 price increase on transmission capacity of hybrid interconnectors

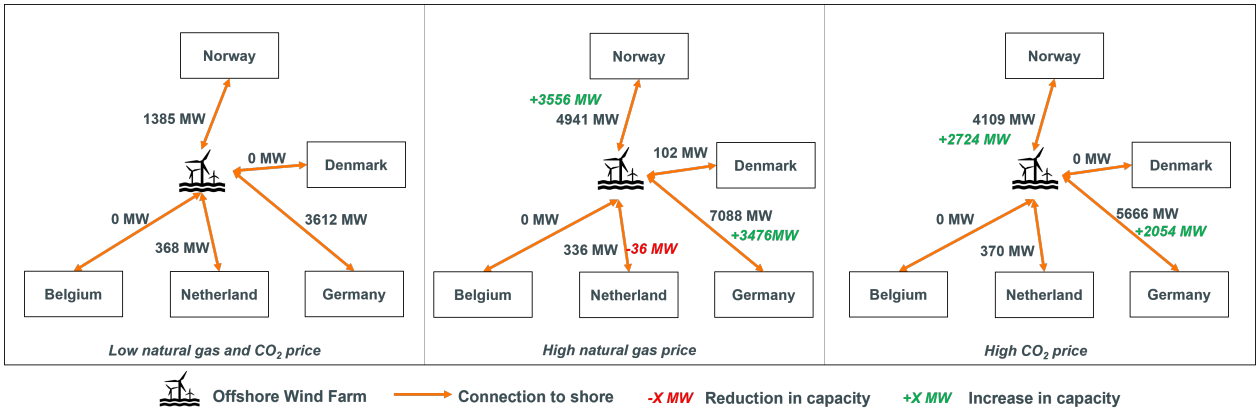

Figure 24: Changes in hybrid interconnector capacity of Hub 7 due to increased natural gas and CO_2 prices

Hub 7 shown in Figure 24 represents the Danish North Sea Energy Island, where the wind farm can potentially connect to five different countries. While doing so, the offshore wind farm's transmission lines act as a hybrid interconnector, enabling power trade between the countries. With an increase in natural gas prices, we observe a significant increase in the capacities of the lines connecting Norway and Germany to the wind farm. Around 20% of Germany's anticipated generation capacity in 2030 is powered by natural gas, which is highly affected by the increase in gas prices leading to high investments in connecting German to the Norwegian market zone. Rather than transferring the surplus hydropower from Norway to pumped hydro storage, the interconnection allows Germany to access this clean and cheap power reducing the need for additional gas power plants. We see a similar effect in the high CO_2 price case but not to the same level as the high natural gas price case. This is because only around 5% of the generation capacity in Germany is highly CO_2 intensive (coal-based power plants). Even though natural gas power plants emit CO_2, the intensity is lower (0.38 tCO_2/MWh vs 0.24 tCO_2/MWh)

compared to coal plants which is the reason for the difference in increase in capacities in both cases. However, these interconnection capacities are extremely high compared to the existing capacity between these countries. While these numbers appear high given the limited scope of the model, they indicate that more interconnection capacity is needed to transport electricity generated by offshore wind to the large demand centers in Europe and withstand a steep rise in natural gas and CO_2 prices in the future.

6.1.3 Investments in additional gas plant capacity

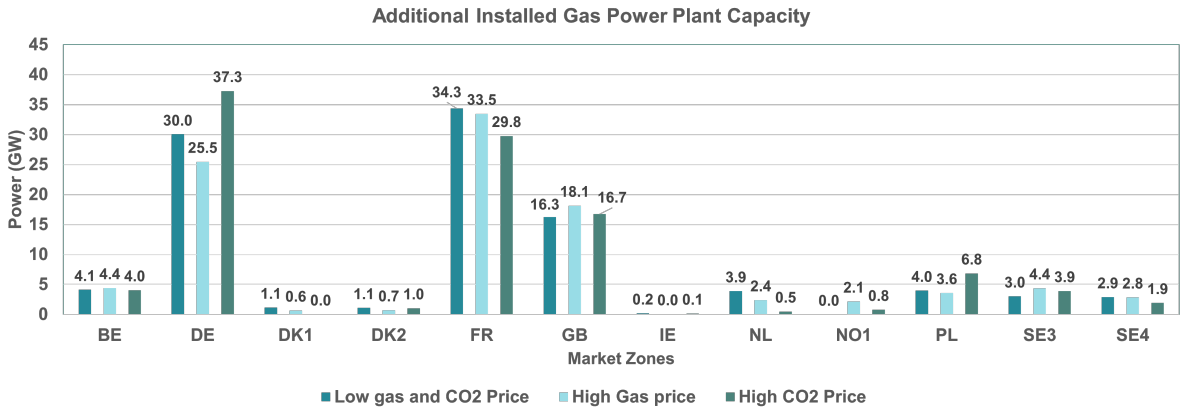

Figure 25: Variation in additional gas capacity installation at different market nodes caused by the change in gas and CO_2 prices

Figure 25 shows the change in additional gas capacities installed in different market zones caused due to the increase in gas and CO_2 prices. In the majority of market zones (DE, NL, PL, FR, IE, DK1 & DK2), we observe that by increasing the price of natural gas, the capacity of additional gas-based power plants that are installed reduces whereas in a few market zones (BE, GB, NO1 & SE3) it increases. As natural gas prices rise, most power exporting market zones are less willing to export the same amount of power as when gas prices were low; hence, their additional installed gas plant capacity decreases. Consequently, the nodes importing power must satisfy their demand by installing more gas plant capacity in their respective market zones. Across import-dependent nodes, higher gas prices led to the installation of more gas power plants. The planned renewable expansion is not enough to compensate the planned phase-outs of existing generation. Based on this, we can infer that there is potential to increase the targeted renewable capacities in import-dependent market zones that could be used instead of additionally installing gas power plants. From a system-wide perspective, we see a reduction in total additional gas plant capacity from 101 GW at a low gas price to 98 GW when the gas price is raised.

Similarly, on increasing the CO_2 price, we see a mixed effect with a few market zones where additional gas capacity increases and a majority where it reduces compared to the case in which

the CO_2 price was set to low. The capacity in market zones such as DE, PL, and IE increases because they are the only market zones with coal and lignite plants running as baseload generation in 2030. With the increase in CO_2 price, these power plants become extremely expensive to operate and are pushed out of the merit order by the low CO_2-intensive gas power plants. Figure 26 shows the difference in the DA dispatch for market zone PL with high and low CO_2 prices where coal power plants are pushed out of the merit order and are utilized only during the peak seasons.

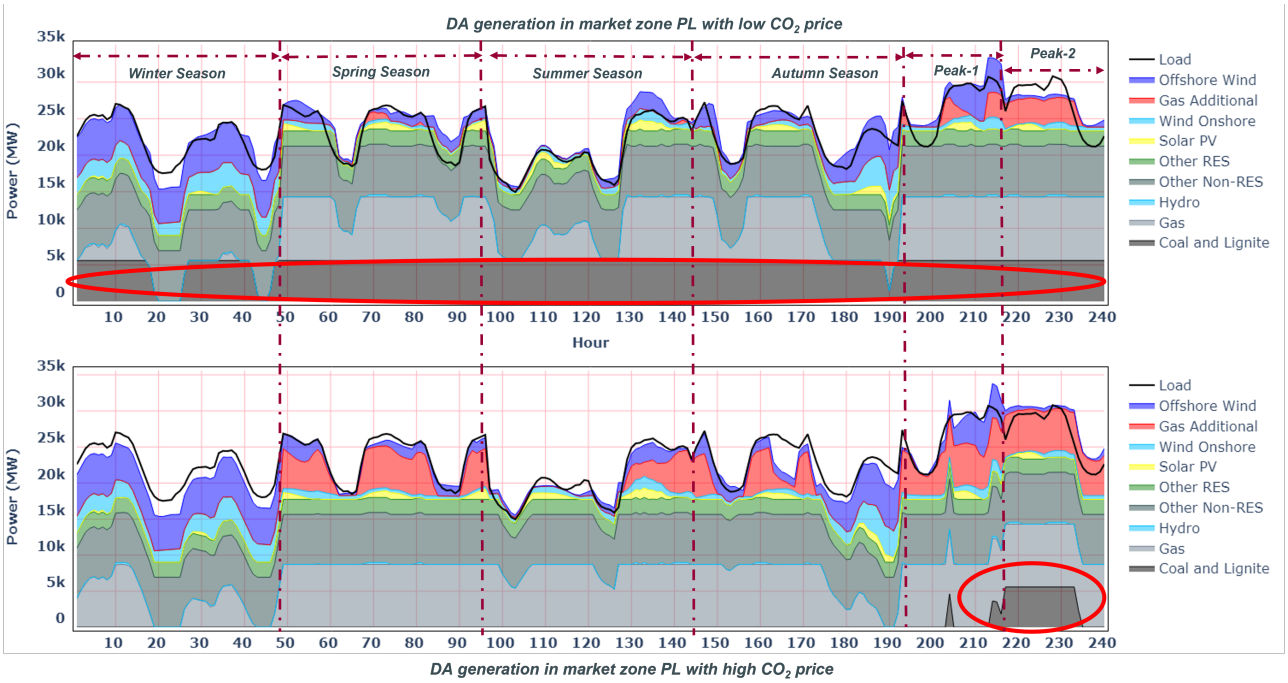

Figure 26: DA dispatch in Poland at high and low CO_2 price

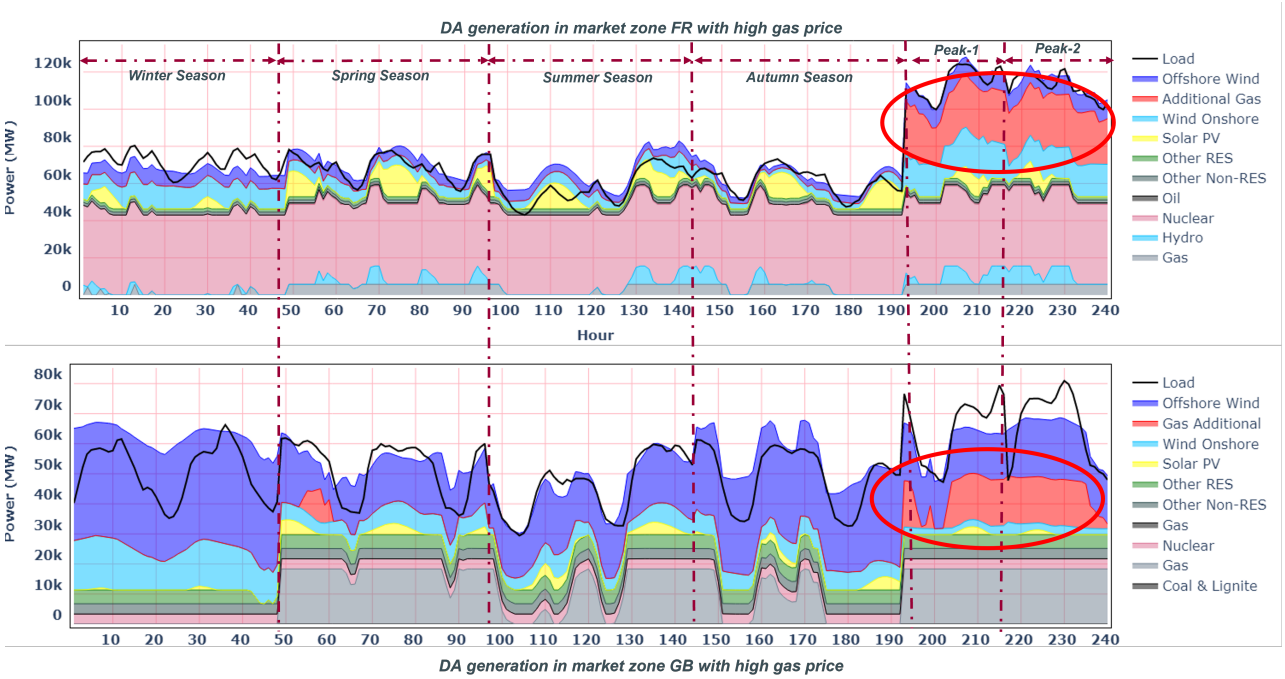

Figure 27: DA dispatch in France and Great Britain at high and low CO_2 price

Overall, in both cases, the installed additional gas capacities are high because of the generation capacity included exogenously in the model is insufficient to meet the demand in the high demand seasons. Majority of the market zones considered in the model have a high expected share (>60%) of renewable capacity in 2030, which makes them vulnerable to adverse climate conditions. The way how the scenario tree is constructed, with the peak scenarios in different market zones occurring at the same time, we probably overestimate the gap between exogenous generation capacity and demand. Market zones that are far away generally experience different climatic conditions. In the event of peak demand and low renewable output, interconnections between different market zones could help alleviate the burden in the system without the need for additionally installed generation capacities. Additionally, unlike the TYNDP data, we consider a fixed electric demand without any options for demand response which also plays a role in installing high gas plant capacity. We further examine the economic dispatch for the nodes GB and FR for all the seasons, as shown in Figure 27. We observe that the additionally installed gas plants are only utilized at their maximum capacity in the two peak seasons when the entire system is short with power.

6.1.4 Investments in storage capacity

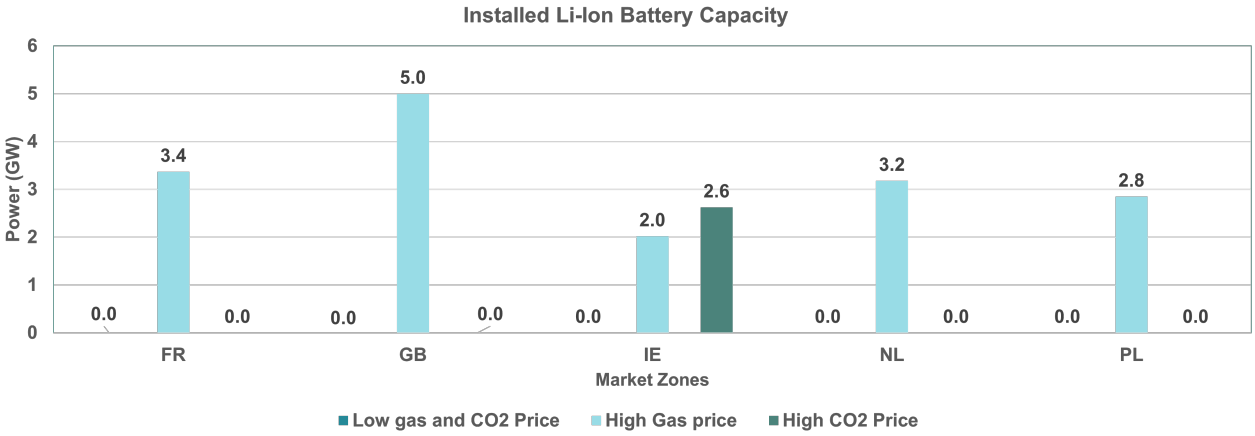

Figure 28: Variation in Li-Ion battery capacity installation at different market nodes caused by the change in gas and CO_2 prices

In the case with high natural gas price, we observe that investment in Lithium-Ion batteries occurs predominantly when the natural gas price is high (Figure 28). The model does so to utilize the cheap offshore wind energy which is curtailed during the low gas price case. At high gas prices, 80% of the curtailment in offshore energy is reduced, which would require additional storage capacity. As a result, market zones with high shares of offshore wind capacities in their generation fleets, such as GB, NL, FR, PL, and IE, see a sudden rise in investment in Lithium-Ion batteries.

6.2 Stochastic Analysis

We use the results from the high gas price case of the deterministic analysis as the basis for the stochastic analysis. We identify for each offshore hub to coast transmission line the operational hour when it transmits at maximum capacity, and introduce outages on the lines on these hours in one scenario per season, causing the model to consider a redispatch of the DA schedule, and possibly adjust the DA schedule. We investigate whether the outages trigger changes in investment and analyze the redispatch options used by the model to deal with the outages. We introduce one outage per season, which equals approximately 18 outage events per year on each line in a scenario. The following paragraphs briefly explain and discuss the results obtained.

6.2.1 Generation, Transmission and Storage investments

We observe no differences in endogenously installed capacities for generation, transmission lines and storage in the entire system in the stochastic set up compared to the deterministic set up. A quick first insight is that so much gas-fired capacity is added, that the deterministic optimal investments can deal with the sudden losses of power accounted for in the stochastic analysis.

6.2.2 Redispatch due to outages

Figure 29 and Figure 31 give an overview of the redispatch decisions caused by the outages of the offshore transmission lines from the hubs. As we consider outage on one transmission link per scenario, each scenario in Figure 29 and Figure 31 represents a separate instance of an outage. We start with Scenario 2 because Scenario 1 includes no outages, and the DA schedule is realized as is. The bars in red represent a negative change to the DA dispatch, whereas the bars in green represent a positive change. In Figure 29 we see the changes to the DA schedule caused due to the transmission outages in wind farm hubs connected to a single market zone, while Figure 31 displays the changes caused due to outages of transmission lines of wind farm hubs connected to more than one market zones.

Redispatch: Scenario 2 - Scenario 7

First, we analyze the redispatch through Scenario 2 - Scenario 7 (Figure 29) which consider outages on hubs which are connected to a single market zone. Following are the observations:

- In the majority of the scenarios, gas-based power plants respond to the outages.
- Pumped hydropower plants and Li-Ion batteries also support the system in conjunction with the gas-based power plants.

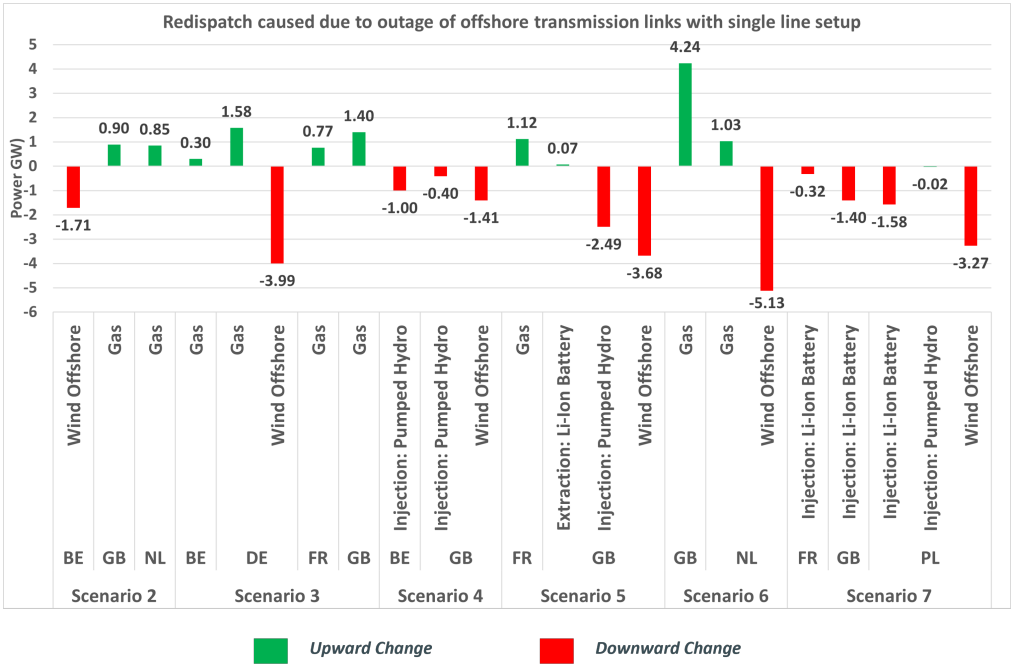

Figure 29: Redispatch with single line setup: Scenario 2-7

- **Activation of gas based power plants**

  Except for Scenario 7 and Scenario 4, gas-based power plants play a role in providing power in all scenarios. We observe that a market zone losing power flow is supported by its gas power plants and gas plants from interconnected markets. Further, we observe that the gas plants providing power are the existing ones rather than the additionally installed ones. A power plant must be part of the DA economic dispatch to provide balancing power. As additional gas plants are non-operational during most of the year (normally operational only during peak seasons), they cannot provide quick balancing power during regular seasons. Due to the losses in transmission, when gas plants from neighboring market zones support another node for power, the neighboring nodes need to generate more than the actual loss of power at the receiving node. The power support from the gas power plants is similar to the activation of balancing power from the FCR reserves and shows that with the current cost assumptions, it is the cheapest way to deal with high-capacity outages. The gas plants can ramp up instantly as they are already in operation in the DA market and support the system in times of need.

- **Support from storage assets**

  In Scenario 7, we observe that a 3.3 GW outage on the link from Baltyk-3 wind farm to Poland is wholly dealt with by the flexibility in operation provided by the storage assets. Pumped hydro and Lithium-Ion batteries reduced their intake during the outage, providing the necessary power to keep the system stable. This scenario indicates that storage assets such as Lithium-Ion batteries and pumped hydro can respond well to the require-

ments of the balancing market. As they can regulate power in both directions, they can be beneficial in dealing with sudden changes in the system by providing quick balancing power.

Other Observations

Figure 30 shows the changes in the topology of Hub 4 caused by the possibility of an outage of transmission line from Doggerbank B offshore wind farm to the shore.

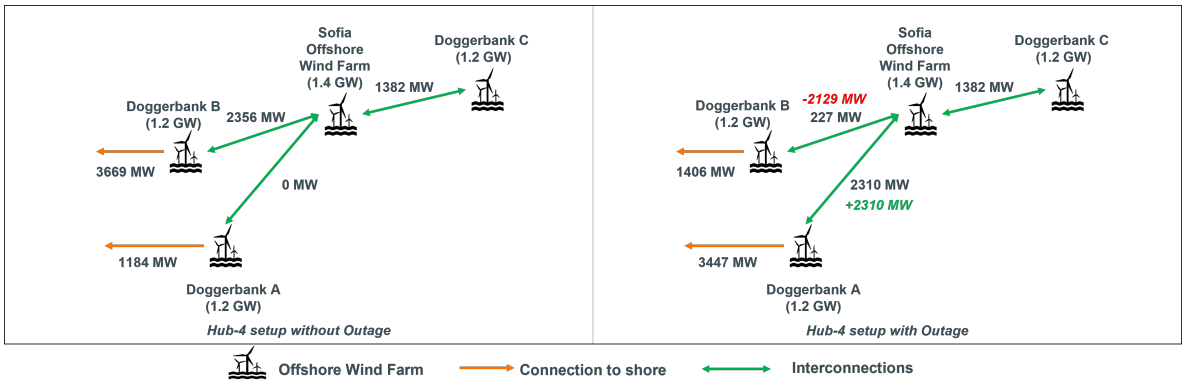

Figure 30: Change in hub interconnection caused due to the outage (Hub 4 c.f. Figure 15)

As a consequence of an outage probability, we observe that the model reroutes the power by investing in an alternate pathway for the power flow. Instead of transmitting power through Doggerbank B, the model connects the Sofia Offshore wind farm to Doggerbank A, which effectively reduces the power loss after an outage from approximately 3.7 GW to 1.4 GW. As shown in Figure 29 in Scenario 4, this 1.4 GW loss is dealt with by a combination of pumped hydro and lithium-ion batteries, which reduce their injection during the hour of outage. Hence, transmission topology changes can also effectively reduce the impact of the loss of power from high-capacity offshore wind farm hubs.

Redispatch: Scenario 8 - Scenario 10

Scenarios 8-10 represent outages on Hubs 7 and 8 (c.f. Figure 16. Scenarios 8 and 9 consider outages in Hub 7 for the transmission lines connecting the offshore wind farm to Germany and Norway, respectively. In Scenario 10, we consider outages for Hub 8 on the line connecting the offshore wind farm and Germany. These hubs connect to more than one market zone and serve as hybrid interconnectors. Analyzing the redispatch in Scenarios 8 - 10 (Figure 26), we observe the following points:

- **Outages on hybrid interconnectors affect multiple nodes**

  Compared to redispatch in Scenarios 2-7, we observe multiple redispatch decisions occurring due to the failure of hybrid lines. For example in Scenario 8, outages on a hy-

brid line importing power caused redispatch in seven different market zones. The major reason is that such hybrid interconnectors act as a bridge between regions with high renewable capacity such as Norway and other countries which could benefit from importing cheap renewable energy. Hence, outages on hybrid creates a ripple effect in the system. Or, in other words, can benefit from their multiple connections to mitigate the consequences of an outage.

- **Outages on power exporting lines can cause curtailment of renewables**

  Further, in Scenario 8, as market zone NO2 was exporting power, an outage caused a curtailment of power from onshore (0.3 GW) and offshore (1.6 GW) wind. As most of the power from the offshore wind farm was flowing towards market zone DE, the unavailability of transmission capacity forced the curtailment of power from the offshore wind farm. To an extent, the model rerouted power to flow from the offshore wind farm to the pumped hydro system (0.9 GW) at market zone NO2 but could only minimize curtailment to 1.6 GW instead of 2.5 GW of offshore wind power. Hence, the unavailability of transmission capacity can push clean and cheap renewable energy out of the system leading to increased curtailment. This may be socially undesirable, but is in our model setting the lowest cost solution.

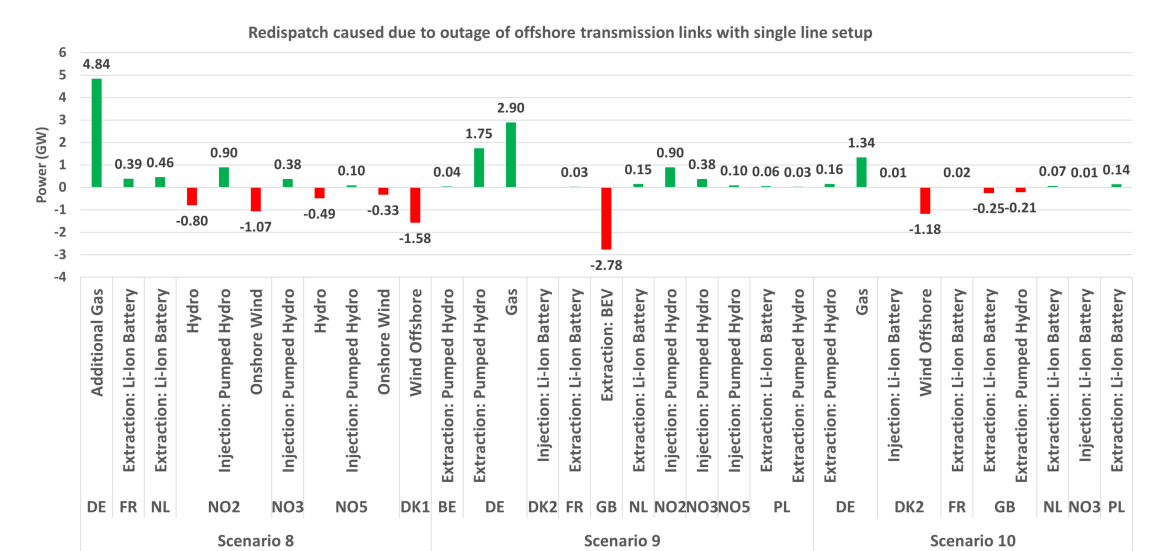

Figure 31: Redispatch with single line setup: Scenario 8-10

6.3 Sensitivity Analysis

We perform sensitivity analyses to determine the feasibility of installing second, parallel, lines connecting the hubs to the shore. We identify two parameters that can affect the decision to install a second line; fixed investment costs of the dual line system and the probability of occurrence of outages. First, we vary the fixed costs of the double line system to be 200%,

150%, 120%, and 100% compared to the single line setup cost. In addition, we vary the probability of occurrence of outages from 1% as in the analysis above, to 3% and 5% for the 150% and 120% cases. Table 4 provides an overview of the sensitivity analysis results. The table entries marked in green highlight where investment in double lines happen.

Table 4: Results- Sensitivity analysis

Probability of Outages	**1%**				**3%**		**5%**	
Fixed Cost of Double Line =	**2X**	**1.5X**	**1.2X**	**1X**	**1.5X**	**1.2X**	**1.5X**	**1.2X**
Hub-1	✗	✗	✗	✓	✗	✓	✓	✓
Hub-2	✗	✗	✗	✓	✓	✓	✓	✓
Hub-3	✗	✗	✗	✓	✓	✓	✓	✓
Hub-4	✗	✗	✗	✗	✗	✗	✗	✗
Hub-5	✗	✗	✗	✓	✓	✓	✓	✓
Hub-6	✗	✗	✗	✓	✗	✗	✓	✓
Hub-7 (DE)	✗	✗	✗	✗	✗	✗	✗	✗
Hub-7 (NO)	✗	✗	✗	✓	✗	✓	✓	✓
Hub-8	✗	✗	✗	✗	✗	✗	✓	✓

X Fixed cost of Single Transmission system line from hubs.
✗ No investment in double line setup from the hub.
✓ Investment in double line setup from the hub.
(DE) Line from wind farm to Germany, **(NO)** Line from wind farm to Norway.

We observe that for Hub 4 and Hub 7 (line from the wind farm to Germany), there is no investment in the double line setup for all considered probabilities of outages and fixed investment costs. In the case of Hub 4, as the power is rerouted (c.f. Section Other Observations) through a different path, increasing the fixed cost and probability of occurrence will not affect the topology of the hub. As the link facing outages in Hub 4 can now at a maximum transport 1.4 GW, the disruption is handled onshore by pumped hydro storage (c.f. Figure 29, Scenario 4). On the other hand, outages on the hybrid interconnector connecting the offshore wind farm to Germany do not warrant an investment in a second line, mainly due to the significant distance (320 km) between the wind farm and Germany. As the transmission cost correlates positively to transmission length, it is more economical to run the installed gas power plants (c.f. Figure 31, Scenario 8) than to invest in additional transmission capacity.

At a 1% probability of occurrence of outages, we see no investments in a parallel line until there are no additional fixed costs to install another line. This is an unlikely case in reality, as installing a second line would require additional fixed costs, such as the cost of setting up cable trenches in the subsea environment. Increasing the probability of outages to 3%, we see a more likely result where three of the five hubs invest in a parallel line when additional fixed costs of the parallel line setup are 50% of the cost of installing a single line. At the same fixed cost level, with 5% of outage probability, six of the eight hubs install a parallel line system.

Increasing the probability of outages decreases the reliability of the transmission lines, and the model counters this by installing parallel lines and ensuring at least half the installed capacity is available to transmit power at all times.

Figure 34, Figure 35 and Figure 36 (c.f. Appendix 2) show the topology of the hubs with a double line setup (for fixed cost 150% and outage probability 5%). We observe that apart from the transmission capacity of the lines experiencing outages, there are no other changes in the transmission capacity of other lines in the hub. Even though the model was free to set the net capacity of the double line system greater than that of the single lines, the model chooses to invest the same total capacity.

6.3.1 Redispatch due to outages with parallel lines

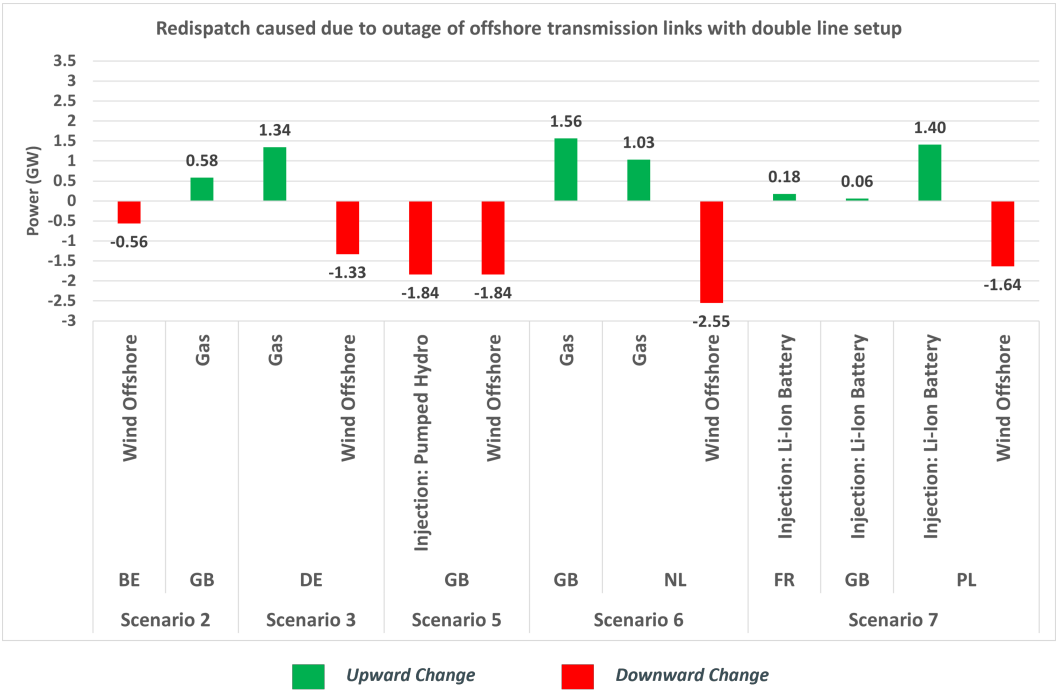

Figure 32: Redispatch with double line setup: Scenario 2,3, 5-7

Installing a parallel line reduces the power outages to half the capacity compared to a single line setup, reducing the need for redispatch. Figure 32 and Figure 33 shows how the system copes with power outages when parallel lines are installed. During an outage event, one of the lines in the double line setup transmits power at its maximum limit to make use of as much energy from the offshore wind farms as possible. As a result, we see fewer activation of redispatch options. Similar to previous observations in the case of outages in single line setup, gas-based power plants, pumped hydro, and Lithium-Ion batteries now respond to outages with reduced power requirements.

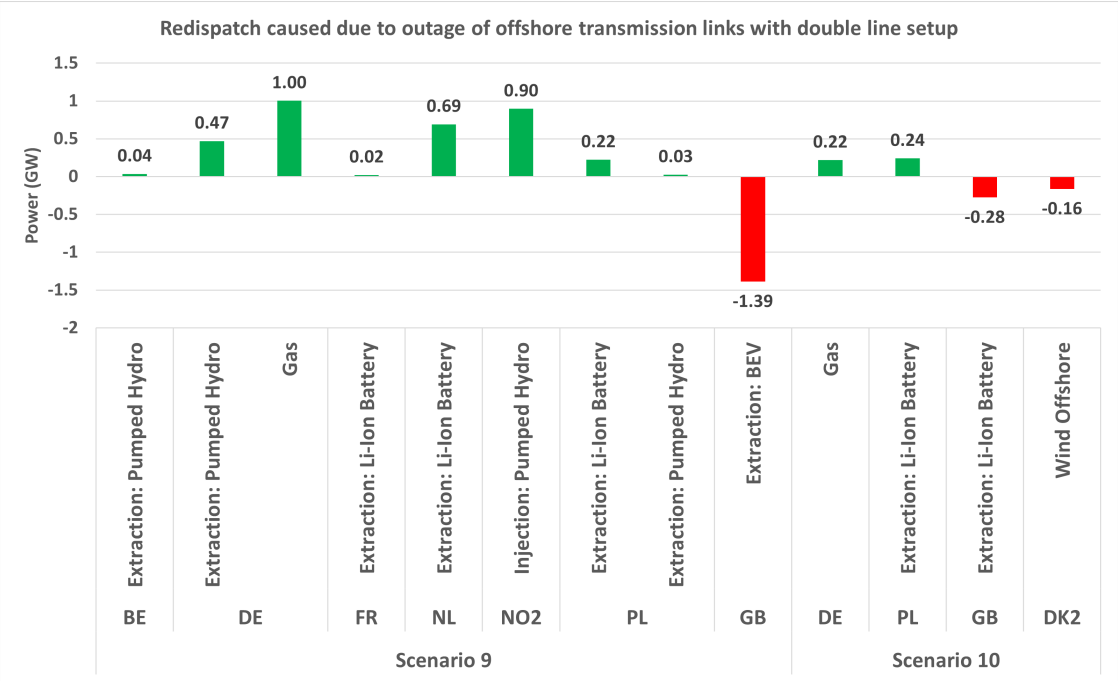

Figure 33: Redispatch with double line setup: Scenario 9 & 10

In Scenario 10 of Figure 33, we see that the installation of double line system reduced the curtailment during an outage instance from 1 GW to nearly 0.2 GW. The offshore wind which would have been curtailed is redirected towards GBwhere the flexible BEVs reduce their power extraction. Subsequently, market zone GB exports lesser power to DE, NL, and PL where we see lithium-ion batteries providing balancing power.

7 Conclusion and Future Research

7.1 Conclusion

We developed a three-stage stochastic model to assess optimal investments in generation, transmission, and storage systems to counter high-capacity HVDC transmission disruptions that may occur on transmission lines transmitting power from large-scale offshore wind farms to the shore. Additionally, we assess redispatch decisions necessary to provide power during sudden loss of power greater 3 than GW. For the analysis we restricted the geographical scope of the model to represent the zonal electricity market covering ten (NSEC, Great Britain and Poland) countries in North-West Europe.

First, we analyze outages of HVDC interconnectors in the North and Baltic Seas and find that offshore power transmission lines face outages due to physical damages to lines or commutation failures in the HVDC converters. However, these events have a very low probability of occurrence. As HVDC transmission will predominantly be used to transmit power from offshore wind farms, we assume a low probability of failure for the transmission lines from offshore wind farms for our analysis. Further, we develop datasets of offshore wind farms in the North, and the Baltic Seas planned to be developed by the NSEC countries, Great Britain and Poland, until 2030. The datasets include information about offshore wind farms, such as approximate location, power capacity, and distance to the shore. We manually cluster offshore wind farms into hubs based on the distance between them.

We then conducted a deterministic analysis without considering outages on transmission lines from offshore wind farm hubs. In the deterministic analysis, we find interconnection capacities for all wind farm hubs and the net capacity connected from the hub to the shore. By varying the CO_2 and the gas price, we discovered a correlation between variation in prices and curtailment of offshore wind. We found that CO_2 and gas prices are negatively correlated to the curtailment of offshore wind in a system with high offshore wind penetration. Increasing CO_2 price to 300 €/tCO_2 pushed CO_2 intensive plants out of the merit order and increased production from gas-based power plants instead. Increasing gas prices caused a slight decrease in export from market zones, causing the installation of gas power plants predominantly in import-dependent market zones. Also, we identified that the planned build-out of renewables is not enough to compensate for the planned phase-outs of existing generation in import-dependent market zones, and there is a need for increased renewable targets.

Next, we conducted a stochastic analysis while considering the disruption of transmission lines from offshore wind farm hubs. There is no change in net transmission capacities from the hubs showing that the choice of topology determined by both deterministic and stochastic analysis

is resilient. No additional investments were required to the existing onshore system to handle sudden power loss greater than 3 GW caused due to the failure of power supply from large offshore wind farm clusters because there is a lot of flexible gas-fired generation available in the system. Redispatch of power from gas-fired power plants, lithium-ion batteries, and pumped hydro capacities was cost-optimal to deal with outage events of low probability. However, outages in hybrid interconnections (Hub 7 and Hub 8) required redispatch in several market zones to deal with the outage. Increased interconnection between market zones provides sufficient flexibility in the system by allowing access to system-wide redispatch options. By conducting a sensitivity analysis, we recognize that increasing the probability of outage and meanwhile decreasing the fixed investment cost to construct a parallel line connecting the offshore wind farm to the shore caused the model to invest in a second line. Installation of a parallel line reduced the magnitude of the power outage, which caused reduced redispatch decisions in the system.

7.2 Scope for Future Research

We identify the following enhancement directions to increase the relevance of our model in real-world scenarios. These enhancements have been identified based on the limitations of our model.

DC Power Flow

In our modeling approach, we consider an economic dispatch in both DA and ID markets without taking into account the physical constraints of the complex AC power grid. Simulating AC flow in the grid using the DC power flow approximation would better represent the dispatch restrictions in the real world.

Flexibility Options

Apart from the flexibility options in our model, there are a few other possible options that have the potential to provide flexibility, such as heat sector coupling, power to gas, and demand-side response. Heat sector coupling enables the option to use co-generating power plants to provide operational flexibility. Even though these plants have a must-run obligation in colder seasons, there is potential to extract flexibility by adjusting heat ratios which can sometimes be cheaper than the flexibility options considered in our model.

Offshore wind growth brings attention to the potential for hydrogen as a fuel. However, in our model, we do not consider the possibility of using the energy from offshore wind to produce alternate energy carriers such as hydrogen. With the help of electrolyzers, electricity can be converted to hydrogen, which is essential for various industrial processes. Member states of

the NSEC plan to construct energy islands with production facilities that can produce hydrogen offshore wind farms. In such a case, if the transmission line from the wind farm goes down, the lost power can be used to generate hydrogen, reducing the curtailment of renewable energy. On the other hand, installing electrolyzers solely to provide flexibility due to outages is not feasible due to their high investment costs.

Another approach to dealing with a sudden power loss is adjusting electricity consumption quickly. Large industries with flexible loads can regulate their demand when needed decreasing the pressure to satisfy all electric demand when the system is under stress.

Cluster Analysis and Geographic Information System Tools

In our model, we made the best effort to assess offshore wind farm areas and the distances between them and manually create wind farm clusters. A clustering process based on distances may not always be realistic because of the various design choices and limitations in individual wind farm projects. However, the model can be extended to support these design choices by incorporating sophisticated clustering algorithms that can replace manual distance-based clustering using Geographic Information System (GIS) tools. Several topological configurations can be set up to test multiple failure scenarios hub configurations.

8 Appendix 1: Input Data

Table 5 - Table 13 provide an overview of the various input data parameters considered in the model.

Table 5: Dispatchable power plant parameters (Backe et al., 2022; Koffi et al., 2017)

Power Plant	Availability (%)	Ramp Rate (% Max Capacity)	Efficiency (%)	CO_2 Content (tCO_2/GJ)
Coal & Lignite	75	70	37	0.1042
Gas	80	85	49	0.0667
Nuclear	75	30	38	0
Oil	85	85	38	1.1016
Other Non-RES	95	85	33	0.037
Other RES	72	81	50	0.0324

Table 6: Generation capacities of market zones in 2030, (ENTSO-e, 2022)

Market Zone	Solar PV (GW)	Wind Onshore (GW)	Wind Offshore (GW)	Hydro (GW)	Other-RES (GW)	Gas (GW)	Coal & Lignite (GW)	Oil (GW)	Nuclear (GW)	Other Non-RES (GW)
BE	5.2	3.7	5.9	0	0.9	8.7	0	0	0	0.8
DK1	2.5	3.0	5.6	0	1.1	1.0	0.2	0	0	0
DK2	1.5	1.9	5.0	0	1.4	0.3	0	0	0	0
DE	40.4	60.3	22.2	1.3	7.6	35.0	9.0	0.9	0	8.7
FR	25.0	28.8	10.9	9.9	2.4	7.2	0	1.0	57.4	1.6
IE	0.4	4.3	5.1	0	0.1	4.1	0	0.3	0	0.1
NL	21.4	6.4	11.4	0	3.9	14	0	0	0.5	1.8
NO1	0.2	0	0	3.5	0	0	0	0	0	0
NO2	0	3.8	3.0	8.5	0	0	0	0	0	0
NO3	0	3.8	0	4.4	0	0	0	0	0	0
NO4	0	3.0	0	5.3	0	0	0	0	0	3.0
NO5	0	0.8	0	10.4	0	0	0	0	0	0
PL	2.6	6.9	6.2	0.3	2.9	10.9	7.5	0	0	7.3
SE1	0.2	1.4	0	5.4	0.3	0	0	0	0	0
SE2	0.3	3.3	3.9	8.1	0.8	0.1	0	0	0	0
SE3	1.7	8.6	0	2.6	2.9	0.1	0	0	3.7	0
SE4	0.5	2.3	2.0	0.3	0.8	0	0	0	0	0
GB	7.9	21.3	39.5	0	6.3	22.9	0	0.1	4.5	3.6

The table gives an overview of the maximum generation capacity of each technology. However, the hourly production is based on availability parameter as explained in Chapter 5.

Table 7: Battery technology parameters, (Backe et al., 2022; Cole and Frazier, 2021)

Storage Technology	Charging Efficiency (%)	Discharging Efficiency (%)	Energy Retention Efficiency (%)
Li-Ion Battery	90	99	100
PH	80	85	90
BEV	75	90	100

Table 8: NTC between market zones in 2030 in GW, (Tosatto, 2022)

	BE	DK1	DK2	DE	FR	IE	NL	NO1	NO2	NO3	NO4	NO5	PL	SE1	SE2	SE3	SE4	GB
BE				3	4.3		3.4											1
DK1			0.6	3.5			0.7		1.64							0.74		1.4
DK2		0.6		1													1.7	
DE	3	3.5	1		4.8		5		1.4				3				1.3	1.4
FR	4.3			4.8		0.7												5.4
IE					0.7													1
NL	3.4	0.7		5					0.7									1
NO1									4.8	1.05		5.4				2.1		
NO2		1.64		0.7			0.7	4.8				1.2						1.4
NO3								1.05			2	0.7			1			
NO4										2		0		0.7	0.35			
NO5								5.4	1.2	0.7								1.4
PL				3										0			0.6	
SE1												0.7			3.3			
SE2										1	0.35					10.3		
SE3		0.74						2.1							10.3		3.2	
SE4			1.7	1.3									0.6			2		
GB	1	1.4		1.4	5.4	1	1		1.4			1.4						

Table 9: Transmission investment costs, (Vrana and Härtel, 2018)

Transmission Type	Fixed Cost (M€)	Length Cost (M€/km)	Length Power Cost (€/MW-km)	Power (M€/MW)
Single Line Offshore-Onshore (OWF)	84.45	0.27	980	0.836
Double Line Offshore-Onshore (OWF)	168.90	0.54	980	0.836
Single Line Onshore-Onshore (IC)	50.63	0.27	980	0.225
Double Line Onshore-Onshore (IC)	101.26	0.54	980	0.225
Single Line OWF-OWF (Links)	3.63	0.27	980	0

Offshore - Onshore: Connection from offshore wind farm to the shore.

Onshore - Onshore: Connection between two onshore zones.

OWF - OWF: Interconnection between offshore wind farms.

Table 10: BEV capacity in each market zone in 2030, (ENTSO-e, 2022)

Market Zone	**Capacity (GWh)**
BE	4.165
DK1	1.698
DK2	1.105
DE	26.668
FR	23.298
IE	1.994
NL	6.843
NO1	9.696
NO2	4.523
NO3	0.362
NO4	0.311
NO5	10.164
PL	5.358
SE1	0.453
SE2	0.746
SE3	3.019
SE4	1.024
GB	19.906

10% of the capacity is available for providing flexibility.

Table 11: Generator fuel and variable costs, (Backe et al., 2022)

Generator	**Variable O&M Cost (€/MWh)**	**Fuel Costs (€/GJ)**
Coal & Lignite	2.70	2.30
Gas	2.31	8.70
Oil	2.76	15.60
Other Non-RES	0.82	0
Nuclear	7.50	1.06
Hydro	0.32	0
Solar PV	0.05	0
Onshore Wind	0.18	0
Offshore Wind	0.39	0
Other-RES	1.88	6.26
Additional Gas	2.31	8.70

Table 12: Generator investment Costs, (Backe et al., 2022)

Generator	**Capital Cost (€/kW)**	**Fixed O&M Cost (€/kW)**
Additional Gas	400	19.5

Table 13: Storage related investment Costs, (Backe et al., 2022; Cole and Frazier, 2021)

Storage	**Capital Cost (€/kWh)**	**Fixed O&M Cost (€/kW)**
Li-Ion Battery	198.41	5.16

9 Appendix 2: Additional Figures

Figure 34, Figure 35, and Figure 36 show the topology of the wind farm hubs after a parallel line connecting the hub to the shore is installed.

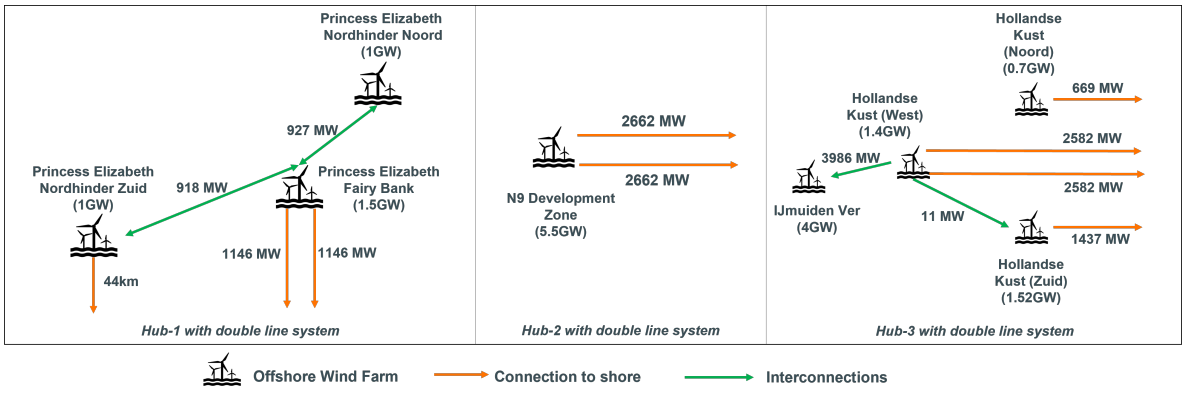

Figure 34: Wind farm Hubs 1-3 with double line setup

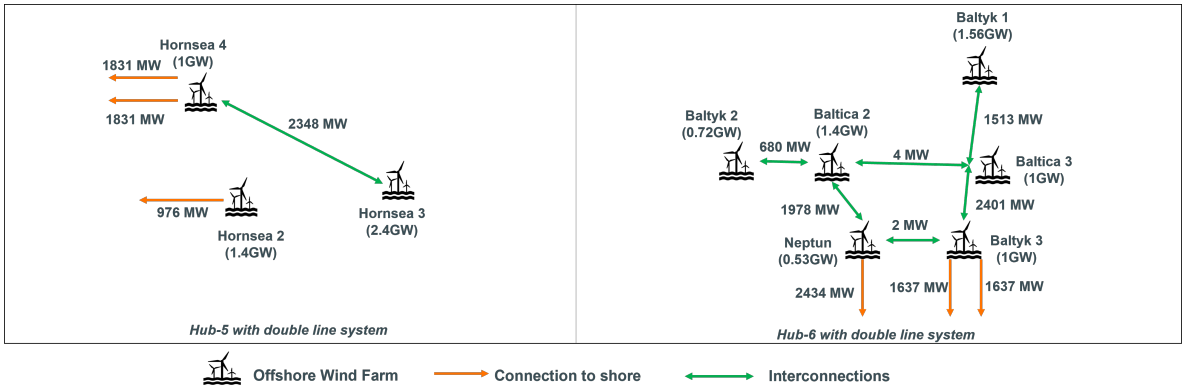

Figure 35: Wind farm Hubs 5 & 6 with double line setup

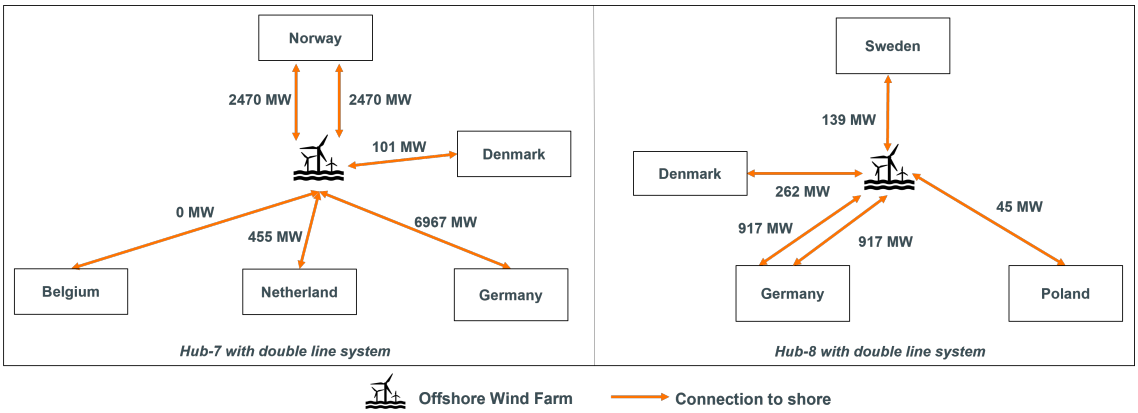

Figure 36: Wind farm Hubs 7 & 8 with double line setup

References

4C Offshore (2021). "Global Offshore Renewable Map". https://map.4coffshore.com/offshorewind. Accessed: 2022-06-20.

50Hertz Transmission GmbH (2020). "Combined Grid Solution". https://www.50hertz.com/de/News/Details/7331. Accessed: 2022-05-22.

Amaral, S. S., Costa, M. A. M., Soares Neto, T. G., Costa, M. P., Dias, F. F., Anselmo, E., Santos, J. C. dos, and Carvalho, J. A. de (2019). "CO_2, CO, hydrocarbon gases and $PM_{2.5}$ emissions on dry season by deforestation fires in the Brazilian Amazonia." In: *Environmental Pollution* 249, 311–320.

Anderson, T. R., Hawkins, E., and Jones, P. D. (2016). "CO_2, the greenhouse effect and global warming: from the pioneering work of Arrhenius and Callendar to today's Earth System Models." In: *Endeavour* 40.3, 178–187.

Backe, S., Skar, C., del Granado, P. C., Turgut, O., and Tomasgard, A. (2022). "EMPIRE: An open-source model based on multi-horizon programming for energy transition analyses." In: *SoftwareX* 17, 100877.

Bakirtzis, G. A., Biskas, P. N., and Chatziathanasiou, V. (2012). "Generation Expansion Planning by MILP considering mid-term scheduling decisions." In: *Electric Power Systems Research* 86, 98–112.

Bañol Arias, N., Hashemi, S., Andersen, P. B., Træholt, C., and Romero, R. (2020). "Assessment of economic benefits for BEV owners participating in the primary frequency regulation markets." In: *International Journal of Electrical Power & Energy Systems* 120, 105985.

Becker, S., Rodriguez, R., Andresen, G., Schramm, S., and Greiner, M. (2014). "Transmission grid extensions during the build-up of a fully renewable pan-European electricity supply." In: *Energy* 64, 404–418.

Benjamin, S., Fleischer, C., Kilmartin, A., and Langhelle, O. (2020). *Opportunities and barriers to interconnector expansion in the North Sea Region*. Tech. rep. Brussels, Belgium: University of Stavanger.

Bilgili, M., Yasar, A., and Simsek, E. (2011). "Offshore wind power development in Europe and its comparison with onshore counterpart." In: *Renewable and Sustainable Energy Reviews* 15.2, 905–915.

Birge, J. R. and Louveaux, F. (2011). *Introduction to stochastic programming*. New York, NY: Springer.

Brauers, H., Oei, P.-Y., and Walk, P. (2020). "Comparing coal phase-out pathways: The United Kingdom's and Germany's diverging transitions." In: *Environmental Innovation and Societal Transitions* 37, 238–253.

Cole, W. J. and Frazier, A. (2021). *Cost projections for utility-scale battery storage*. Tech. rep. National Renewable Energy Lab.(NREL), Golden, CO (USA).

EIA (2021). *Climate Considerations in the International Energy Outlook 2021*. Tech. rep. Washington DC, USA: U.S. Energy Information Administration (EIA).

Elia Group (2021). *Roadmap to Net Zero*. Tech. rep. Brussels, Belgium: Elia Group.

Elliott, M., Swan, L. G., Dubarry, M., and Baure, G. (2020). "Degradation of electric vehicle lithium-ion batteries in electricity grid services." In: *Journal of Energy Storage* 32, 101873.

ENTSO-e (2018a). *All CE TSOs' proposal for the dimensioning rules for FCR in accordance with Article 153(2) of the Commission Regulation (EU) 2017/1485 of 2 August 2017 establishing a guideline on electricity transmission system operation*.

– **(2018b)**. *Explanatory note for the FCR dimensioning rules proposal*. Tech. rep. Brussels, Belgium: European Network of Transmission System Operators for Electricity (ENTSO-e).

– **(2021)**. *HVDC Utilisation and Unavailability Statistics 2020*. Tech. rep. Brussels, Belgium: European Network of Transmission System Operators for Electricity (ENTSO-e).

– **(2022)**. *Ten-Year Network Development Plan (TYNDP) 2022*. Tech. rep. Brussels, Belgium: ENTSO-e.

Europe Beyond Coal (2020). "Austria's last coal plant closes, Increasing European coal phase-out momentum". https://beyond-coal.eu/2020/04/17/austrias-last-coal-plant-closes-increasing-european-coal-phase-out-momentum/. Accessed: 2022-05-22.

– **(2021a)**. "Portugal becomes fourth European country to go coal free". https://beyond-coal.eu/2021/11/22/portugal-becomes-fourth-european-country-to-go-coal-free/. Accessed: 2022-05-22.

– **(2021b)**. "Sweden follows hot on Austria's heels to go coal free." https://beyond-coal.eu/2020/04/21/sweden-follows-hot-on-austrias-heels-to-go-coal-free/. Accessed: 2022-05-22.

European Commission (2017). *Commission Regulation (EU) 2017/1485, Establishing a guideline on electricity transmission system operation*.

– **(2019)**. *Clean energy for all Europeans*. Publications Office.

European Union (2020). *Offshore wind energy in Europe*. Tech. rep. Brussels, Belgium: European Union.

Fodstad, M., Crespo del Granado, P., Hellemo, L., Knudsen, B. R., Pisciella, P., Silvast, A., Bordin, C., Schmidt, S., and Straus, J. (2022). "Next frontiers in energy system modelling: A review on challenges and the state of the art." In: *Renewable and Sustainable Energy Reviews* 160, 112246.

Fraunhofer ISE (2021). *Levelized Cost of Electricity Renewable Energy Technologies*. Tech. rep. Freiburg, Germany: Fraunhofer ISE.

Gephart, M., Boeve, S., and Klessmann, C. (2020). *Recommendations for an integrated framework for the financing of joint offshore wind projects: final report*. Tech. rep. Brussels, Belgium: European Commission, Directorate-General for Energy.

Glensk, B. and Madlener, R. (2019). "The value of enhanced flexibility of gas-fired power plants: A real options analysis." In: *Applied Energy* 251, 113125.

Göke, L. and Kendziorski, M. (2022). "Adequacy of time-series reduction for renewable energy systems." In: *Energy* 238, 121701.

Gough, R., Dickerson, C., Rowley, P., and Walsh, C. (2017). "Vehicle-to-grid feasibility: A techno-economic analysis of BEV-based energy storage." In: *Applied Energy* 192, 12–23.

GWEC (2022). *Global Wind Report 2022*. Tech. rep. Brussels: GWEC.

Hannah, E., John, M., Jelle, V., and Uden (2020). *PROMOTioN – Progress on Meshed HVDC Offshore Transmission Networks D12.4 - Final Deployment Plan*. Tech. rep. Brussels, Belgium: European Union.

Hausfather, Z. (2018). "Analysis: How much 'carbon budget' is left to limit global warming to 1.5C?" https://www.carbonbrief.org/analysis-how-much-carbon-budget-is-left-to-limit-global-warming-to-1-5c/. Accessed: 2022-05-22.

Hernandez, D. D. and Gençer, E. (2021). "Techno-economic analysis of balancing California's power system on a seasonal basis: Hydrogen vs. lithium-ion batteries." In: *Applied Energy* 300, 117314.

Hu, J., Yang, G., Ziras, C., and Kok, K. (2019). "Aggregator Operation in the Balancing Market Through Network-Constrained Transactive Energy." In: *IEEE Transactions on Power Systems* 34.5, 4071–4080.

IEA (2021a). *Global Energy Review: CO_2 Emissions in 2021*. Tech. rep. Paris: IEA.

– (2021b). *Offshore Wind Outlook 2019*. Tech. rep. Paris: IEA.

– (2021c). *World Energy Outlook 2021*. Tech. rep. Paris, France: International Energy Agency (IEA).

IPCC (2022). *Global Warming of 1.5℃: IPCC Special Report on Impacts of Global Warming of 1.5℃ above Pre-industrial Levels in Context of Strengthening Response to Climate Change, Sustainable Development, and Efforts to Eradicate Poverty*. Cambridge University Press.

Koffi, B., Cerutti, A., Duerr, M., Iancu, A., Kona, A., and Janssens-Maenhout, G. (2017). "Covenant of Mayors for Climate and Energy: Default emission factors for local emission inventories, Version 2017." In: *EUR 28718 EN*.

Krukanont, P. and Tezuka, T. (2007). "Implications of capacity expansion under uncertainty and value of information: The near-term energy planning of Japan." In: *Energy* 32.10, 1809–1824.

Kucukvar, M., Onat, N. C., Kutty, A. A., Abdella, G. M., Bulak, M. E., Ansari, F., and Kumbaroglu, G. (2022). "Environmental efficiency of electric vehicles in Europe under various electricity production mix scenarios." In: *Journal of Cleaner Production* 335, 130291.

Li, Y. and Huang, G. (2012). "Electric-power systems planning and greenhouse-gas emission management under uncertainty." In: *Energy Conversion and Management* 57, 173–182.

Liu, Z., Wu, Q., Christensen, L., Rautiainen, A., and Xue, Y. (2015). "Driving pattern analysis of Nordic region based on National Travel Surveys for electric vehicle integration." In: *Journal of Modern Power Systems and Clean Energy* 3.2, 180–189.

Ludin, G. A., Nakadomari, A., Yona, A., Mikkili, S., Rangarajan, S. S., Collins, E. R., and Senjyu, T. (2022). "Technical and Economic Analysis of an HVDC Transmission System for Renewable Energy Connection in Afghanistan." In: *Sustainability* 14.3.

Öberg, S., Odenberger, M., and Johnsson, F. (2022). "Exploring the competitiveness of hydrogen-fueled gas turbines in future energy systems." In: *International Journal of Hydrogen Energy* 47.1, 624–644.

Ocker, F. and Jaenisch, V. (2020). "The way towards European electricity intraday auctions – Status quo and future developments." In: *Energy Policy* 145, 111731.

Olk, C., Sauer, D. U., and Merten, M. (2019). "Bidding strategy for a battery storage in the German secondary balancing power market." In: *Journal of Energy Storage* 21, 787–800.

Østergaard, P. A. (2012). "Comparing electricity, heat and biogas storages' impacts on renewable energy integration." In: *Energy* 37.1. 7th Biennial International Workshop "Advances in Energy Studies", 255–262.

Perveen, R., Kishor, N., and Mohanty, S. R. (2014). "Off-shore wind farm development: Present status and challenges." In: *Renewable and Sustainable Energy Reviews* 29, 780–792.

Pfenninger, S., Hawkes, A., and Keirstead, J. (2014). "Energy systems modeling for twenty-first century energy challenges." In: *Renewable and Sustainable Energy Reviews* 33, 74–86.

Poplavskaya, K., Lago, J., Strömer, S., and de Vries, L. (2021). "Making the most of short-term flexibility in the balancing market: Opportunities and challenges of voluntary bids in the new balancing market design." In: *Energy Policy* 158, 112522.

Ramezanzadeh, S. P., Mirzaie, M., and Shahabi, M. (2021). "Reliability assessment of different HVDC transmission system configurations considering transmission lines capacity restrictions and the effect of load level." In: *International Journal of Electrical Power & Energy Systems* 128, 106754.

Rodrigues, R., Pietzcker, R., Fragkos, P., Price, J., McDowall, W., Siskos, P., Fotiou, T., Luderer, G., and Capros, P. (2022). "Narrative-driven alternative roads to achieve mid-century CO2 net neutrality in Europe." In: *Energy* 239, 121908.

Ryndzionek, R. and Sienkiewicz, Ł. (2020). "Evolution of the HVDC Link Connecting Offshore Wind Farms to Onshore Power Systems." In: *Energies* 13.8.

Skar, C., Doorman, G., and Tomasgard, A. (2014). "The future European power system under a climate policy regime." In: *2014 IEEE International Energy Conference (ENERGYCON)*, 318–325.

TenneT Holding B.V. (2020). "BorWin1". https://tennet.eu/our-grid/offshore-projects-germany/borwin1/. Accessed: 2022-05-22.

– (2021). "What kind of markets are there and how do they work?" https://netztransparenz.tennet.eu/electricity-market/about-the-electricity-market/what-kind-of-markets-are-there-and-how-do-they-work/. Accessed: 2022-02-15.

Thangavelu, S. R., Khambadkone, A. M., and Karimi, I. A. (2015). "Long-term optimal energy mix planning towards high energy security and low GHG emission." In: *Applied Energy* 154, 959–969.

The Wind Power (2021). "World wind farms database". https://www.thewindpower.net/country_list_en.php. Accessed: 2022-06-20.

Tosatto, A. (2022). "European Transmission and Market Models". https://github.com/antosat/European-Transmission-and-Market-Models. Accessed: 2022-06-20.

UNEP (2011). *Decoupling natural resource use and environmental impacts from economic growth, A Report of the Working Group on Decoupling to the International Resource Panel*. Tech. rep. United Nations Environment Programme International Resource Panel.

van der Veen, R. A. and Hakvoort, R. A. (2016). "The electricity balancing market: Exploring the design challenge." In: *Utilities Policy* 43, 186–194.

Vorushylo, I., Keatley, P., and Hewitt, N. (2016). "Most promising flexible generators for the wind dominated market." In: *Energy Policy* 96, 564–575.

Vral, T. (2018). *Using electric vehicles to balance the network*. Tech. rep. Brussels, Belgium: Elia Group.

Vrana, T. K. and Härtel, P. (2018). "Estimation of investment model cost parameters for VSC HVDC transmission infrastructure." In: *Electric Power Systems Research* 160, 99–108.

Wind Europe (2019). *Our energy, our future, How offshore wind will help Europe go carbon-neutral*. Tech. rep. Brussels, Belgium: Wind Europe.

Yuan, Y., Cheng, H., Zhang, H., Wang, Z., and Zhou, W. (2022). "Transmission expansion planning with optimal transmission switching considering uncertain n-k contingency and re-

newables." In: *Energy Reports* 8. ICPE 2021-The 2nd International Conference on Power Engineering, 573–583.

Zhou, H., Yao, W., Ai, X., Li, D., Wen, J., and Li, C. (2022). "Comprehensive review of commutation failure in HVDC transmission systems." In: *Electric Power Systems Research* 205, 107768.

Zhu, Y., Zhang, S., Liu, D., Zhu, L., Zou, S., Yu, S., and Sun, Y. (2019). "Prevention and mitigation of high-voltage direct current commutation failures: a review and future directions." In: *IET Generation, Transmission & Distribution* 13.24, 5449–5456.

Zweifel, P., Praktiknjo, A., and Erdmann, G. (2017). *Energy Economics*. Springer Texts in Business and Economics. Berlin, Heidelberg: Springer Berlin Heidelberg.

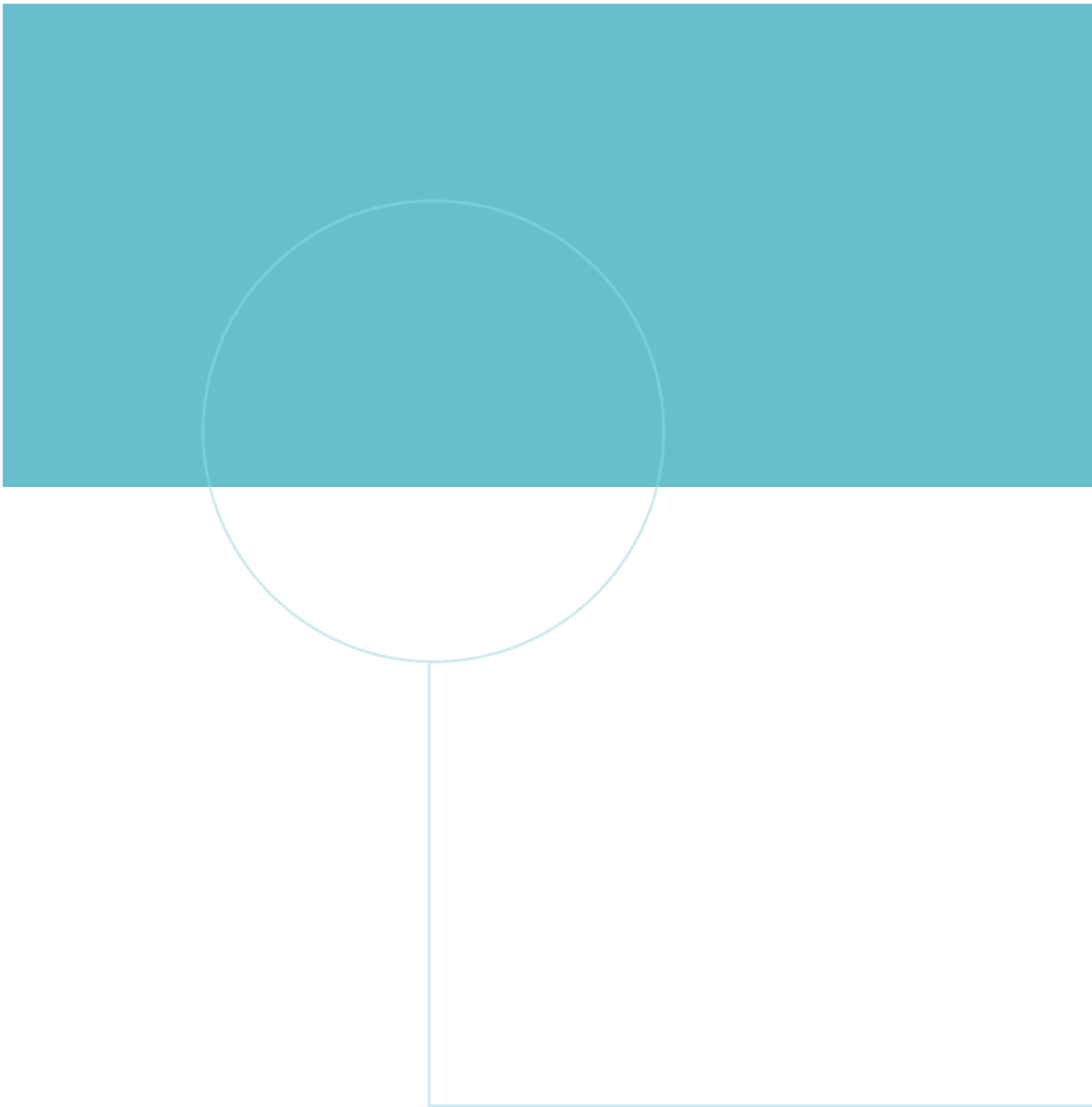

NTNU
Norwegian University of
Science and Technology

TECHNISCHE
UNIVERSITÄT
BERLIN